FHWA -NJ-2002-005

Circular Elastomeric Bearings

FINAL REPORT
December 2004

Submitted by

Husam Najm
Hani Nassif
N. Ozgur Bezgin
Raxit Patel
Anand Patel

Dept. of Civil & Environmental Engineering
Center for Advanced Infrastructure & Transportation (CAIT)
Rutgers, The State University
Piscataway, NJ 08854-8014

NJDOT Research Project Manager
Mr. Robert Sasor

In cooperation with

New Jersey
Department of Transportation
Bureau of Research
and
U.S. Department of Transportation
Federal Highway Administration

Disclaimer Statement

"The contents of this report reflect the views of the author(s) who is (are) responsible for the facts and the accuracy of the data presented herein. The contents do not necessarily reflect the official views or policies of the New Jersey Department of Transportation or the Federal Highway Administration. This report does not constitute a standard, specification, or regulation."

The contents of this report reflect the views of the authors, who are responsible for the facts and the accuracy of the information presented herein. This document is disseminated under the sponsorship of the Department of Transportation, University Transportation Centers Program, in the interest of information exchange. The U.S. Government assumes no liability for the contents or use thereof.

TECHNICAL REPORT STANDARD TITLE PAGE

1. Report No.	2. Government Accession No.	3. Recipient's Catalog No.
FHWA-NJDOT-2002-005		

4. Title and Subtitle	5. Report Date
Circular Elastomeric Bearings	December 2004
	6. Performing Organization Code: CAIT/Rutgers

7. Author(s)	8. Performing Organization Report No.
Husam Najm, Hani Nassif, N. Ozgur Bezgin, Raxit Patel, Anand Patel	FHWA-NJDOT-2002-005

9. Performing Organization Name and Address	10. Work Unit No.
Center for Advanced Infrastructure and Transportation (CAIT) Rutgers University Piscataway, NJ 08854-8014	11. Contract or Grant No.

12. Sponsoring Agency Name and Address		13. Type of Report and Period Covered
New Jersey Department of Transportation, P.O. Box 600 Trenton. NJ 08625	Federal Highway Administration U.S. Department of Transportation Washington D.C.	Final Report 1/01/2001 - 12/31/2004
		14. Sponsoring Agency Code

15. Supplementary Notes

Dr. Najm's e-mail address is: hnajm@rci.rutgers.edu

16. Abstract

Reinforced and unreinforced elastomeric bearing pads have been used for bridges in NJ for about five years. The shape of these bearings is square or rectangular and their orientation is generally in the direction of thermal movements. Circular elastomeric bearings are not used in NJ but have been used in several states. These bearings may be more suitable on skewed and curved bridges with limited space on pier cap or abutment seat, however, their behavior needs to be studied and evaluated. A nationwide survey has been conducted to evaluate state DOT's experience with circular elastomeric bearings and a finite element and experimental investigation was performed to compare various bearing geometries. Survey results showed circular elastomeric bearings are being used in several states and more states are willing to consider them. Very few states had instrumented elastomeric bearings and most states that used circular bearings reported insignificant cost difference compared to rectangular and square bearings. Results from the finite element investigation showed that laminated circular bearings have higher axial stiffness than rectangular or square bearings of the same area. For the same area, rotational stiffnesses of circular bearings were higher than those of square bearings. The finite element analysis also showed non-linear distribution of normal stresses across the bearing and the existence of tensile stresses at the interface between the elastomer top layer and the steel shim under compressive and shear loads. Results from the experimental study showed that the stress-strain relations in compression of circular, square, and rectangular laminated bearings tested in this study show a similar trend to those from the finite element analysis. They also show similar trend to those of AASHTO LRFD design guide curves in Section 14.7.5.3.4. The effective compression moduli Ec of circular and square bearings from tests were about 10% higher, and for rectangular bearings, was about 20% higher than AASHTO LRFD approximate values. Comparisons of the rotational stiffnesses of circular, square, and rectangular bearings from finite element analysis and from experimental results were not conclusive and more research is needed in this area.

17. Key Words	18. Distribution Statement
circular bearings, square bearings, survey, elastomer, plain, shims, skewed bridges, curved bridges, wide bridges, laminates, cost	

19. Security Classif (of this report)	20. Security Classif. (of this page)	21. No of Pages	22. Price
Unclassified	Unclassified	101	

Form DOT F 1700.7 (8-69)

Acknowledgements

The authors wish to acknowledge the support of the personnel from the New Jersey Department of Transportation (NJDOT). In particular the authors would like to thank Mr. Robert Sasor, Mr. Nicholas Vitillo, Mr. Jose Lopez, and Mr. Jerry Sellner for their technical support and constructive comments. Also, the authors would like to thank Mr. Anthony Chmiel for his helpful suggestions on the survey.

The financial support of this project was provided by the State of New Jersey Department of Transportation (NJDOT) and the Federal Highway Administration (FHWA). Mr. Robert Sasor was the NJDOT Research Project Manager. Drs. Husam Najm and Hani Nassif were the project Principal Investigators.

TABLE OF CONTENTS

Page

LIST OF FIGURES

Page

Page

Page

LIST OF TABLES

SUMMARY

Reinforced and unreinforced elastomeric bearing pads have been used for New Jersey bridges for approximately five years. The shape of these bearings is square or rectangular, and their orientation is generally in the direction of thermal movements. Although, the direction of thermal movement for straight bridges can be reasonably predicted, the direction of displacements of skewed and curved bridges may not be well defined. For rectangular bearings, if the direction of movement is not oriented along one of the principal axes of the bearing, distortion of the bearing may occur. The problem is worsened if the fatigue loading is significant, which could cause delamination at the elastomer-steel shim interface bond. For very wide bridges, circular bearings perform better than square or rectangular bearings. For square and rectangular bearings, transverse, as well as longitudinal, movement must be considered when the direction of movement is not along the centerline of the beam. Moreover, rectangular bearings often need to be notched to provide edge clearance for certain capital geometries, which increases the cost of the bearing and adds more corners to its shape. Also, in some instances, these bearings may not be properly oriented in the field as required by the contract drawings. Circular elastomeric bearings are not direction dependent and they generally exhibit the same behavior in all directions. The circular shape, moreover, does not have edge corners, which eliminates stress concentrations and the possibility of distortions. These bearings are less likely to be notched in comparison to the rectangular bearings and their orientation in the field is simple. Circular elastomeric bearings have been used on many projects in several states. Their advantages on skewed, curved, and wide bridges make them an attractive alternative to rectangular bearings, however, their behavior needs to be studied and evaluated. A nationwide survey has been conducted to evaluate state DOT's experience with circular elastomeric bearings. A similar survey was sent to bridge consultants in the New York/New Jersey area. Bearing manufacturers and suppliers were contacted by phone and electronic mail. The results of the surveys and results from the analytical and experimental investigation of circular, square, and rectangular bearings are presented with conclusions and recommendations.

INTRODUCTION

During the last 30 years elastomeric bearings have been used with increasing frequency in highway bridges. These bearings, which are economical and require less maintenance, can support heavy gravity loads while accommodating large deformations of the elastomer. The early use of such bearings was limited to the unreinforced elastomeric pads. Today, steel-laminated elastomeric pads are often used for situations requiring higher bearing stress and stiffness. More recently, fiberglass reinforced elastomeric pads and fabric reinforced elastomeric pads have been used. AASHTO Standard Specifications allow the use of fiberglass reinforcement in elastomeric bearings. Other materials, such as polyester, have proven to be too flexible and both polyester and cotton are not strong or stiff enough. The strength of the fabric reinforcement governs the compressive strength of the bearing when minimum reinforcement is used. If a stronger fabric with acceptable bond properties is used, the stress limits given in AASHTO [7,20] Section 14.4.1 (AASHTO Method A) may be increased. However, thorough testing over a wide range of conditions, including fatigue will be required prior to acceptance. While elastomeric bearings have been used successfully for the last 30 years, there have been some instances of performance problems. These problems include bearing slip or bearing “walking out “: a phenomenon, which was more evident in natural rubber pads more than in neoprene pads. Another problem was delamination due to the separation of the elastomer-steel bond. Delamination could occur as a result of a poor bond between steel and the elastomer and due to overstressing of the bearing.

In New Jersey, reinforced and unreinforced elastomeric bearing pads have been used for bridges for approximately five years. The shape of these bearings is square or rectangular and their orientation is generally in the direction of thermal movements. Although the direction of thermal movement for straight bridges can be reasonably predicted, the direction of displacements of skewed and curved bridges may not be well defined. For rectangular bearings, if the direction of movement is not oriented along one of the principal axes of the bearing, distortion of the bearing may occur. The problem is

worsened if the fatigue loading is significant, which could cause delamination of the elastomer-steel bond. Moreover, rectangular bearings often need to be notched to provide edge clearance, which increases the cost of the bearing and adds more corners to its shape. Also in some instances, these bearings may not be properly oriented in the field as required by the analysis.

Circular elastomeric bearings are not direction dependent and they generally exhibit the same behavior in all directions. Moreover the circular shape does not have edge corners, which eliminates stress concentrations and the possibility of distortions. These bearings are less likely to be notched in comparison to the rectangular bearings, and their orientation in the field is simple. Their advantages make them an attractive alternative to rectangular bearings, however, their behavior needs to be studied and evaluated.

The purpose of this study is to evaluate the performance of circular and rectangular bearings in regard to the factors that most affect their cost and behavior. These factors include compressive stress; shear strains, rotations, movements, geometry, and laminates. The study will include a survey of State Department of Transportation's experience with elastomeric bearings, in particular, circular bearings. Based on a literature review and the results of this survey, the results of an analytical investigation, and information from manufacturers, recommendations will be made to the NJDOT on the appropriateness of utilizing circular bearings in bridges in New Jersey. The study will also evaluate the use of composite laminates between elastomer pads in terms of strength and stiffness, and make recommendations to the NJDOT on the potential of these composite materials in bridge bearings.

RESEARCH OBJECTIVES

The objective of this research is to evaluate and compare the behavior and performance of circular, square, and rectangular bearings with regard to critical parameters and overall cost and to determine whether using circular bearings can result in cost savings

over square and rectangular elastomeric bearings. Another objective is to make recommendations, based on the comparison of performance and cost, on whether to allow the use of circular bearings in bridges in New Jersey and to evaluate the use of high performance composites instead of steel between elastomer pads in terms of strength, stiffness, durability, and cost. In order to achieve these objectives, the following was done. First, surveys of current DOT experiences in circular elastomeric bearings, as well as the experiences of area consultants and manufacturers, were conducted. Second, a comprehensive finite element investigation of circular versus square and rectangular elastomeric bearings was completed. Third, an experimental evaluation of circular, square, and rectangular bearings was completed.

LITERATURE REVIEW

The literature survey provided here includes an overall review of all research work performed on bridge elastomeric bearings. Up-to-date experimental and analytical research, as well as current State DOT and design code specifications, are reviewed.

Movements in bridge structures are caused by joint expansion and contraction, deflection, earth pressures, and other forces, and are usually accommodated by bearings. A variety of bearing devices has been used, including sliding plates, small and large-diameter roller nests, large single rollers, rockers, isolation bearings, and elastomeric bearings. Bearing components are generally specified by an AASHTO or ASTM designation that includes material and inspection requirements to assure quality and performance. In searching for more satisfactory bridge bearings, the desire is to develop bearings with no moving parts that can freeze, corrode, or deteriorate, easy to install and maintain; and are aesthetically pleasing. Elastomeric bearings satisfy many of these desired features. Elastomeric bearings have been used with increased frequency in highway bridges during the last 30 years. These bearings, which are economical and require less maintenance, can support heavy gravity loads while accommodating large deformations of the elastomer. The early use of such bearings was limited to the unreinforced elastomeric pads. Today, steel-laminated elastomeric

pads are often used for situations requiring higher bearing stress and stiffness. More recently, fiberglass reinforced elastomeric pads and fabric reinforced elastomeric pads have been used. AASHTO Standard Specifications allow the use of fiberglass reinforcement in elastomeric bearings. Other materials such as polyester have proven to be too flexible and both, polyester and cotton are not strong or stiff enough. The strength of the fabric reinforcement governs the compressive strength of the bearing when minimum reinforcement is used. If a stronger fabric with acceptable bond properties is used, the stress limits given in AASHTO [7,20] Section 14.4.1 (AASHTO Method A) may be increased. However, thorough testing over a wide range of conditions, including fatigue will be needed before being accepted.

While elastomeric bearings have been used successfully for the last 30 years, there have been some instances of performance problems in the past. These problems included bearing slip or bearing "walking out ", a phenomenon, which was more evident in natural rubber pads more than in neoprene pads. Another problem was delamination due to the separation of the elastomer-steel bond. Delamination could happen due to poor bond between steel and the elastomer and due to overstressing of the bearing. The performance of elastomeric bearings has been also questioned under low temperatures because the natural rubber and neoprene both become stiffer once subjected to extreme cold temperatures.

Minor and Egen[13] (1970) produced the most comprehensive study to date (NCHRP Report 109) on elastomeric bearings. They tested a wide range of neoprene, natural rubber, neoprene-dacron, and ethylene-propylene dimonomer elastomers. They introduced the shear modulus as a design parameter and pointed out that quality control during fabrication is important. NCHRP Report 248, " *Elastomeric Bearing Design, Construction, and Materials*" by Roeder and Stanton [21] (1982) concentrated on the development of improved specifications (Method A) for unconfined, plain, and reinforced elastomeric bridge bearings. The recommendations of this report were adopted in the AASHTO *Standard Specifications for Highway Bridges* in 1985.

Roeder and Stanton [18] (1987) in NCHRP Report 298, " *Performance of Elastomeric Bearings"* included laboratory testing of actual bridge bearings to correlate bearing performance and test data with the theories upon which Method A specifications were based. The research was performed on bearings of natural rubber and neoprene with different shape factors, different thickness and number of laminates, different bearing shapes (rectangular, circular, and square). Both steel and fiberglass reinforced specimens were tested. The report also included the development of special specifications for special applications (Method B). It also provided more rational bearing specifications that would allow bearing pressures as high as 1600 psi under certain design conditions.

In their third NCHRP study, Report 325 in 1989, Roeder and Stanton[17] sought to develop recommendations for low temperature behavior and acceptance test procedures of elastomeric bearings. They concluded that low temperatures might cause dramatic increases in the stiffness of the bearing, which may result in significant forces transmitted by the bearing to the substructure. Neoprene pads in their study showed more increase in stiffness compared to natural rubber. Muscarella and Yura [18] (1995) conducted an experimental study for the Texas DOT on elastomeric bridge bearings. Their research proved that tapered elastomeric bearings performed equally as well as flat bearings, and that manufacturing tapered bearings with the steel laminates parallel to each other offers several benefits over spacing shims radially. They also concluded that elastomers with lower hardness has some advantages over harder elastomers in terms of the additional rotational capacity they provide and that highly reinforced bearings performed better in compression and fatigue tests. The effects of square and rectangular elastomeric bearing pads on performance AASHTO precast I-beams were reported by Yazdani, Eddy, and Cai [24] (2000). Their study indicated that the performance characteristics of precast bridge I-beams are slightly enhanced by the effects of restraints from laminated neoprene bearing pads. McDonald, Hemysfield, and Avent [10] (2000) studied the slippage of neoprene pad bridge bearings. In particular, they were interested in why those pads tend to slip or "walk" out-of-place. Their study showed the slope of the bottom of the girder in contact with the bearing remains

relatively constant and that slippage in bearings occurs on a daily basis due to thermal movements.

An analytical investigation using the finite element analysis by Hamzeh, Tassoulas, and Becker [5] (1998) of square and rectangular elastomeric bearings yielded higher stresses and strains at the elastomer-steel shim interface. They also observed tensile stresses in the cover elastomer layers particularly near the tips of the steel shims.
The use of the finite element method in the analysis of elastomeric bearings began about twenty years ago. Lindley[8,9] (1971, 1975) first developed a large deformation plane stress finite element computer program, which was later modified to include bulk compression and plain strain. This program was then used to compute effective compression moduli (at small strains) for infinite long strips with different shape factors and material properties. Analytical investigations by Herrmann, Hamidi, Safigh-Nobari, and Ramaswamy [6] (1988) have resulted in the development of a composite three-dimensional finite element procedure based on an equivalent homogeneous continuum. Seki [19] (1987) investigated multiplayer elastic bearings at the Technical Research Laboratory of the Bridgestone Corporation. Strip biaxial testing provided details of the strain energy function used to define the elastomer material properties. A five-layer bearing was analyzed and it was claimed that the analyses agree well with experimental results. Takayama et al. [22] (Takayama 1990) has fitted five material constants from biaxial elongation tests and has successfully analyzed a full-scale 500 mm (19.7 inches) diameter bearing. This 3D model contained 4136 elements and 7120 nodes. The model was compressed to 100Mpa (14.5ksi) and it achieved a shear deformation of 380%. Billing [3] (1992) performed extensive finite element analysis regarding the elastomeric bearings. He studied low shape-factor and Malaysian Rubber Producer's Research Association twelve layers test bearings by two-dimensional and three dimensional models, and made some comparison with the test results. However, his work was concentrated on the performance of elastomeric bearing as a base isolation for the buildings.

SURVEY OF STATE DOT'S

A general survey was conducted of state bridge engineers at different DOT's across the United States. The main purpose of the survey was to learn which states use circular elastomeric bearings, which bridge types it was specified for, cost comparison with square and rectangular bearings, and their experiences and comments. An example of circular elastomeric bearings is shown in Fig. 1. The survey also investigated which states are willing to consider circular bearings in the future. Other information obtained from the survey was related to bearing design methods, bearing inspection and maintenance, and bearing failure. Surveys were distributed to forty-nine states, and responses were received from thirty-nine states, about an 80% participation ratio.

Figure 1. Circular elastomeric bearings used in concrete box girders in Massachusetts.

Results of the survey showed which states already used circular bearings, and the states that are willing to consider these bearings, are summarized in Table 1. Eight out of the thirty-nine states (21%) that participated in the survey have used circular

bearings. Eighteen states (46%) said they are willing to consider circular elastomeric bearings for their bridges. Ohio indicated that they will consider bearings, but they thought they are more expensive than square and rectangular bearings. Other states, such as South Dakota, Oregon, and Hawaii, mentioned that their willingness to consider them would be based on what advantages they offer over square or rectangular bearings. The states that used circular bearings gave the following information about circular bearings:

Table 1. Survey of State DOT's - Circular versus square and rectangular elastomeric bearings.

STATE DOT	Use circular elast. bearings	Willing to consider using circular elastomeric bearings		Additional State DOT comments
Alabama				
Alaska		Yes		
Arizona			No	
Arkansas			No	
California				
Colorado		Yes		
Connecticut	Yes			
Delaware	Yes			
Florida				
Georgia		Yes		
Hawaii		Yes		If their use is justified
Idaho	Yes			
Illinois		Yes		
Indiana			No	
Iowa			No	There is no reason to use them
Kansas			No	
Kentucky		Yes		
Louisiana				
Maine	Yes			
Maryland				
Massachusetts	Yes			
Michigan			No	
Minnesota		Yes		
Mississipi		Yes		
Missouri		Yes		
Montana		Yes		
Nebraska				
Nevada			No	
New Hampshire	Yes			
New Mexico		Yes		
New York	Yes			

North Carolina			No	
North Dakota			No	
Ohio		Yes		Though they think they are expensive
Oklahoma			No	
Oregon		Yes		Would consider them but right now
Pennsylvania			No	do not see any reason to use them
Rhode Island				
South Carolina		Yes		
South Dakota			No	Unless convinced there was an
Tennesseee		Yes		advantage for circular bearings
Texas	Yes			
Utah				
Vermont		Yes		
Virginia			No	
Washington		Yes		
West Virginia				
Wisconsin		Yes		
Wyoming				

The majority of these states used 12 in to 24 in diameter bearings; only New Hampshire has used diameters less than 12 in. The thickness of the bearings varied from 2 in to 4 in with Connecticut using less than 2 in thickness and New Hampshire using more than 4 in thick bearings. None of the states have used the circular bearings for straight bridges. The survey results also showed that 29% of the circular bearings were used for mild skew bridges, 50% for larger skew, and 21% for curved bridges. As for bridge length and type, most of the bridges with circular bearings have short spans (less than 100 ft long) and two-thirds of these bridges were precast concrete girder bridges while the remaining third were steel bridges.

Table 2, Page 11 shows circular elastomeric data reported by various states. Standard bearing drawings available on the website of the Texas Department of Transportation shows typical dimension for various bearing geometries based on location, beam type, and end clip angle. The drawing specifies circular bearings for Type IV and Type 72 beams with beam clip angles ranging from 30 degrees to 60 degrees. The New Hampshire Department of Transportation provides standard bearing drawings for circular bearings as well as design guidelines and specifications for bridge shoes. The New Hampshire DOT specifies circular elastomeric bearings for all concrete girder

structures. For steel girders, they recommend circular bearings for skewed structures; however, they do not recommend round bearings for steel girders with high live load rotations.

More than 50% of the states using circular elastomeric bearings specify neoprene for the elastomer layers. The remaining states specify natural rubber (20%) and polychloroprene (20%). The steel shims used by most states are mild steel, with the exception of Delaware, which reported the use of stainless steel shims in their bearings. On the question of maintenance of circular bearings, Texas, New York, and Connecticut reported no difference in maintenance requirements for circular bearings versus square or rectangular bearings. The remaining states stated that insufficient data was available to compare maintenance requirements. Cost comparisons between circular and square bearings indicated that most states did not have enough data to make such comparison. Texas reported a 10% increase when using the circular bearings and Connecticut saying the cost is about the same. Overall, these states reported that circular bearings in their state comprised less than 10% of the total elastomeric bearings in the state. In New York, New Hampshire, and Texas the percentage was between 10% and 30%. The remaining questions in the survey were related to bearing design methods, inspection, maintenance, and damage, rather than to comparisons between circular and square bearings. However, information obtained from responses to these questions is applicable to all elastomeric bearings and will be presented and discussed in the following paragraph.

Table 2. Survey of state DOT's circular elastomeric bearing data.

STATE DOT	Diameter	Thickness	Elastomer Type	Shim Type	Maintenance vs. square bearings	Cost vs. square bearings	Bridge Type
Connecticut	21"-24"	2"- 3"	Neoprene	Mild Steel	Similar	Minor differences	Mild and large skews; less than 100 ft and from 100 - 150 ft
Delaware	12"- 24"	< 2", 2"- 3"	Neoprene	Stain. Steel	Not enough info	Not enough info	-
Idaho	12"- 24"		Neoprene	Mild Steel	Not enough info	Not enough info	Large skew bridges
Maine	12"- 24"	2"- 4"	Neoprene	Mild Steel	Not enough info	Not enough info	PPC girders; large skew and curved;less than 100 ft

Massachusetts	12"- 24"	3"- 4"	Polychloroprene	Mild Steel	Not enough info	Not enough info	PPC girders; Large skew; less than 100 ft
New Hampshire	12"- 36"	2"- 4"	Natural Rubber	Mild Steel	Not enough info	Not enough info	PPC and steel girders; mild and large skew; less than 100 ft and 100-150 ft
New York	12"- 24"	-	Neoprene and Natural Rubber	Mild Steel	Similar	Not enough info	Steel girders; Large skew and curved; less than 100 ft
Texas	12"-24"	2"-3"	Neoprene and Polychloroprene	Mild Steel	Similar	More expensive by about 10%	PPC girders; Mild and large skew and curved less than 100 ft, 100-150 ft

On the question of the design methods used in practice, AASHTO standard specification Method A is used by 50% of the states, compared to 12% using LRFD AASHTO Method A and 12% using LRFD Method B. In-house design methods are used by 8% of the participating states. The remaining 18% did not give a response. For the survey, only the state of Texas reported they had instrumented and monitored elastomeric bearings (rectangular only) for longitudinal displacements, however, 35% of the states said that they would be interested in instrumentation and monitoring elastomeric bearings in the future. On the question of bearing replacement due to failure, 28% of the states stated that they have replaced a bearing due to failure. The common mode of failure observed in elastomeric bearings was bearing movement – bearing walking out- and excessive rotation, with 50% of the states reporting this type of problem with elastomeric bearings. Other reported failure modes included: bulging of elastomer layers (29%), delamination at the elastomer-shim interface (10%), and material deterioration with age (12%).

COMMENTS FROM SURVEY OF STATE DOT'S

Some states provided additional general comments on circular and elastomeric bearings. Washington State commented that load versus rotation could be an issue with circular bearings and design criteria will be necessary for designers. Another issue they pointed out was top and bottom attachment details, saying it is easier to fabricate these attachments for rectangular bearing, but they added this can be overcome with experience. Massachusetts said that design Method B is too conservative, and results in very tall bearings due to rotation limits. Massachusetts also said that these limits are too restrictive due to insufficient rotational tests. Iowa DOT added more comments to

the issue of rotation limits. Information provide by the Iowa DOT bridge office showed that using rubber layer thickness rather than the total rubber thickness in Method A, is better than Method B in predicting realistic bearing rotations. Minnesota DOT reported they have been using a curved plate bearing detail for almost twenty years that eliminated any consideration for rotation in their elastomeric bearing design.

The Minnesota DOT details for the curved plate bearing assembly are shown in Figure. 2. Alaska DOT only allows natural rubber for elastomers due to cold weather concerns.

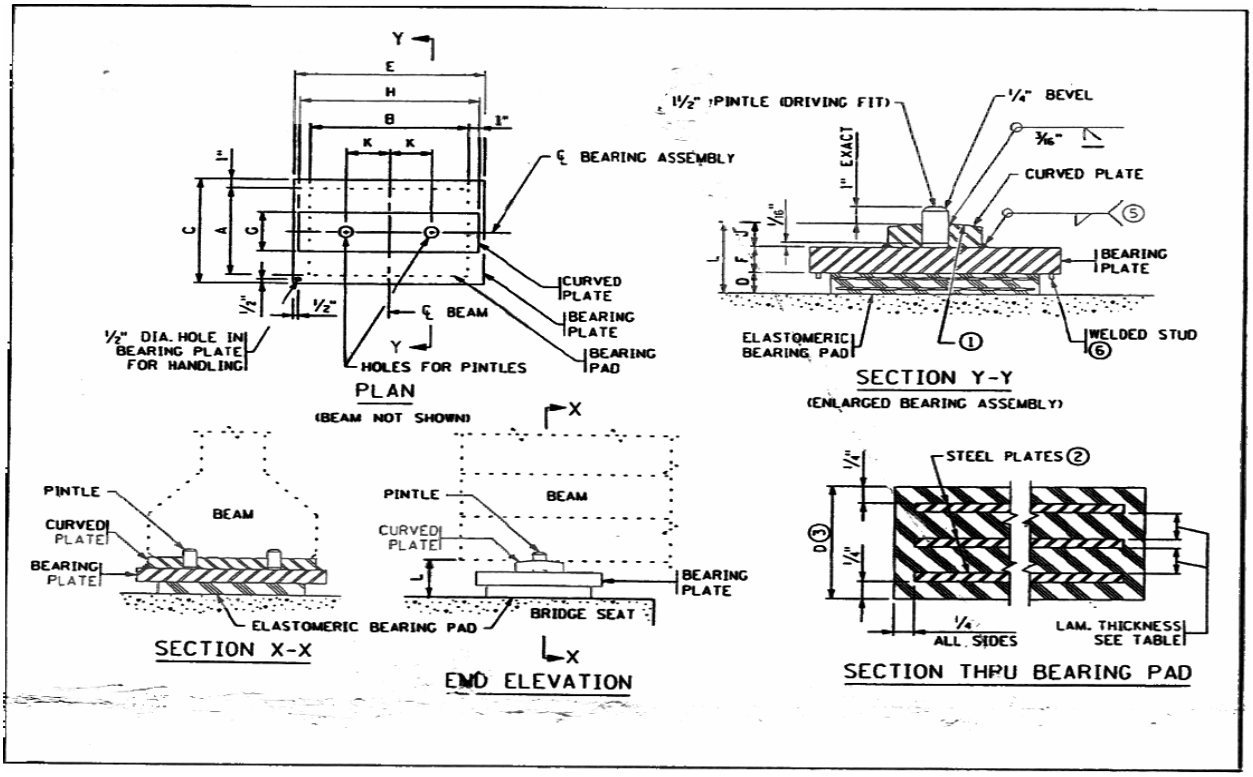

Figure 2. Minnesota DOT detail for curved bearing assembly.

The Oregon DOT indicated that their bearing supplier informed them it is much easier and cheaper to manufacture rectangular bearings compared to round bearings and that is why they did not them. The Texas DOT mentioned that they might discontinue use of circular bearings because higher stress rectangular pads could satisfy bearing seat room limitations in skewed conditions. Finally, the Connecticut DOT commented that excessive rotations were the most critical in elastomeric bearings and that installation tolerances should be maintained to prevent overstressing one edge.

CONSULTANT AND SUPPLIER SURVEYS

A second survey was conducted of bridge designers and consultants in the New York/New Jersey area on whether they have designed circular elastomeric bearings, and what experience they had with these types of bearings relating to their use, cost, and other considerations associated with them. Questionnaires were distributed to seventeen consultants and only seven responded to our survey. Three consultants (42%) said they have designed circular elastomeric bearings for bridges. Among those who designed circular bearings, (66%) stated that there are only minor differences in cost between circular and square bearings. Two consultants, out of the seven who participated in the survey said they would be willing to consider circular elastomeric bearings in certain cases. On the question of design methods, most respondents said they use standard AASHTO method A in their design. Several of them also use method B, however, only one consultant stated that they use the LRFD AASHTO methods for bearing design. On the question of using carbon or glass fiber composite laminates instead of steel shims between elastomer layers, more than 50% of consultants who participated in the survey believe this material can be used for low-stress elastomeric bearings. Finally, only one consultant reported they have done instrumentation and monitoring of bearing horizontal movements but did not provide further information.

A third survey was conducted of bearing manufacturers in the United States to compare cost between circular and square bearings, and determine whether composite laminates have been used in place of steel shims between elastomer layers. This survey was conducted by telephone and by electronic mail. Table 3 shows cost comparison between circular and square bearings for the same area, thickness, and number of steel plates. The results of this survey yielded minor differences in cost between the circular and the square bearings. Most manufacturers/suppliers indicated that there is no significant difference in molding and compressing circular bearings compared to square or rectangular bearings. Only two manufacturers reported that they have been involved in research type work involving using composite laminates to replace steel shims between elastomers in elastomeric bearings, but they said they do not produce these

types of bearings on a commercial scale. They cited difficulty in compressing and vulcanizing the bearing because the composite laminates are flexible and cannot remain straight during the formation process. Others cited concerns with proper bonding between the elastomer and the composite. No cost estimates were given for elastomeric bearings using composite laminates. However, a couple of manufacturers suggested that the price of an elastomeric bearing with composite laminates probably is higher than those with steel shims.

Table 3. Cost comparison of circular versus square elastomeric bearings from manufacturer/supplier survey*.

Manufacturer	Square 12"x12"x3"	Circular Φ14"x3"
Seismic Energy Products, TX	$225	$245
AMSCOT Company, NJ	$175-$200	$225-$250
Granor Rubber Inc.	$100	$130
Tobi Engineering, IL	$70	$75
Scougal Rubber Inc.	$400	$425
Average price	$200	$225

* 4 to 5 steel plates per bearing

INSTRUMENTED ELASTOMERIC BEARINGS

The Ohio DOT performed a study in 2000 on instrumented laminated rectangular elastomeric bearings. Their study was published in Report No. FHWA/OH-2000/010. One of the goals of their study was to assess the feasibility of using instrumented elastomeric bridge bearings as monitoring and condition assessment devices during the life of the bridge. This was based on the assumption that due to loading and changes in bridge conditions, the loads and deformations of the bearings would vary in a way that

when measured could be related to the changes and the conditions of the bridge. In their study, bearing deformations were measured in the field for a three-span slab-girder bridge near Cincinnati. The bridge had continuous rolled beams and integral abutments. Measurements were made during deck concrete pour and static truck load-test. They reported that instrumenting bearings for short-term deformations is more practical, can be easily measured in the field, and can provide useful information about bridge movement and overall bridge service behavior. Long-term assessment measurements and accurate bearing force prediction is not practical. Because of the non-linear behavior of the bearing and the effects of creep and thermal effects, and the variation of bearing stiffness with time, it was difficult to predict the force associated with measured displacements. At deck-pour, the maximum measured bearing deformations were 0.07 in (1.78 mm) horizontal and 0.02 in (51 mm) vertical and 0.003 radian rotation. The maximum measured horizontal deformations during a static truckload test were 0.012 in (0.3 mm) horizontal. Over time the variation of bearing properties makes these measurements difficult and not practical. They also discovered that the bearings in the field developed a permanent shear offset prior to live load application.

To study whether this initial offset would lead to premature failure, they ran fatigue tests in the lab on bearings with 25% and 50% initial shear offset and cyclic shear displacement +-50% up to 2000 cycles. The results showed that bearings did not have a substantial loss of vertical or shear stiffness and did not fail and those bearings in the field would serve their intended function.

From the DOT survey, only the state of Texas reported monitoring and instrumentation of rectangular elastomeric bearings. They collected longitudinal thermal movements at several locations in the state. In their response to our questionnaire, they did not indicate any specific comments on thermal movements or whether measured data agreed with predicted data, however, they mentioned measured data were within anticipated design movements.

EVALUATION OF COST SAVINGS

From the responses of the State DOT's, consultants, and manufacturers/suppliers, the cost differentials between circular, square, and rectangular bearings with steel plates are about 10%. As shown in Table 3, Page 15, in the survey section, the average cost of a circular elastomeric bearing with the same area, thickness, and number of layers is approximately 10% higher than a square bearing. The average cost of the circular bearing was about $ 225, compared to $ 200, for square bearings. Since the cost of the bearings is only a small part of the overall cost of the bridge, the impact of this cost differential on the overall cost of the bridge is insignificant. Cost comparison of plain bearings showed that a circular plain bearing with the same area and thickness as those shown in Table 3, cost about $ 25 compared to $ 20 for a square plain bearing. Although the cost difference is higher (about 25%) for plain bearings, it is not considered significant because of the generally lower cost of plain bearings.

EVALUATE THE EFFECT OF COMPOSITE LAMINATES ON BEARING BEHAVIOR

The advantages of using an elastomeric bearing with carbon fiber or glass-fiber composite laminates is to eliminate corrosion in bearings and extend their service life as well as reducing their weight. On the other hand, the lower stiffness of the composite materials compared to steel, would reduce the vertical stiffness of the bearing and reduce its allowable vertical stress. Therefore, the use of these bearings may be limited to locations on the bridge where loads are small (short span bridges). Because of the very limited research work that was reported on elastomeric bearings with carbon fiber or glass-fiber composite laminates, an analytical investigation of these types of bearings was initiated to compare them to steel laminated bearings. The use of composite laminates to replace steel shims between elastomer layers was evaluated using the ABAQUS finite element analysis as explained in detail in the next section. As reported earlier in the survey section, manufacturers and suppliers commented that elastomeric bearings with carbon fiber composite laminates, although possible, are not a commercially available product. The results of the finite element analysis showed lower stiffness for the bearings with composite laminates for the same bearing shape, as

shown in Figures 51 and 52. Comparing circular and square bearings with composite laminates, the circular bearing showed more vertical stiffness as was the case with the bearings with steel laminates. This comparison is shown in Figure 53**.**

FINITE ELEMENT ANALYSIS

Description of Computer Model

The purpose of the finite element analysis (FEA) is to evaluate the behavior of circular, square, and rectangular elastomeric bearings under various loading conditions. The types of bearings evaluated included plain elastomeric bearings and layered (laminated) elastomeric bearings. The loading conditions investigated were as follows: compression only, compression and shear, and compression and rotation. The bearing parameters included: bearing geometry, stiffness, thickness, and bearing contact area. The analysis program used was ABAQUS Version 5.8. This program is a multipurpose, non-linear analysis program that can handle material and geometrical non-linearities. The elastomer layers and the steel and composite shims were modeled using three-dimensional eight-node solid elements. Boundary conditions at the top and bottom of the bearing were modeled assuming rigid plates for all cases.
To obtain a better understanding of elastomeric bearings' behavior, two sets of models were developed; one set for the analysis of the plain elastomeric bearings and the other set for the analysis of laminated elastomeric bearings.

In order to achieve this comparison, computer models with similar parameters, such as surface area, total bearing thickness, internal elastomer layer thickness, and steel layer thickness, were generated so that the only difference between these models would be the difference in their geometric shapes. The dimensions of the square bearing was set up to a typical value of 16 inches which gave a surface area of 256 in^2. Based on this value, the rectangular bearing with the same surface had dimensions of 12 inch by 21.33 inch, and the circular bearing had a diameter of 18.05 inches. In order to maintain ease of modeling and finite element generation the generated rectangular model had 12 inch by 21.5 inch dimensions which resulted in a slightly higher area (258 in^2) and the

circular model had a diameter of 18 inches which resulted in a slightly lower surface area (254.47 in^2). These differences in surface areas were taken into consideration when lateral loads were determined. However, in general, this adjustment of dimensions was very small and did not have an impact on the comparison of the bearing behavior. The Neo-Hookean and the Mooney-Rivlin material models for rubber were used to model the elastomer. The elastomer was modeled as non-linear elastic material. These two models are modifications of the general material model studied by James, Green, and Simpson (1975). The model studied by James is based on a strain-energy function W given by:

$$W = C_{10}(I_1 - 3) + C_{01}(I_2 - 3) + C_{11}(I_1 - 3)(I_2 - 3) + C_{20}(I_1 - 3)^2 + C_{30}(I_2 - 3)^2 \quad (1)$$

This potential function W is expressed as a function of I1 and I2. The accuracy of the model depends on the C constants. To simplify the general model, the constant C_{01}, C_{11}, C_{20}, and C_{30} were set equal to zero. The remaining constant C_{10} was obtained from compressive test data on rubber made by the Malaysian Rubber Producer's Research Association. The model then is known as the Neo-Hookean Model given by:

$$W(I_1, I_2) = C_{10}(I_1 - 3) \quad (2)$$

and

$$C_{10} = \frac{G}{2} \quad (3)$$

When only constants C_{10} and C_{01} are retained, the model is known as the Mooney-Rivlin Model, given by the following equation:

$$W(I_1, I_2) = C_{10}(I_1 - 3) + C_{01}(I_2 - 3) \quad (4)$$

The steel shims were modeled using bilinear stress-strain model for low-carbon A36 structural steel. The material models for neoprene and steel shims are shown in Figures 4 and 5 respectively. The properties of neoprene and steel materials were as follows:

Properties of the elastomer (neoprene):

Hardness: 55±5

Shear modulus ≅ 200 psi (at -10°C)

Properties of the steel:

Mild steel, F_y=36 ksi

Elastic modulus ≅ 29000 ksi

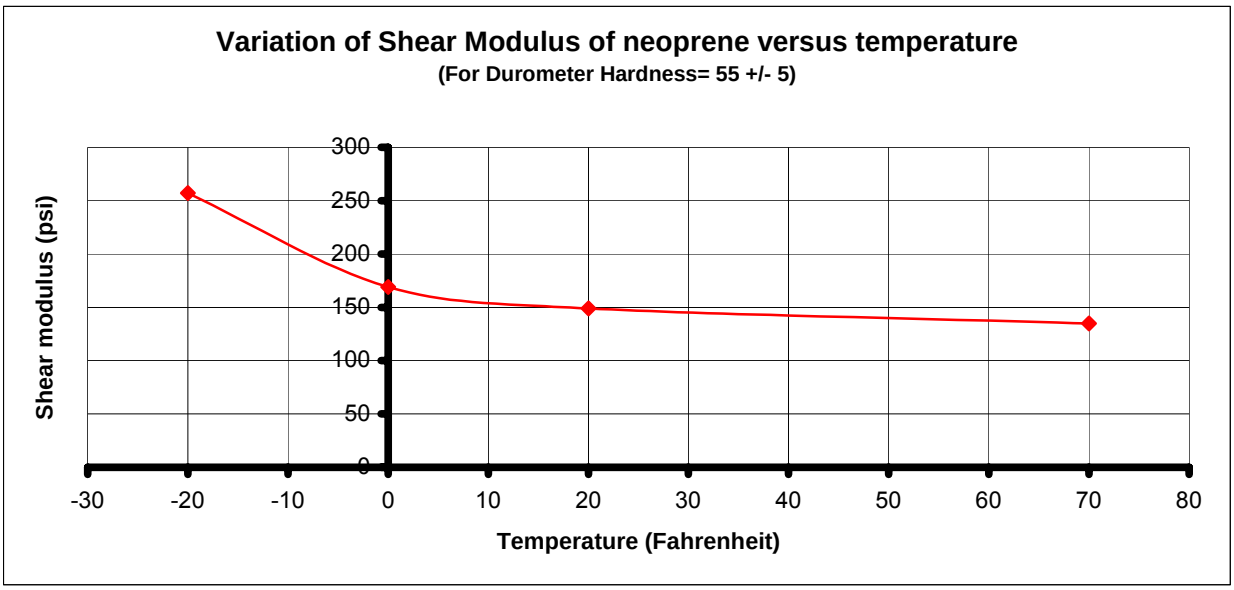

Figure 3. Variation of shear modulus with temperature.

The variation of neoprene shear modulus with corresponding temperature is shown in Figure 3. A spreadsheet was prepared in order to establish the geometry and the loading data used in the FE model. Model data is shown in Table 4. Eight node brick elements were used in the modeling of the bearings (Hybrid elements were used to take into account the incompressible nature of the elastomer). The loading was applied incrementally and the geometric non-linearity of the material was included in the generation of the model.

Table 4. Bearing geometry and loading data for the finite element analysis.

SQUARE									Lateral load components (lb)		Number of nodes		Load per node (lb)	
Length (in)	Width (in)	Thickness (in)	Area (in2)	Load (psi)	Total vertical load (lb)	Lateral load percentage	Lateral load (lb)	Angle with the bearing (°)	Length	Width	Length	Width	Length	Width
16.0	16.0	3.0	256.0	1000	256000	0.2	51200	45.0	36204	36204	19	19	100.3	100.3

Number of steel layers	Steel thickness (in)	Edge layer thickness (in)	Intermediate layer thicknesses (in)	Shape Factor (S)
5	0.075	0.25	0.531	7.5

$$\text{Shape Factor} = S = \frac{W.L}{2x(W+L)x\text{Layer Thickness}}$$

Note: No holes within the plate.

RECTANGLE									Lateral load components (lb)		Number of nodes		Load per node (lb)	
Length (in)	Width (in)	Thickness (in)	Area (in2)	Load (psi)	Total vertical load (lb)	Lateral load percentage	Lateral load (lb)	Angle with the bearing (°)	Length	Width	Length	Width	Length	Width
21.5	12.0	3.0	258.0	1000	258000	0.2	51600	29.2	45057	25148	19	19	124.8	69.7

Number of steel layers	Steel thickness (in)	Edge layer thickness (in)	Intermediate layer thicknesses (in)	Shape Factor (S)
5	0.075	0.25	0.531	7.2

$$\text{Shape Factor} = S = \frac{W.L}{2x(W+L)x\text{Layer Thickness}}$$

Note: No holes within the plate.

CIRCULAR

Diameter (in)	Thickness (in)	Area (in2)	Load (psi)	Total vertical load (lb)	Lateral load percentage	Lateral load (lb)
18.0	3.0	254.5	1000	3E+05	0.2	50894

Number of steel layers	Steel thickness (in)	Edge layer thickness (in)	Intermediate layer thicknesses (in)	Shape Factor (S)
5	0.075	0.25	0.531	8.5

$$\text{Shape Factor} = S = \frac{D^2}{4x\text{Layer Thickness } xD}$$

Note: No holes within the plate.

BEHAVIOR OF PLAIN BEARINGS UNDER COMPRESSION (FEA)

In order to clearly visualize the behavior of the elastomeric bearings under the loadings, 3-D models were generated by ABAQUS 5.8 using three-dimensional brick elements. The analytical investigation included two bearing groups: plain elastomeric bearings and steel reinforced elastomeric bearings. Each set or group had three different bearing shapes: circular, square, and rectangular. For the first set of bearings, the total thickness of the bearing was pure elastomer (neoprene) material and material properties at an ambient temperature of –10°C (14°F) were used. For the second set of bearings, the bearing had both elastomer layers and steel shims (plates) rigidly attached to each other at the interface. Eight node hybrid brick elements are used in the model. In order to generate a realistic pressure distribution on the bearing, i.e. through the bottom flange of a girder, a distributed load is applied to the elastomer bearing through a rigid layer. The assumption was that the friction between the bearing and the rigid layer was infinite, such that no slip occurred during the loading, and also that the bearing is supported such that no movement at the plane of support is allowed (later in the investigation, bearings with slip were evaluated). A distributed load of 1,000 psi was applied according to the ASSHTO specifications for load limits on elastomeric bearings.

Deformations of Plain Bearings

The undeformed and deformed shapes of a square plain bearing are shown in Figures 4 and 5 respectively. Figures 6 and 7 show the undeformed and deformed shapes for a rectangular plain bearing, while Figures 8 and 9 show the undeformed and deformed shapes for a circular plain bearing. The deformed shapes under compressive loads show the effect of bearing geometries on bearing deformations. It can be observed that for circular bearing, there are no local deformations compared to deformations of square and rectangular bearings. Since the square and rectangular bearings lack the radial symmetry, there are excessive deformations at the corners.

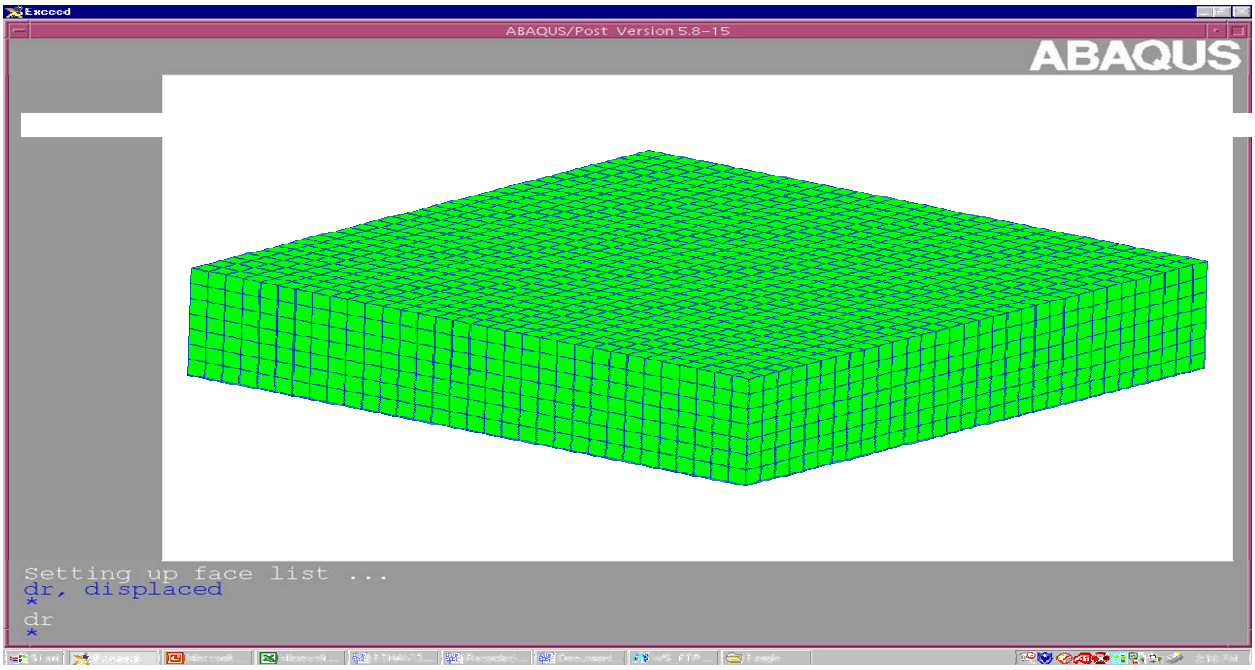

Figure 4. Finite element model of plain square bearing.

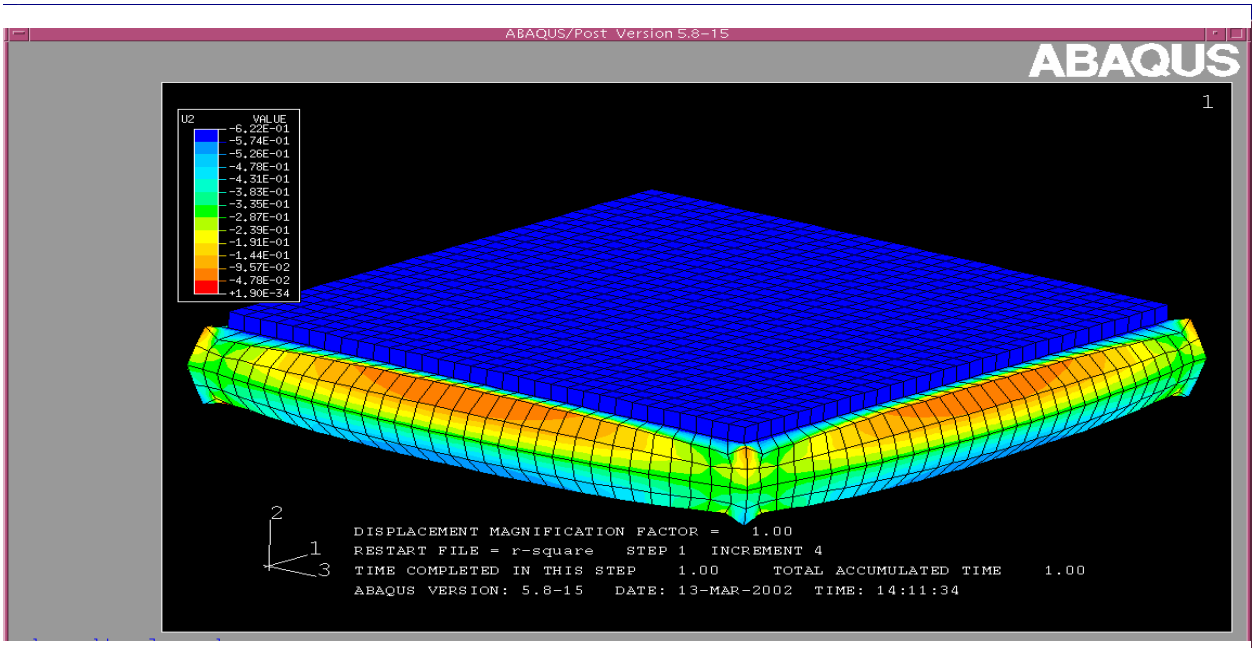

Figure 5. Displacements in the plain square bearing.

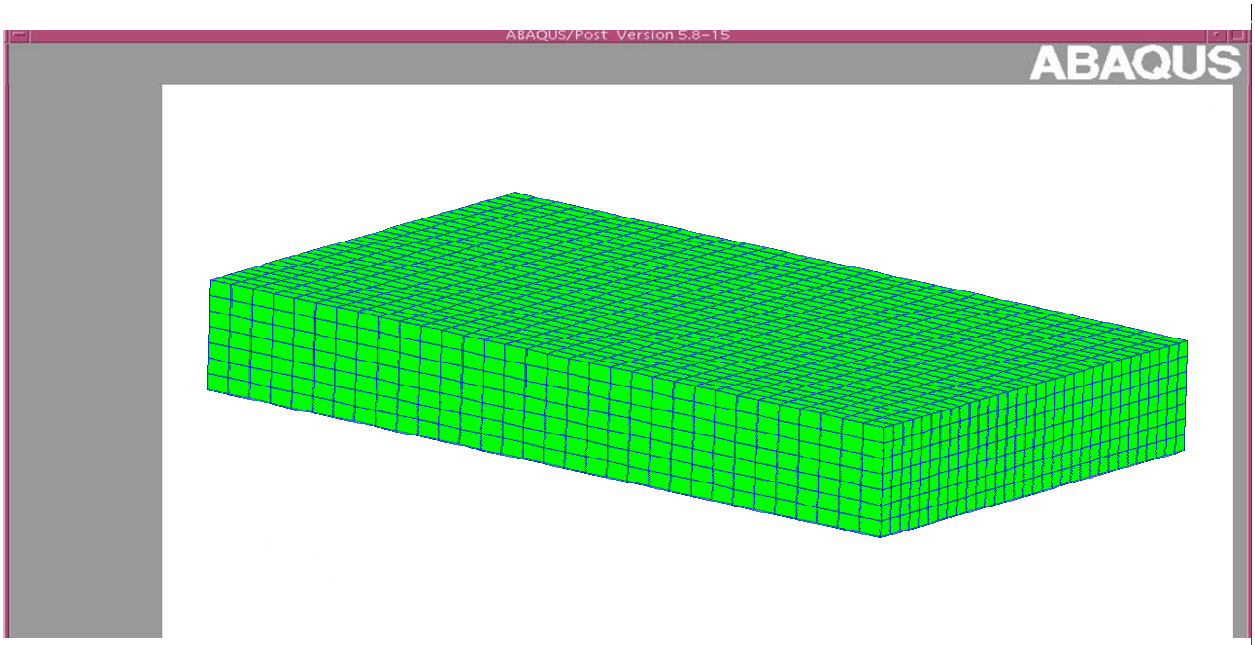

Figure 6. Finite element model of plain rectangular bearing.

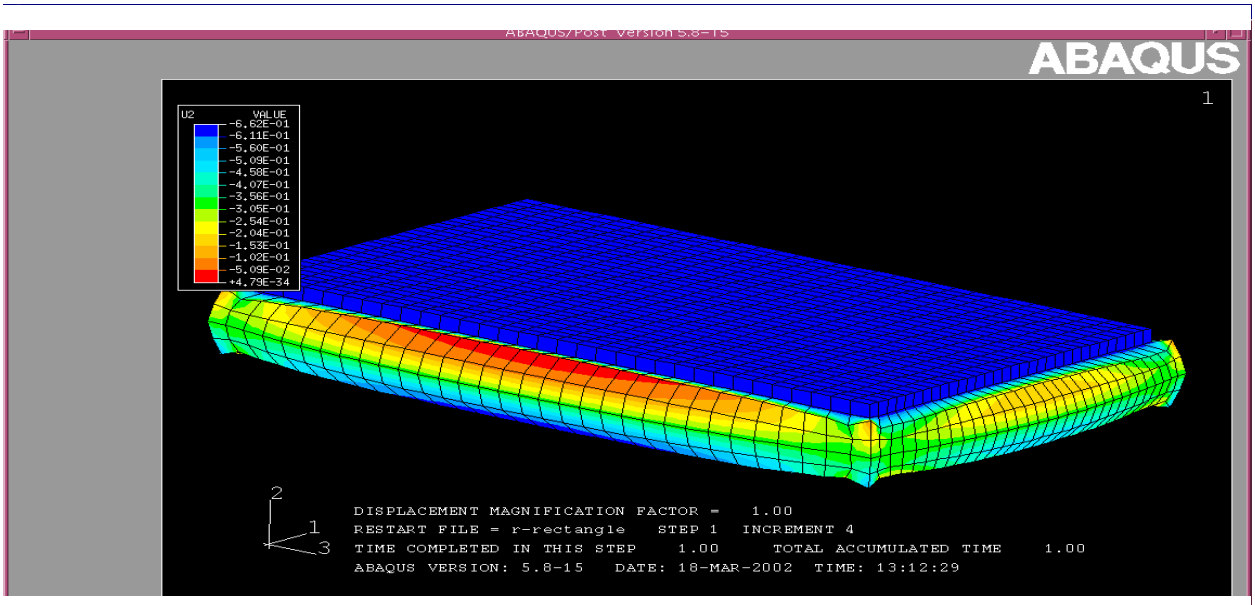

Figure 7. Displacements in plain rectangular bearing.

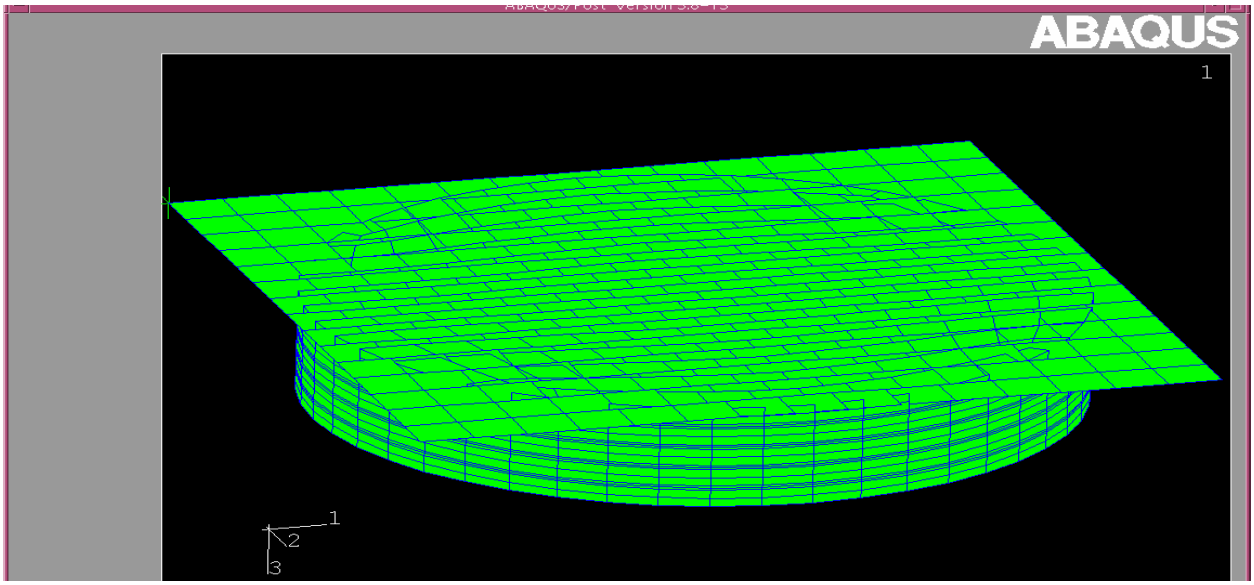

Figure 8. Finite element model of plain circular bearing.

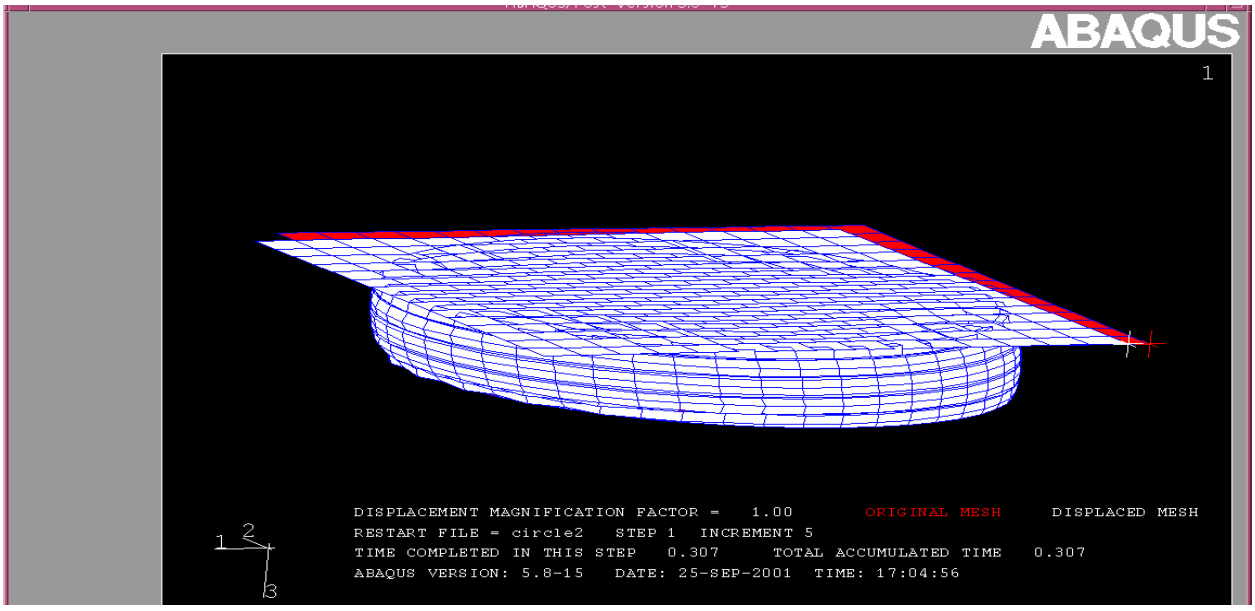

Figure 9. Deformed shape of plain circular bearing.

BEHAVIOR OF LAMINATED BEARINGS UNDER COMPRESSION (FEA)

In bridge bearings, laminates such as steel or fiber reinforced composite plates are provided in order to make the plain elastomeric bearing stiffer. There are two factors for this increase in stiffness:

1. When a laminate with a higher translational stiffness than the elastomer is introduced within a bearing, it replaces a hypothetical layer of elastomer with a lower translational stiffness, which increases the overall stiffness of the bearing.
2. When a plain elastomeric bearing is compressed, it bulges. When laminates are introduced to the bearing, available surface to bulge is reduced and the remaining surfaces that are free to bulge are confined. This confining effect is caused by the tensional stresses induced in the laminates.

The following is a brief discussion of these factors:

Assuming that a plain elastomer bearing is sliced into three hypothetical layers, each of these layers has a translation stiffness of K_e. The total stiffness of the plain elastomeric bearing K_T can be represented in the form:

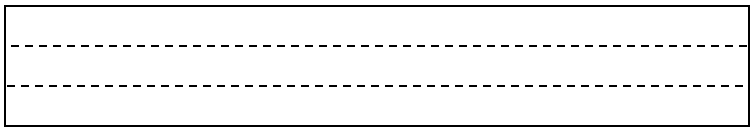

Figure 10. Representation of plain elastomeric bearing.

$$\frac{1}{K_T} = \frac{1}{K_{e1}} + \frac{1}{K_{e2}} + \frac{1}{K_{e3}} \Rightarrow K_T = \frac{K_{e1}.K_{e2}.K_{e3}}{K_{e2}K_{e3} + K_{e1}K_{e3} + K_{e1}K_{e2}} \quad (5)$$

Now, lets assume that one of these layers is replaced by another layer, such as steel or fiberglass, which has a larger stiffness than the elastomer layer denoted by K_s

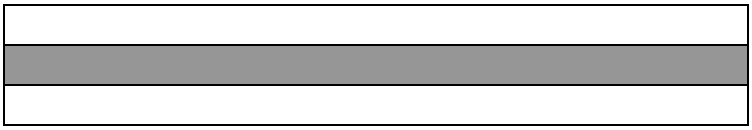

$K_s > K_e$

Figure 11. Representation of layered elastomeric bearing.

The total stiffness of the laminated elastomeric bearing K_P can be represented in the form:

$$\frac{1}{K_L} = \frac{1}{K_{e1}} + \frac{1}{K_s} + \frac{1}{K_{e2}} \Rightarrow K_L = \frac{K_{e1}.K_s.K_{e2}}{K_s K_{e2} + K_{e1}K_{e2} + K_{e1}K_s} \quad (6)$$

If these two equations are compared, it can be observed that in the second equation, the rate of increase in the numerator is higher than the rate of increase in the denominator. Therefore, the total stiffness of the laminated bearing K_L is higher than the total stiffness of the plain bearing K_T

On the other hand, when a plain elastomeric bearing is held under compression, the free exterior surfaces bulge and the cross section of the deformed shape takes the form in Figure 12.

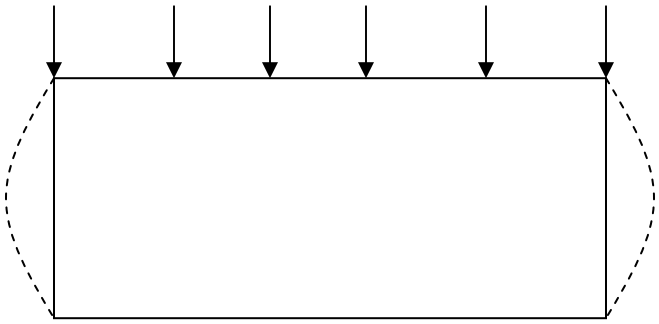

Figure 12. Representation of plain elastomeric bearing deformation.

In this case, it is assumed that the top and the bottom surfaces are rigidly supported, such that no movement is allowed on these surfaces.

The deformed shape of a laminated bearing is shown in Figure 13.

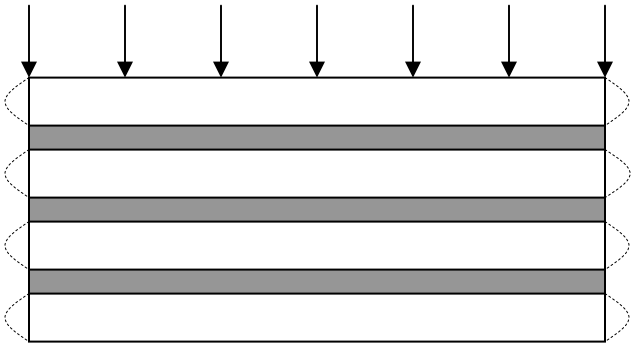

Figure 13. Representation of layered elastomeric bearing deformation.

Since the laminates are bonded to the elastomer layers above and below, they provide confinement. As the free elastomer layer surfaces tend to bulge under compression, the friction between the laminate and the elastomer interface causes tension within the laminates, which confines the elastomer layers.

Variation of Local Stiffness Within The Elastomer

Another important property that must be discussed is the stiffness distribution within the elastomeric material. Stiffness of a material depends on the confinement of the material as well as the properties of the material. Inside a layer of elastomer, the interior regions are more confined than the outer regions, which in return cause the stiffness to be higher at the interior regions. On the other hand, another factor that effects this spatial stiffness variance is the material property of the elastomer. Elastomers are incompressible materials such that the volume of the elastomer remains constant under any type of loading. Unlike other materials, such as metals, this fluid like behavior prevents the elastomer from deforming by changing its volume. The elastomer reacts to the loading by deforming and thereby dissipating the energy that has been induced. This dissipation of energy also relieves the stresses that have been induced. However, when the ability to deform is prevented by confinement, the stresses build up within the elastomer. Since elastomers are incompressible materials, by preventing the elastomer

when the ability to deform is prevented by confinement, the stresses build up within the elastomer. Since elastomers are incompressible materials, by preventing the elastomer from deforming, the only means of dissipating energy has also been prevented. Therefore, as the degree of the confinement increases, the local stiffness is also increased.

The models generated were loaded such that the loads were transmitted to the elastomer through a rigid plate that was rigidly attached to the bearing. The physical outcome of this procedure is that all the points along a bearing surface are forced to move the same amount. Since the interior regions within an elastomer are stiffer than the exterior regions, the stresses that are developed are also higher at interior locations.

Steel-laminated square bearing under compression

Figures 14, 15, and 16 show a bearing model, vertical deformations, and stress distribution in a typical layer in a steel reinforced square bearing. The plots in these figures indicate that 1) the radial rate of change of stiffness is not equal within a square bearing, and 2) local stiffness depends on the local degree of confinement, with the highest stiffness at the center and lower stiffness near the edges and the lowest stiffness at the corners. It is evidenced that there is a tendency towards circular distribution of the stress, however because of the geometry of the bearing, stress distribution near the edges become discontinuous.

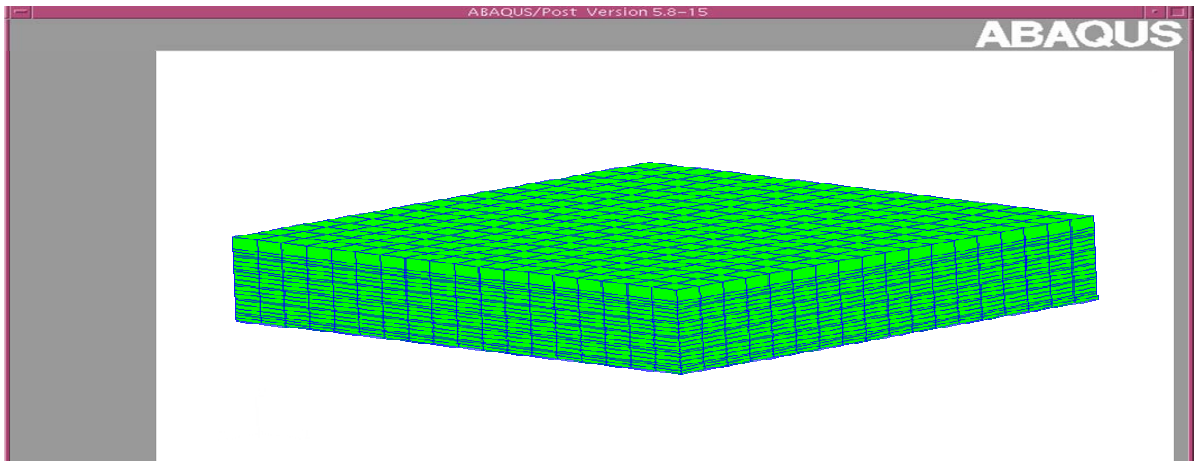

Figure 14. Finite element model of laminated square bearing.

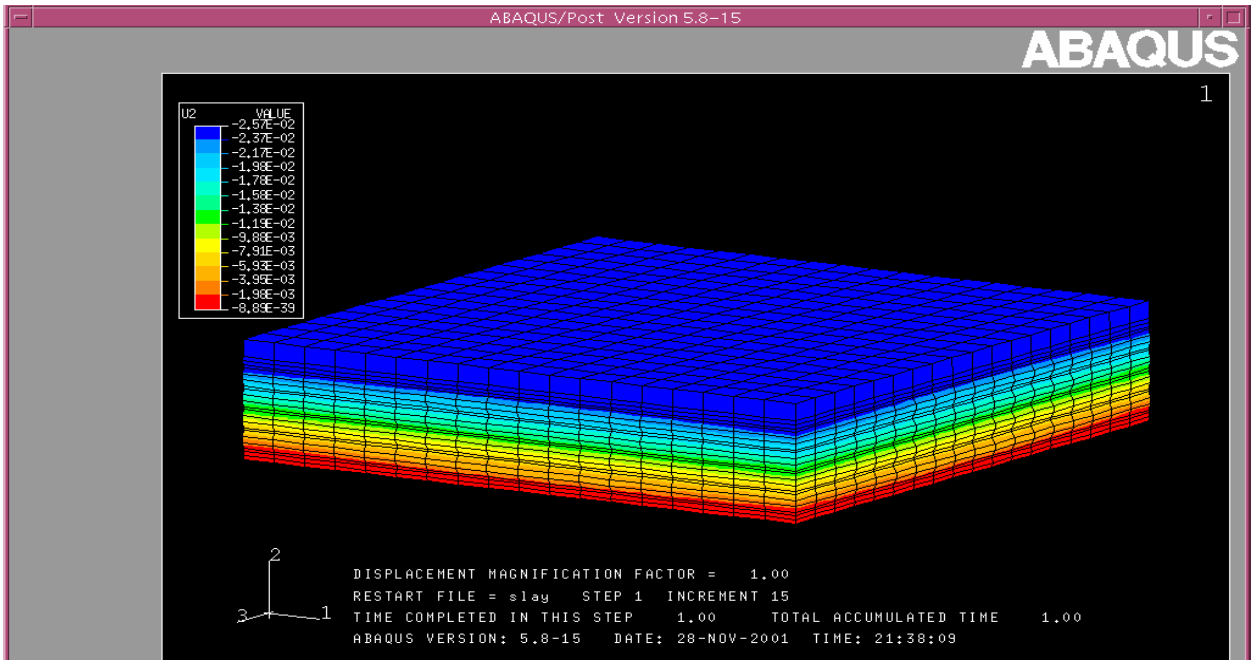

Figure 15. Displacements in a laminated square bearing.

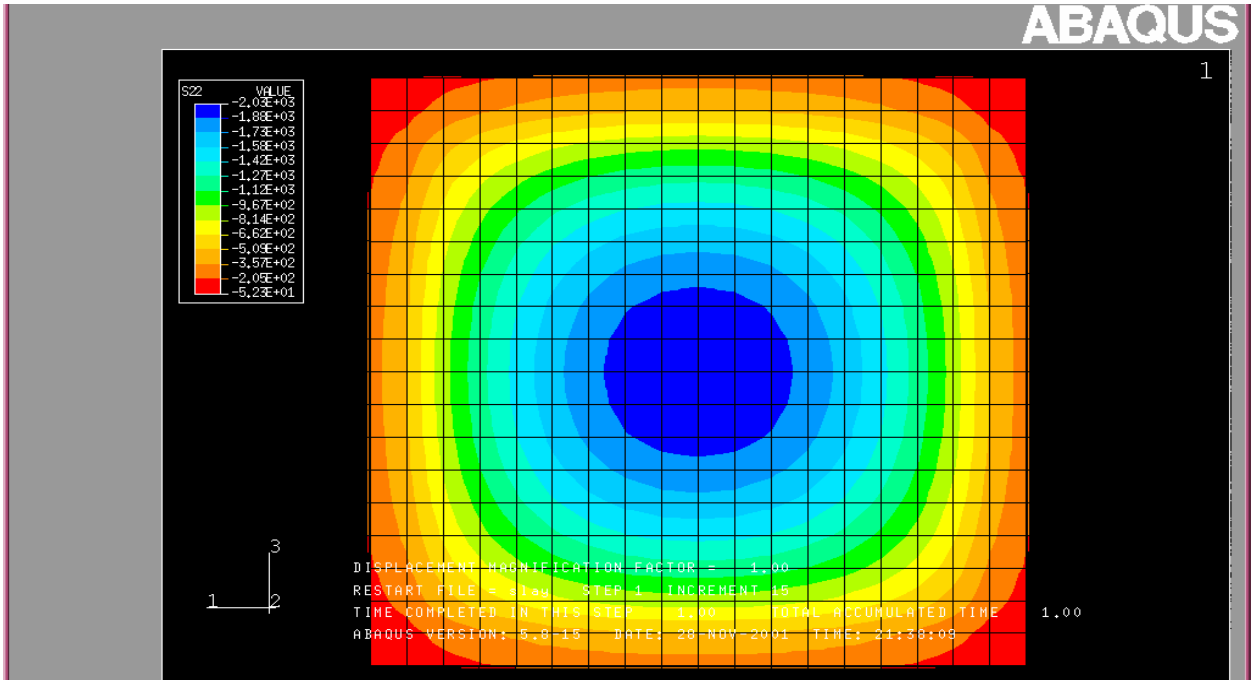

Figure 16. Compressive stress distribution within a typical elastomer layer.

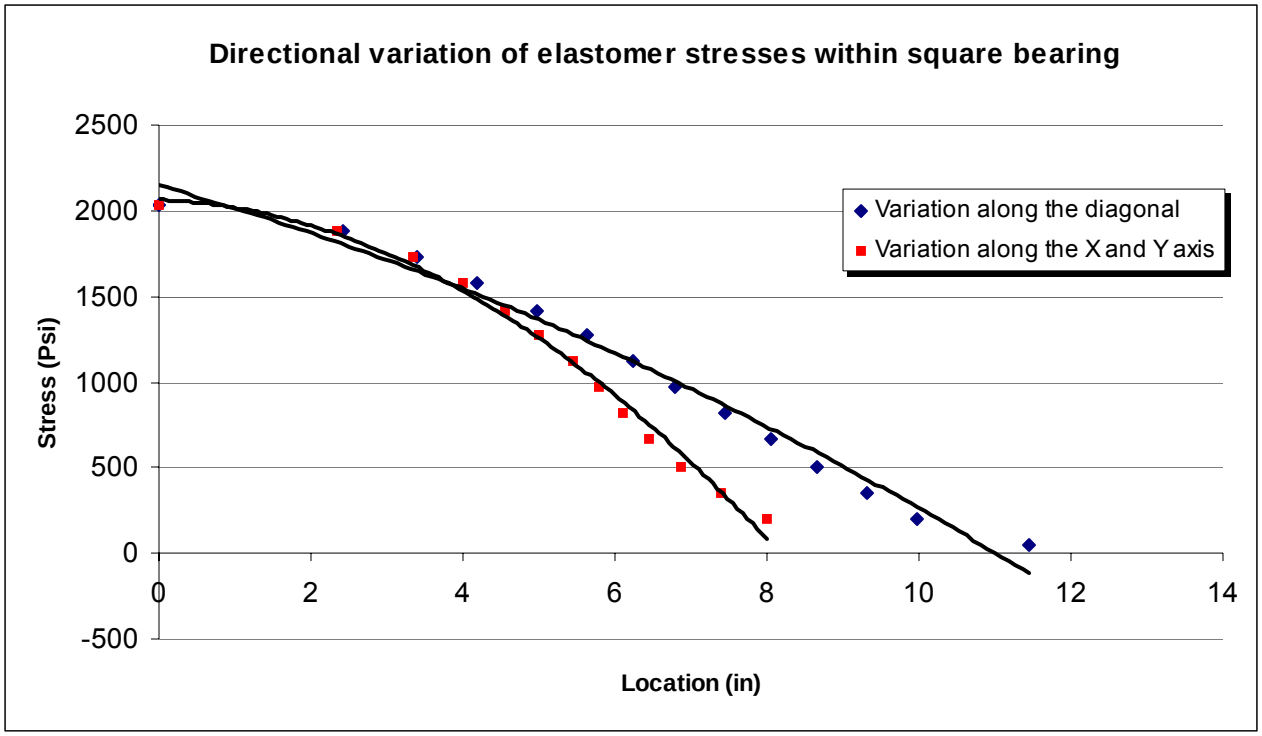

Figure 17. Directional variation of elastomer stresses within the square bearing.

Figure 17 illustrates the difference in stresses at a certain radial distance from the center of the bearing. This change in stress distribution is an indication of the radial rate of change of stiffness within the bearing. Since the material is not stressed the same amount, this change of radial stiffness may create delamination problems.

Laminate stresses in square bearing under compression

Under compression, tension stresses are induced within the laminates in order to prevent bulging. Figures 18 and 19 show tensile stress distribution within the steel laminates along the horizontal and vertical axis. From these figures, it is observed that since the bulging at the midpoints of the edges are the highest, the tensile stresses, which are directly related to displacements are also higher.

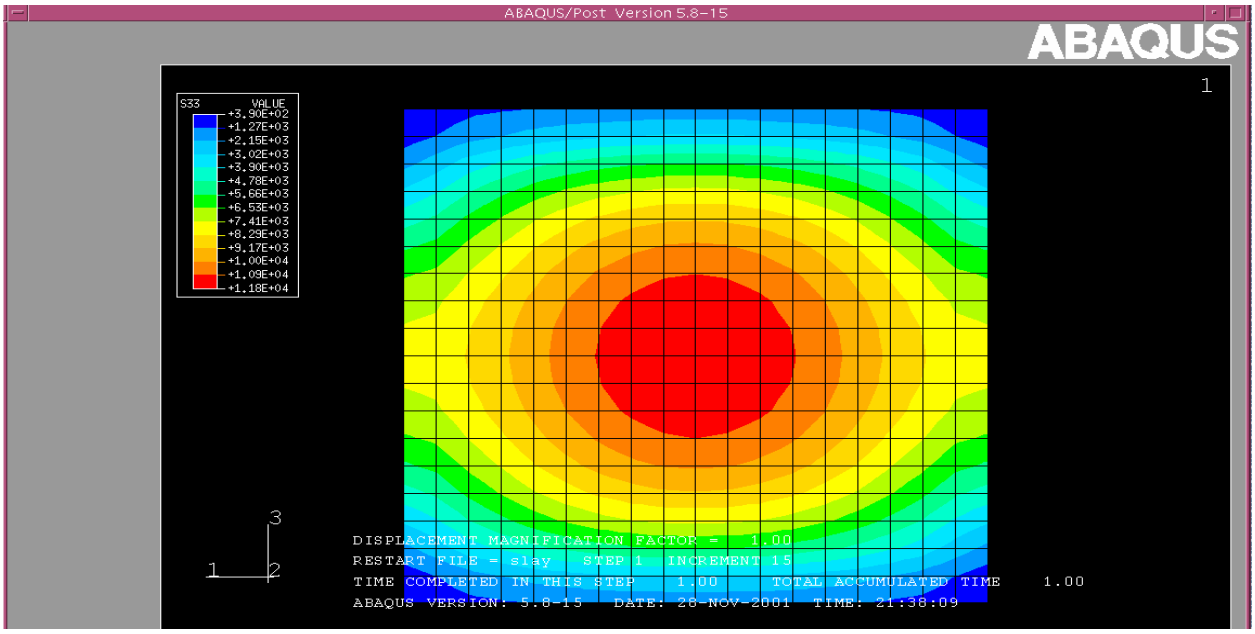

Figure 18. Tension along the horizontal axis in a typical steel laminate.

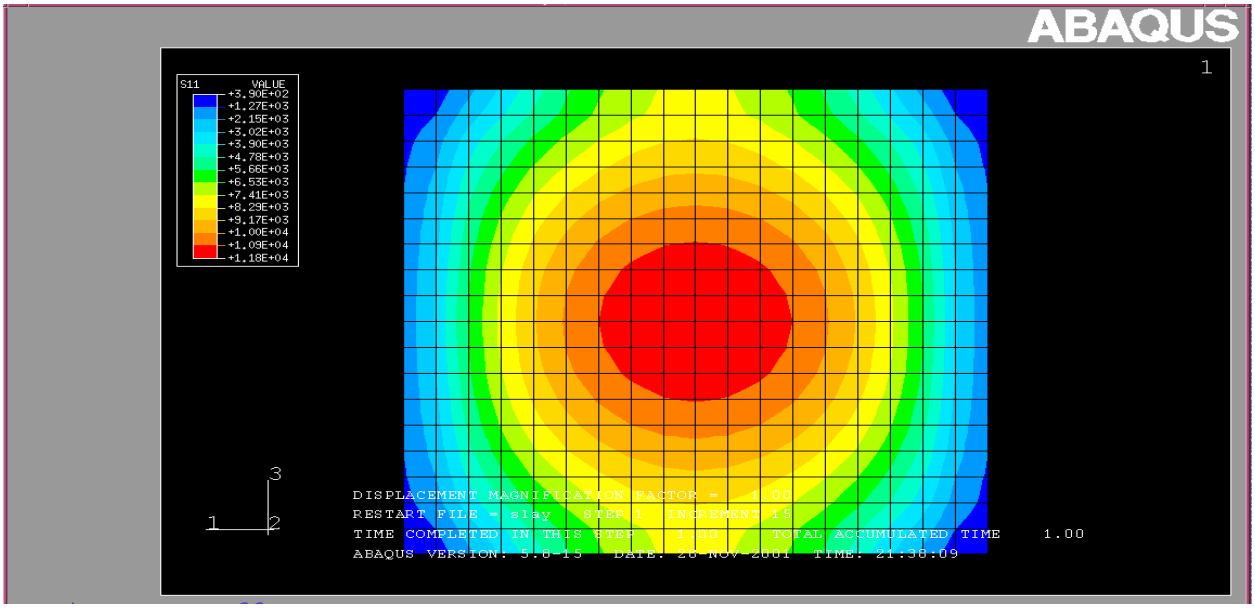

Figure 19. Tension along the vertical axis in a typical steel laminate.

Steel-laminated rectangular bearing under compression

The deformations and stress distribution in a rectangular bearing are shown in Figures 21 and 22 respectively. Compared to the displacement values for the square bearing shown in Figure 15, the deflections of rectangular bearings in Figure 21 are approximately 14% higher. The increase in the vertical deflection in a rectangular bearing is due to a lower shape factor than the square bearing which leads to a lower bearing stiffness. Shape factor is a measure of the ability of the bearing to deform. In layered elastomeric bearings, the ability to deform is proportional to the amount of free-to-bulge surface area, which is provided by the free surfaces of the intermediate elastomer layers. As this free-to-bulge surface area gets higher, the bearing becomes less stiff and more deformable. Note that the radial rate of change of stiffness is also not constant due to rectangular shape of the bearing (Figure 22). Figures 22 and 23 show the stresses and the directional stress profile within elastomer layer. Figure 23 shows that the rate of change of radial stiffness is not the same along 3 directions, which may create delamination problems.

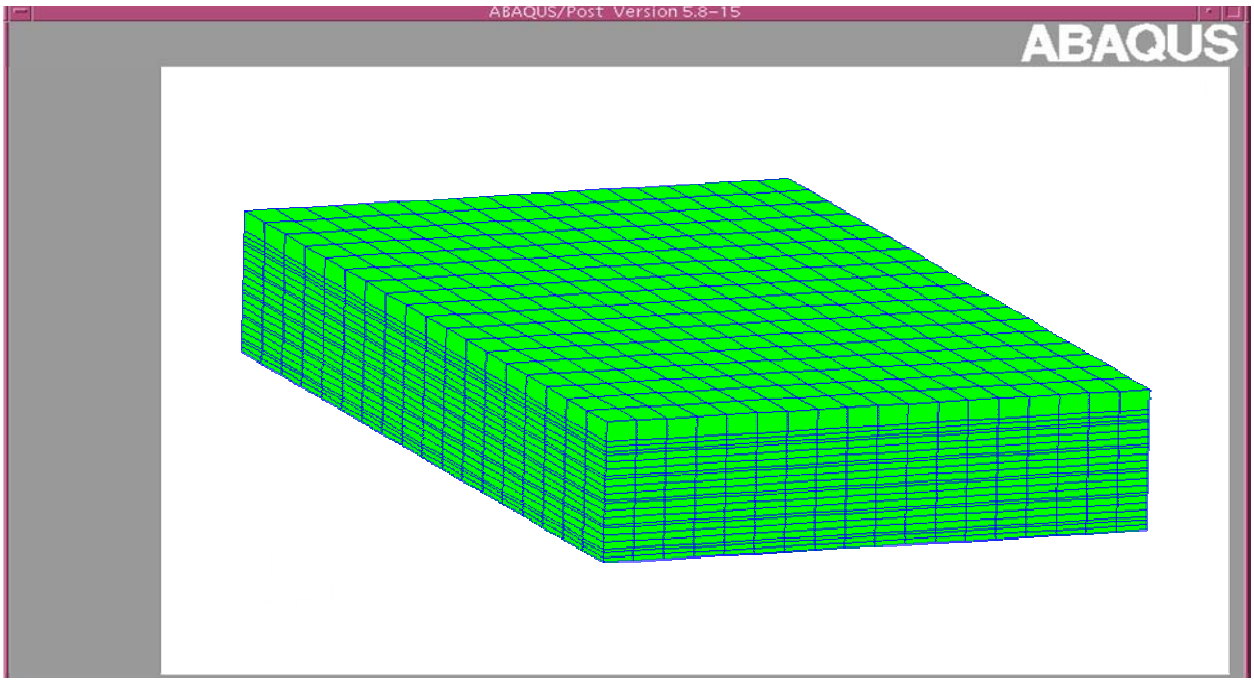

Figure 20. Finite element model of rectangular bearing.

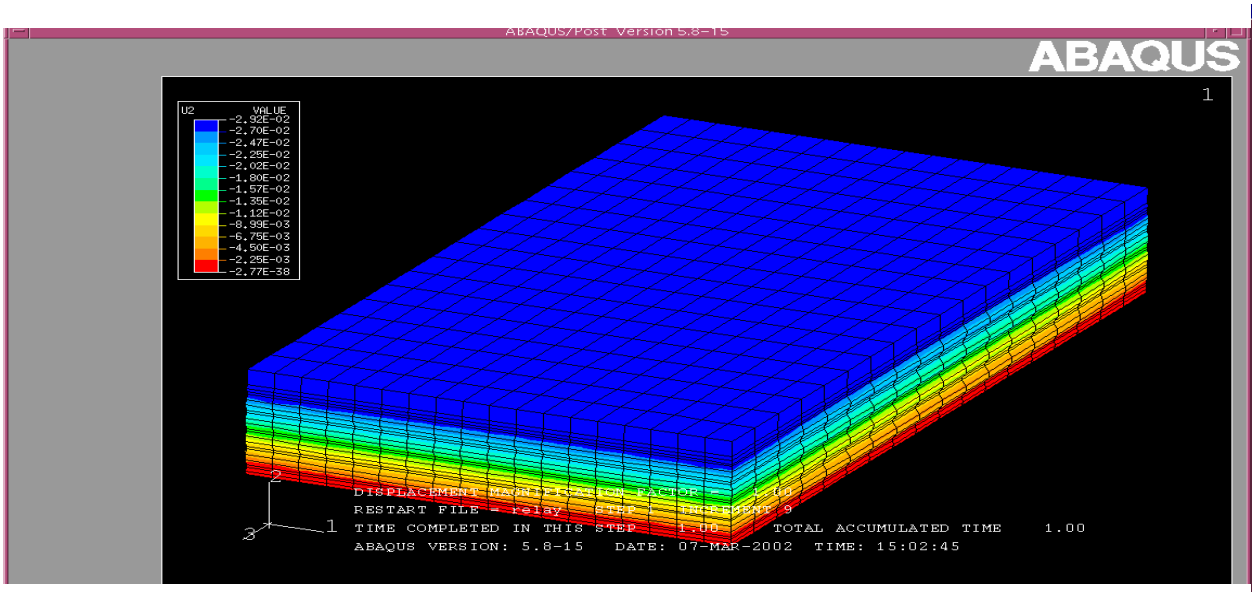

Figure 21. Displacement in a rectangular bearing.

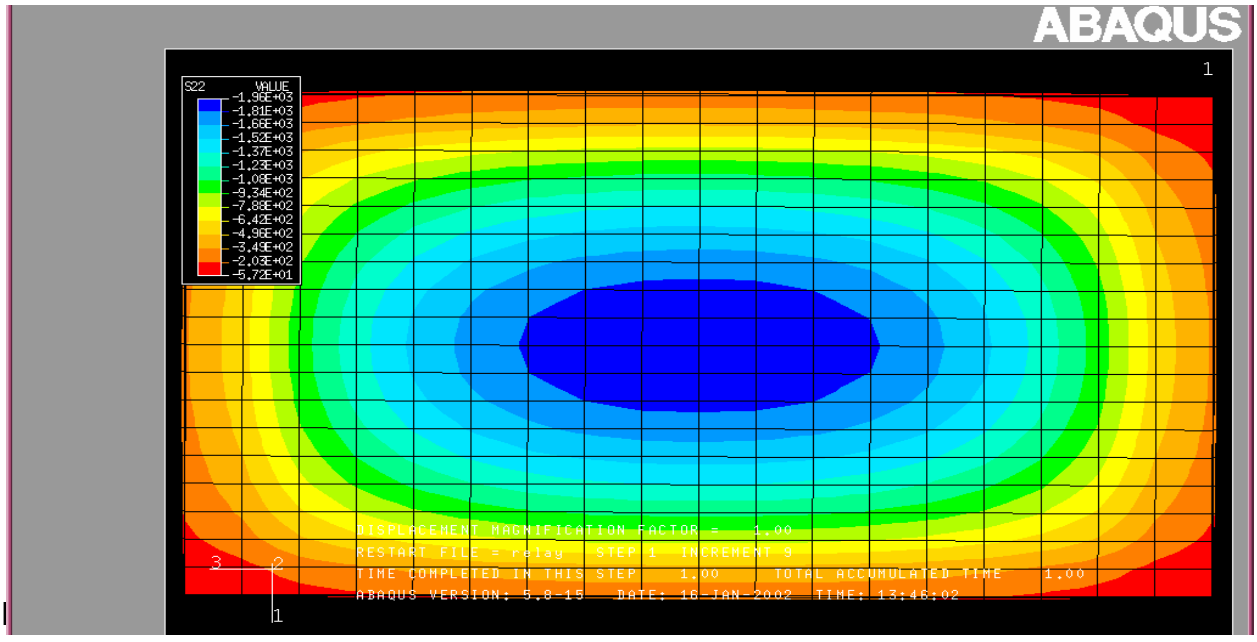

Figure 22. Compressive stress distribution in a typical elastomer layer.

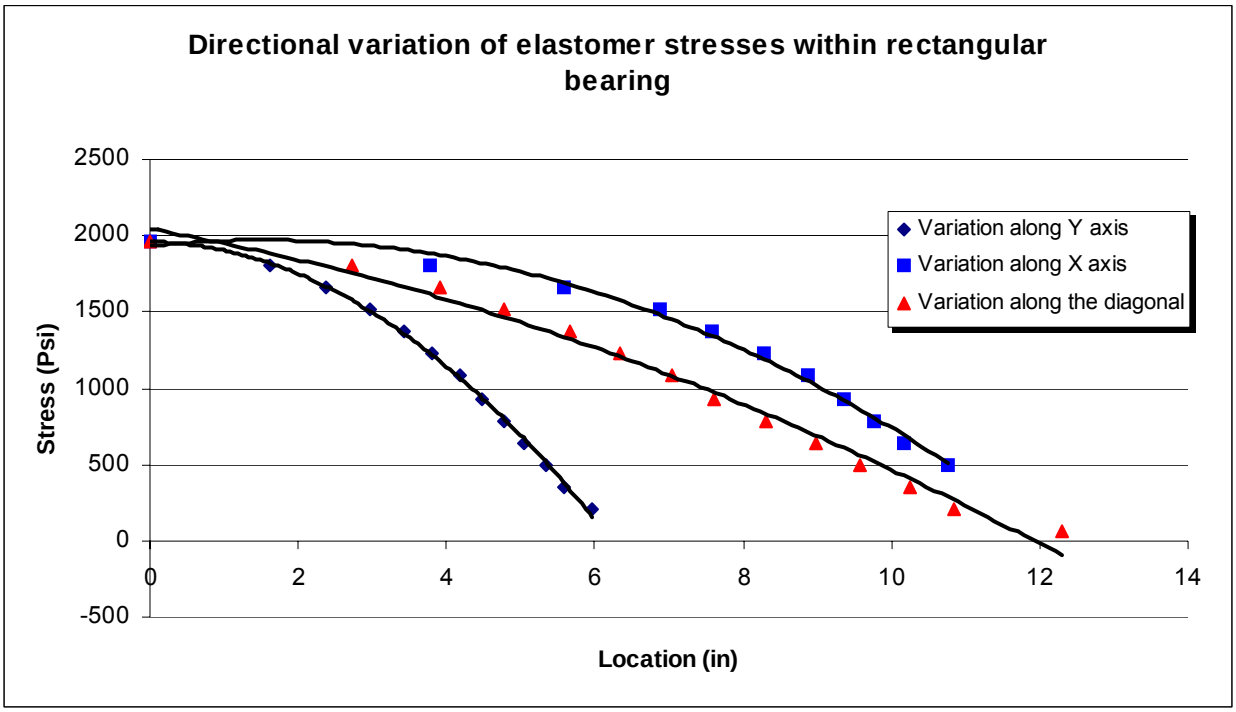

Figure 23. Directional variation of elastomer stresses within the rectangular bearing.

Laminate stresses in rectangular bearing under compression

Since the surface, which is free to bulge, is higher at the longer sides than the shorter sides, the amount of bulging is also higher at the longer sides. Since the amount of bulging is higher, the tensile stresses are also higher, as displayed in the stress contours of the steel laminates in Figures 24 and 25.

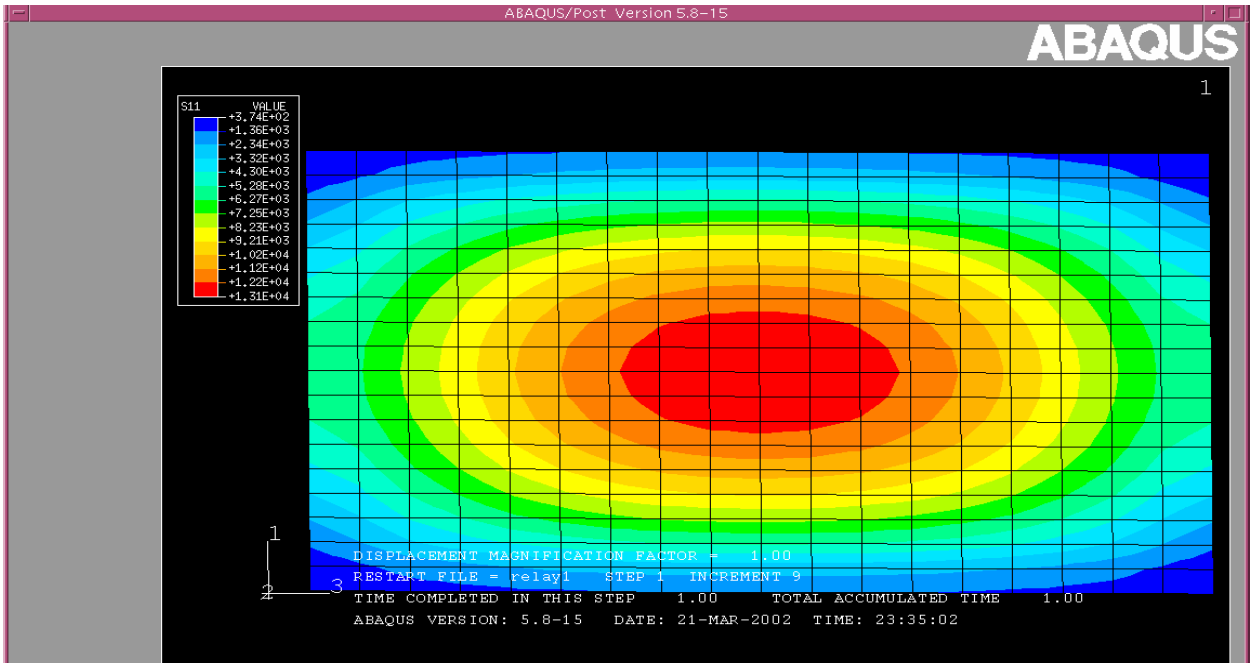

Figure 24. Tension along the horizontal axis in a typical steel laminate.

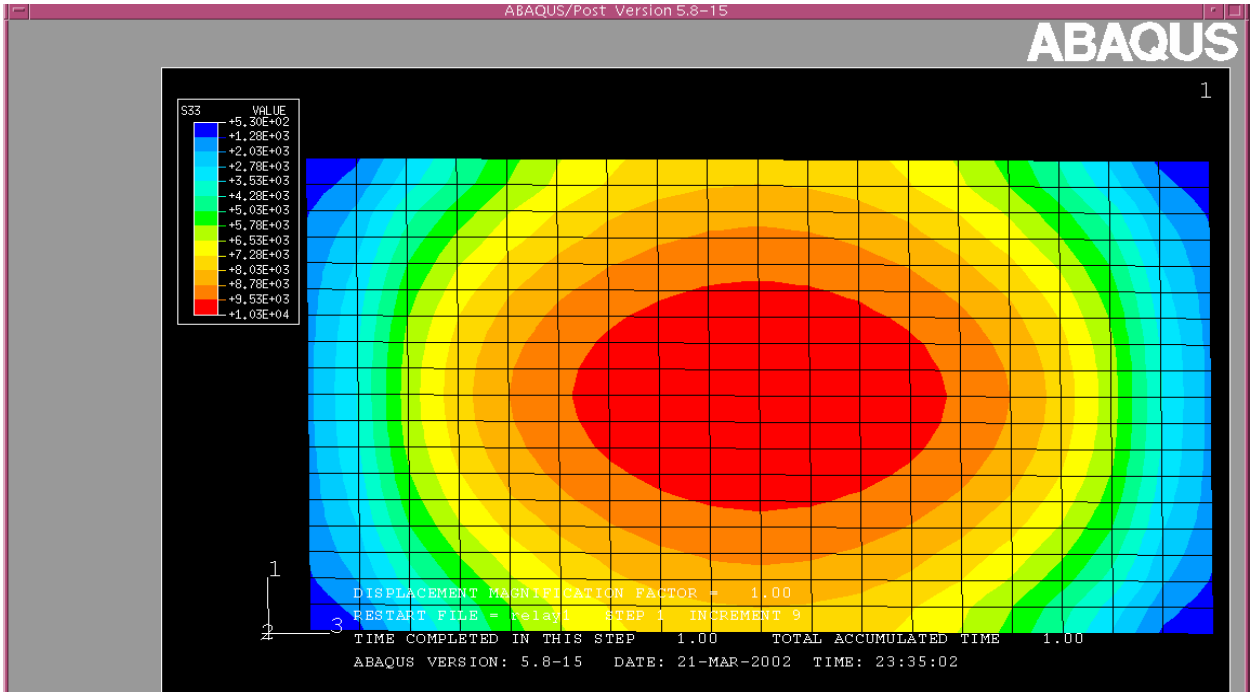

Figure 25. Tension along the vertical axis in a typical steel laminate.

Steel-laminated circular bearings under compression

The circular bearing model is shown in Figure 26. The displacement and the compressive stress distribution are shown in Figures 27 and 28 respectively. Note that the total vertical deflection in the circular bearing is approximately 10% lower (0.0233 in versus 0.0257 in) than the vertical deflection in square bearing (see Figure 15, Page 30). The decrease in the vertical deflection in a circular bearing is due to a higher shape factor than that in the square bearing.

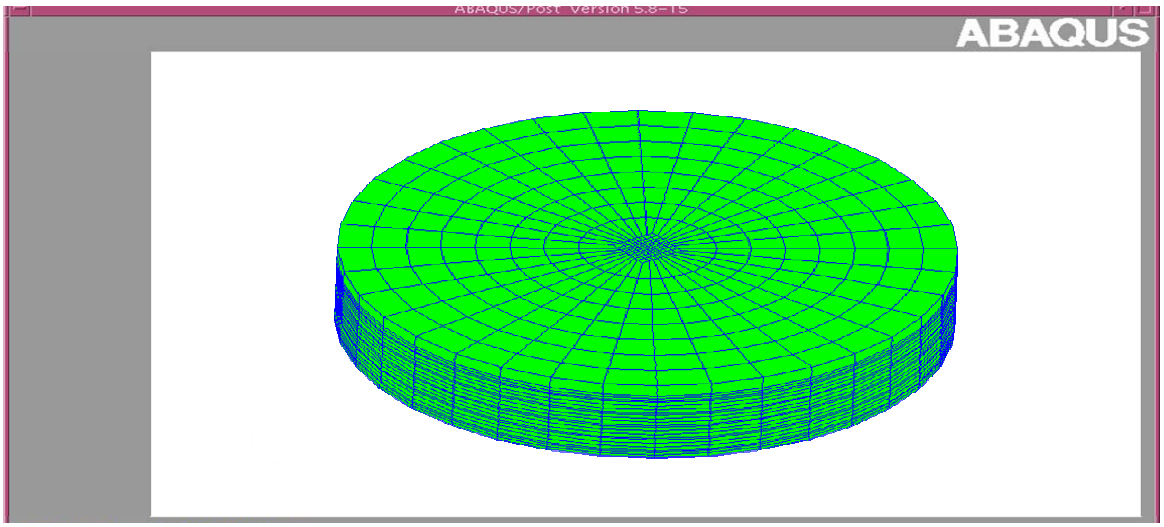

Figure 26. Finite element model of circular bearings.

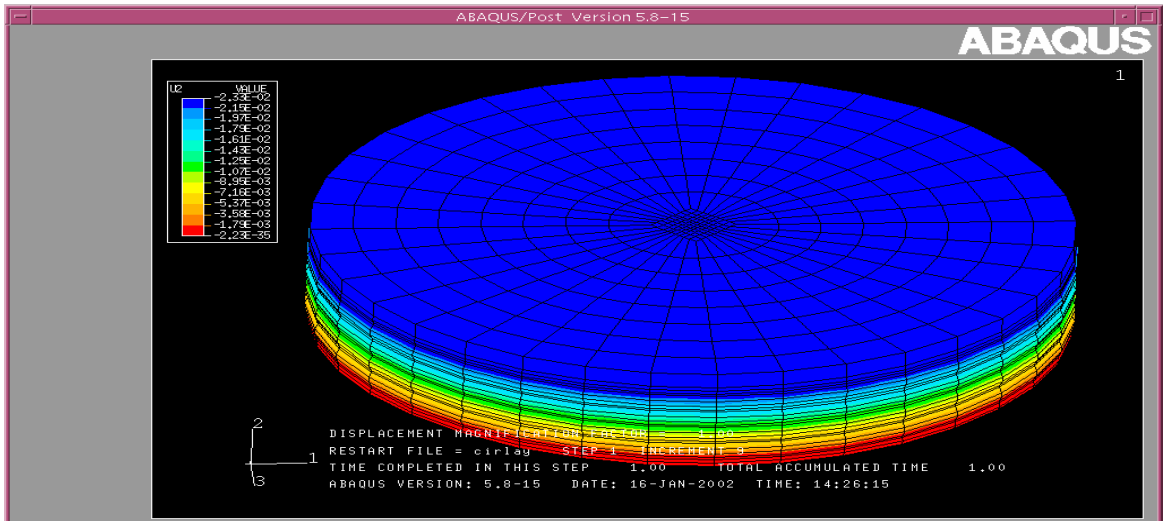

Figure 27. Displacement in circular laminated bearings.

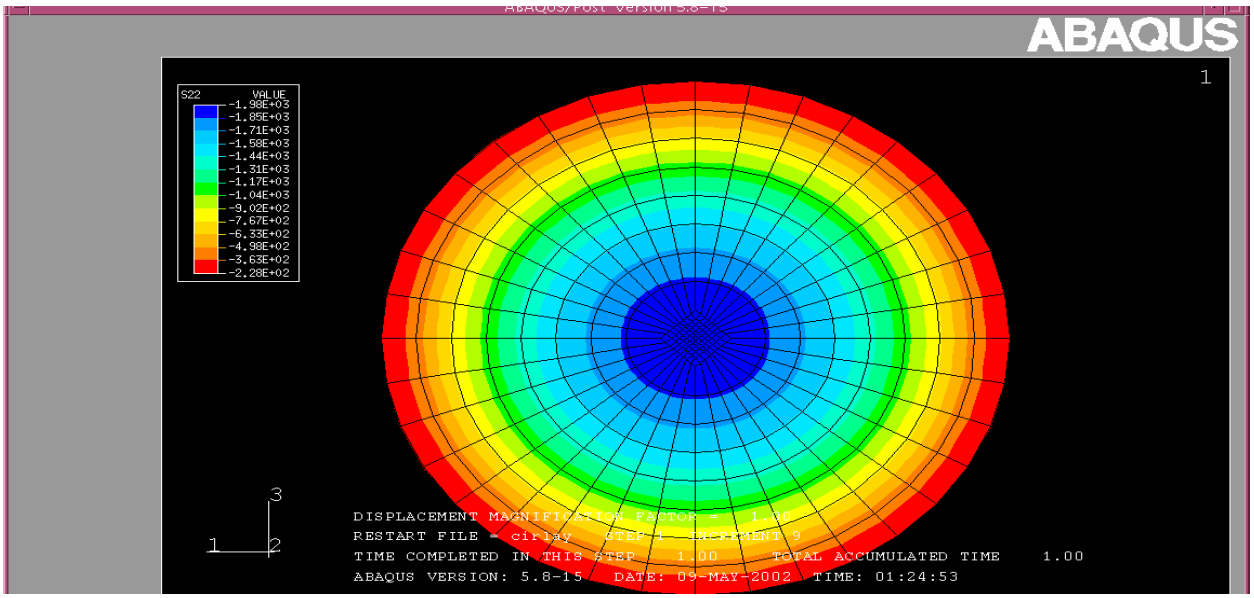

Figure 28. Compressive stress distribution in a typical elastomer layer.

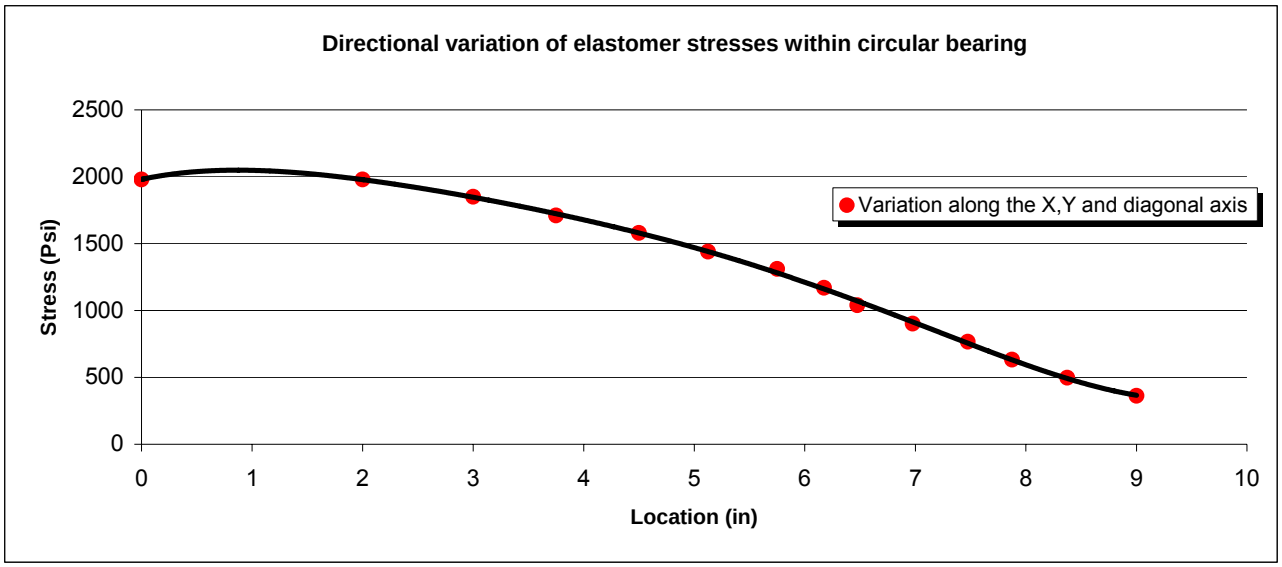

Figure 29. Directional variation of elastomer stresses within a circular bearing.

Figures 28 and 29 show the stress distribution in circular bearings. The stress contours in circular bearings under pure compression are uniform and the radial change of stress is nearly constant.

Laminate stresses in circular bearings under compression

Tensile stress distributions within laminates in circular bearings are shown in Figures 30 and 31. These figures show that there are no directional variances regarding the tensile stresses, meaning that the plate is tensioned equally in all directions. However, in square and rectangular bearings, the stress distribution is not equal. Also, note that the value of the tensile stresses is also lower than the stresses in the square and rectangular bearings. Since in circular bearings, there is less surface that is free to bulge (higher shape factor) than in either square or rectangular bearings, the amount of bulging is less, which in turn causes lower tensile stresses. In square bearings, the diagonal stress distribution is less than the stress distribution along primary axis, due to the fact that bulging occurs along the primary axis. In the rectangular bearing, the laminate is tensioned the highest amount along the vertical axis, due to the fact that bulging occurs the most along the longer sides of the bearing. Since the bulging along the shorter sides is relatively lower, the horizontal stresses are also lower. However, the laminate in the circular bearing is tensioned equally, meaning that due to its circular shape the laminate material is better made use of.

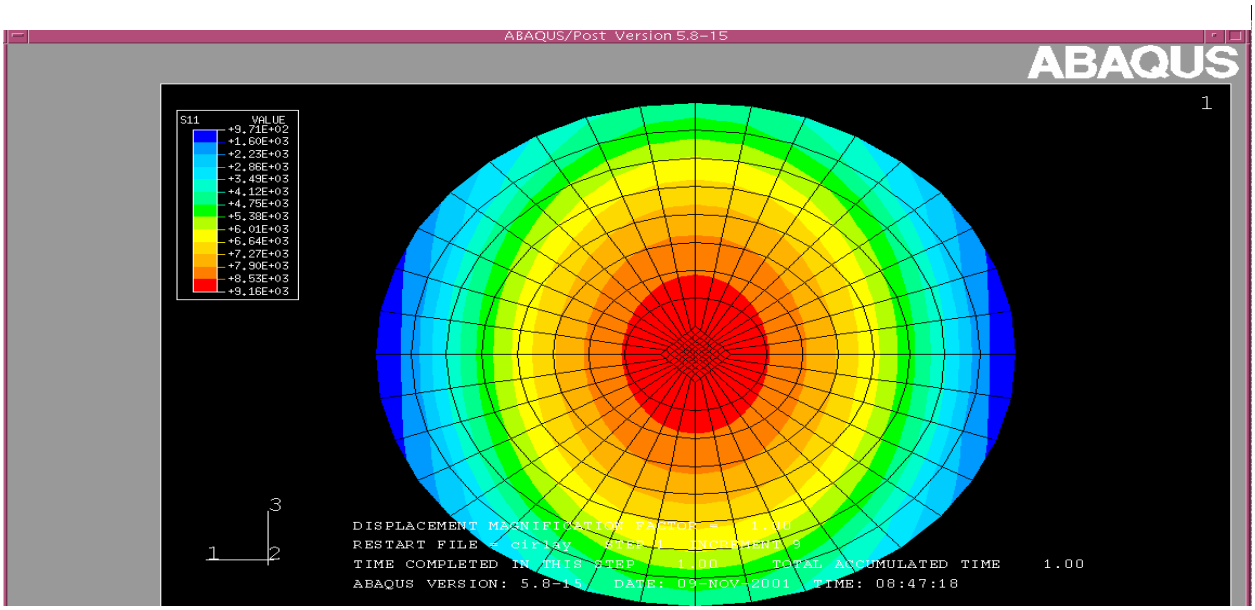

Figure 30. Tension along the vertical axis in a typical steel laminate.

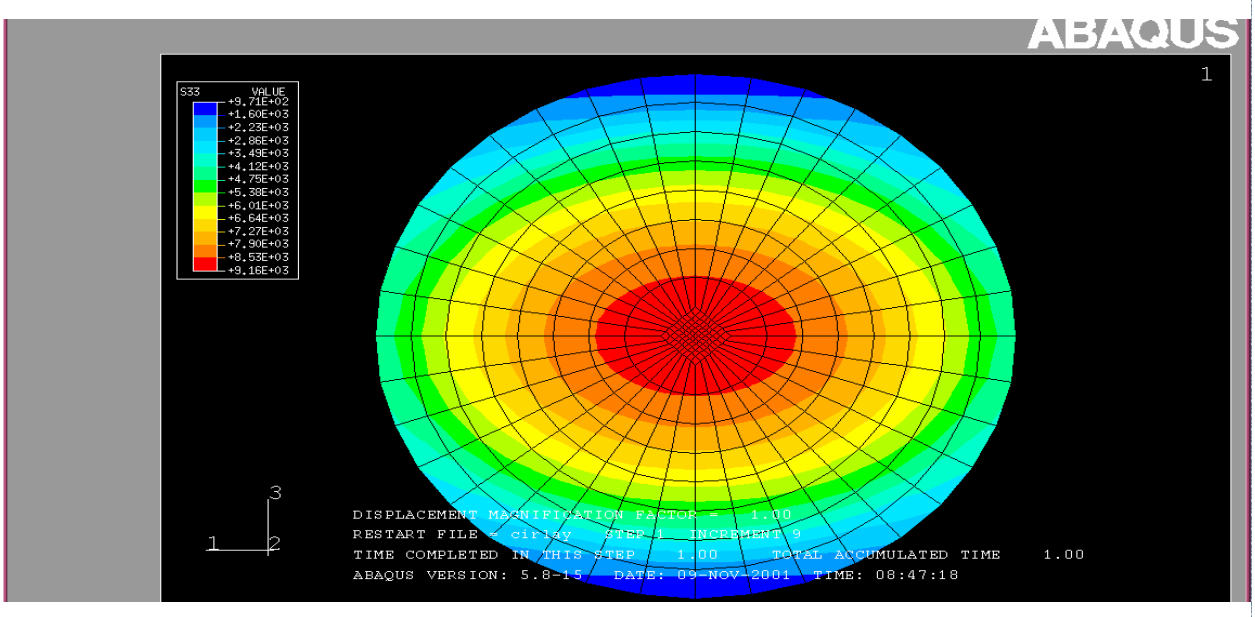

Figure 31. Tension along the horizontal axis in a typical steel laminate.

SUMMARY OF BEHAVIOR OF LAMINATED BEARINGS UNDER COMPRESSION (FEA)

The compressive stress distribution along bearing axes for circular, square, and rectangular elastomeric bearings is shown in Figure 32. In this figures, the location along the X axis of the bearing is normalized with respect to the total length (L). It is observed that the compressive stress values in the circular bearing are less than those of square and rectangular bearings between, approximately, the 0.25 and 0.65 ratios as shown in Figure 32. As mentioned earlier the stress distribution in circular bearings is more uniform due to bearing geometry and the absence of corners. The stress-stain relations for three types of bearings, circular, square, and rectangular are plotted in Figure 33. This figure shows that circular bearings have higher axial stiffness compared to square and rectangular bearings. Hence for the same axial load and same bearing area, circular bearings will have lower compressive strains compared to square and rectangular bearings.

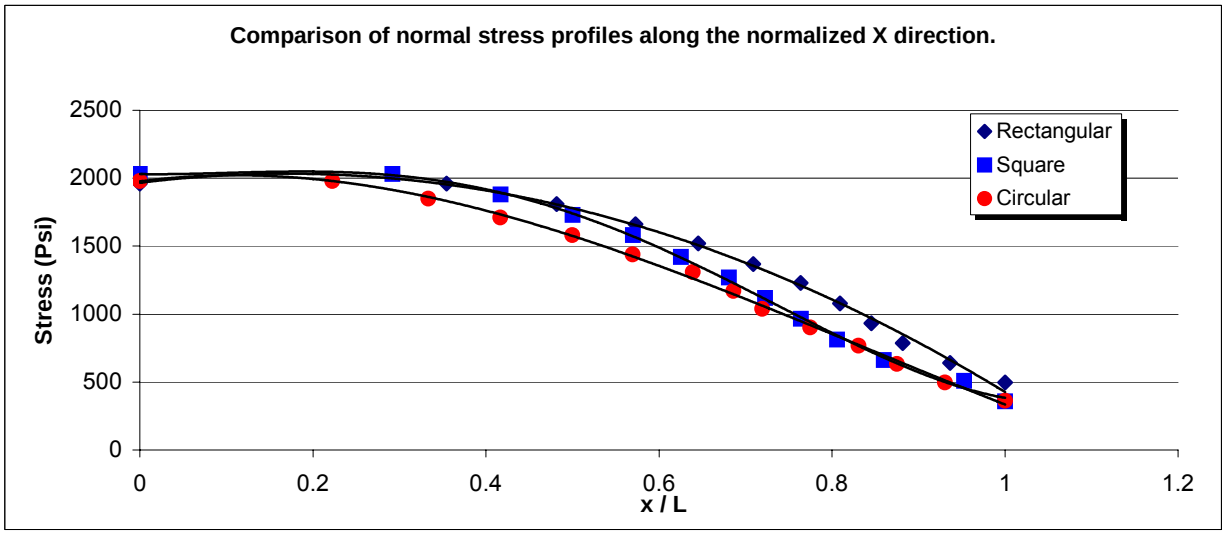

Figure 32. Comparison of normal stress profiles along the normalized X-direction.

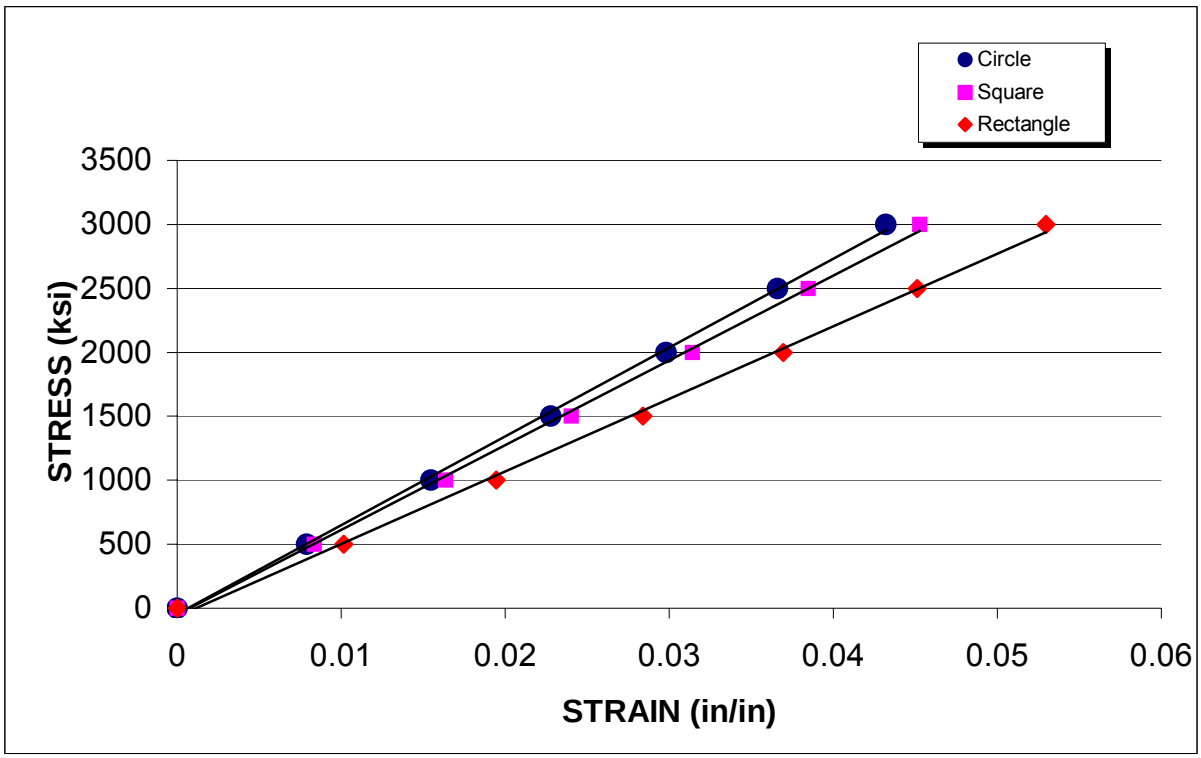

Figure 33. Stress-strain relations for circular, square, and rectangular bearings under compression

STEEL LAMINATED BEARINGS SUBJECTED TO COMPRESSION AND SHEAR (FEA)

In order to analyze the effect of the lateral loads on bearings, which are subjected to vertical loads, the bearings have been simultaneously subjected to a distributed load of 1000 psi and a lateral load that equals to 20 percent of the total vertical load.

The lateral loads were applied along the diagonal for the square and rectangular bearings in order to take into consideration the effect of skew and multi-directional movements. The displacements of laminated square, rectangular, and circular bearings under compression and shear are shown in Figures 34, 35, and 36 respectively. The displaced shapes show the restraining effect of the steel laminates on the elastomer layers. The lateral displacements for all three bearings were the same along the diagonal as shown in Table 5. Table 5 summarizes the applied compressive loads and shear loads and the resulting displacements.

Table 5. Combined data for compression and shear.

	Square	Rectangular	Circular
Distributed load (psi)	1000	1000	1000
Surface area (in^2)	256	258	254.5
Total vertical load (lb)	256000	258000	254500
Lateral load (20% of vertical) (lb)	51200	51600	50900
Maximum deflection (x-axis) (in)	1.86	1.29	1.86
Maximum deflection (y-axis) (in)	1.86	2.3	1.86
Total deflection along the diagonal (in)	2.63	2.64	2.63

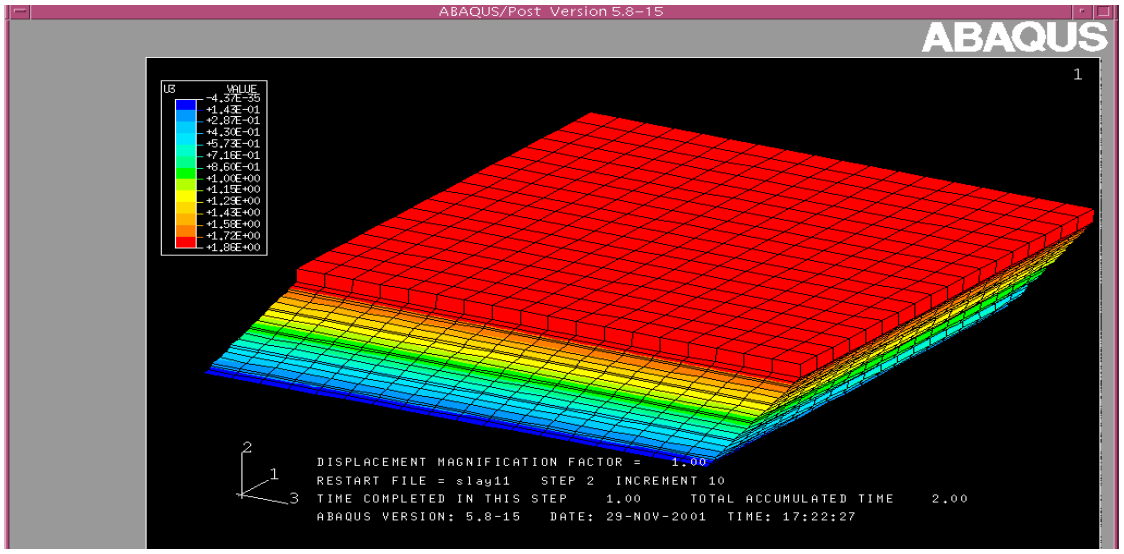

Figure 34. Displacements of square bearing under compression and shear.

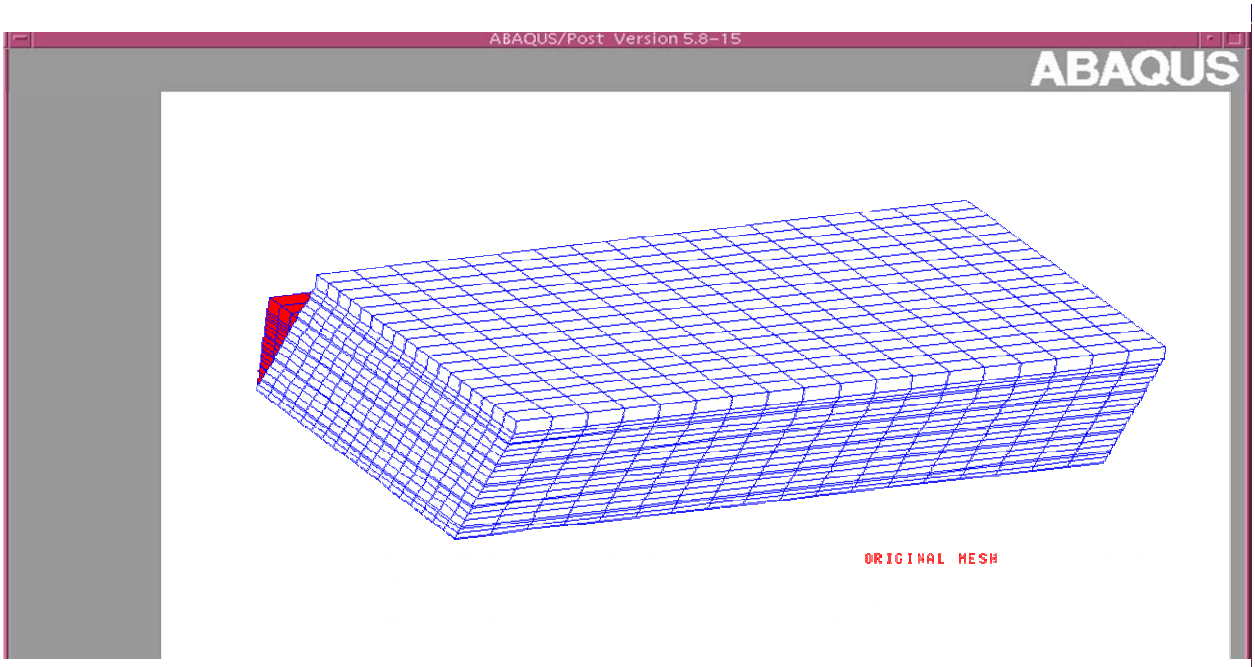

Figure 35. Displacements of rectangular bearing under compression and shear.

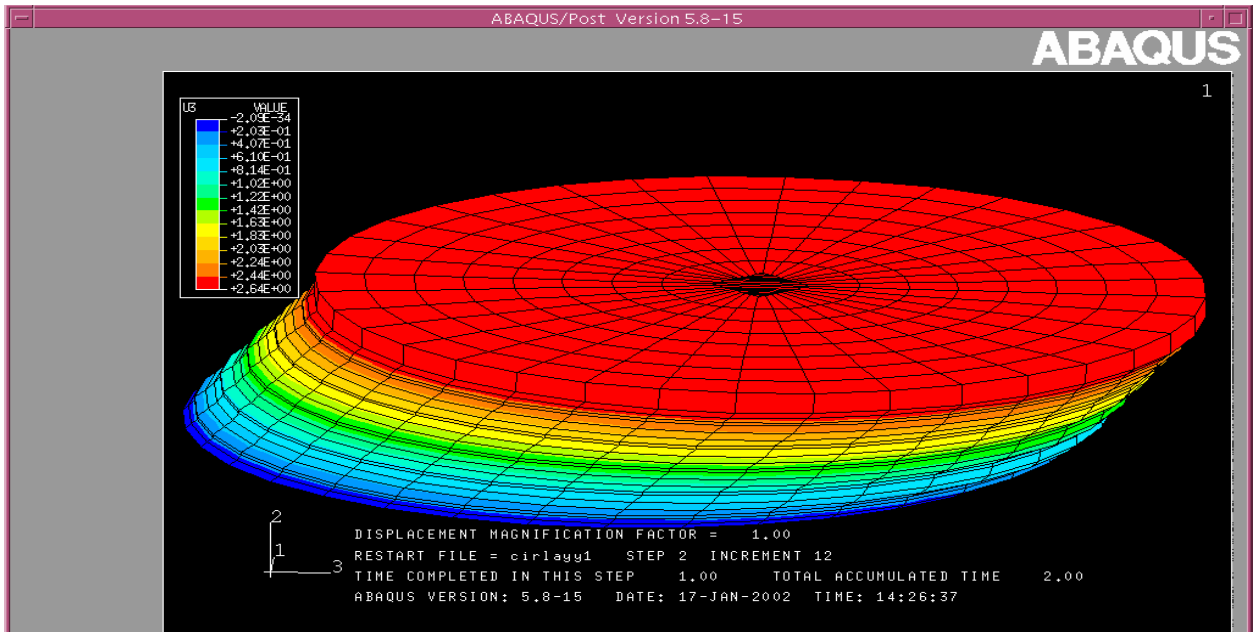

Figure 36. Displacements of circular bearing under compression and shear.

Figures 37 to 39 show the compressive stress distribution for square, rectangular and circular bearings in a typical elastomer. Along the lower and right vertical edges of the square and rectangle bearings the stresses are not continuous and vary along the length. In the long run the material properties change with loadings, and this change will be different locally due to the variation of stresses along an edge. It is important to note that the radial variation of the stress away from the center of the bearing is dependent on the amount of friction between the interface of the bearing and the top platen. However, the variation of the stress along a certain cross section, such as along the edges of the bearing, is a result of the geometry of the bearing.

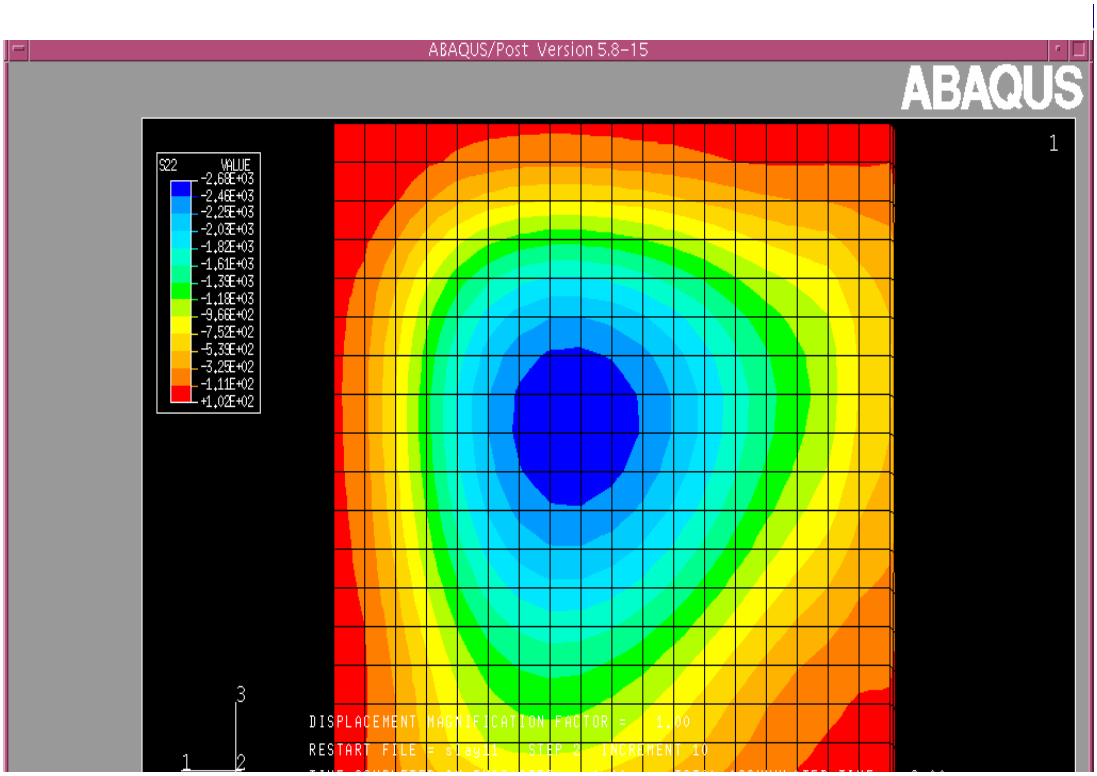

Figure 37. Compressive stress distribution in a square bearing under compression and shear in a typical elastomer layer.

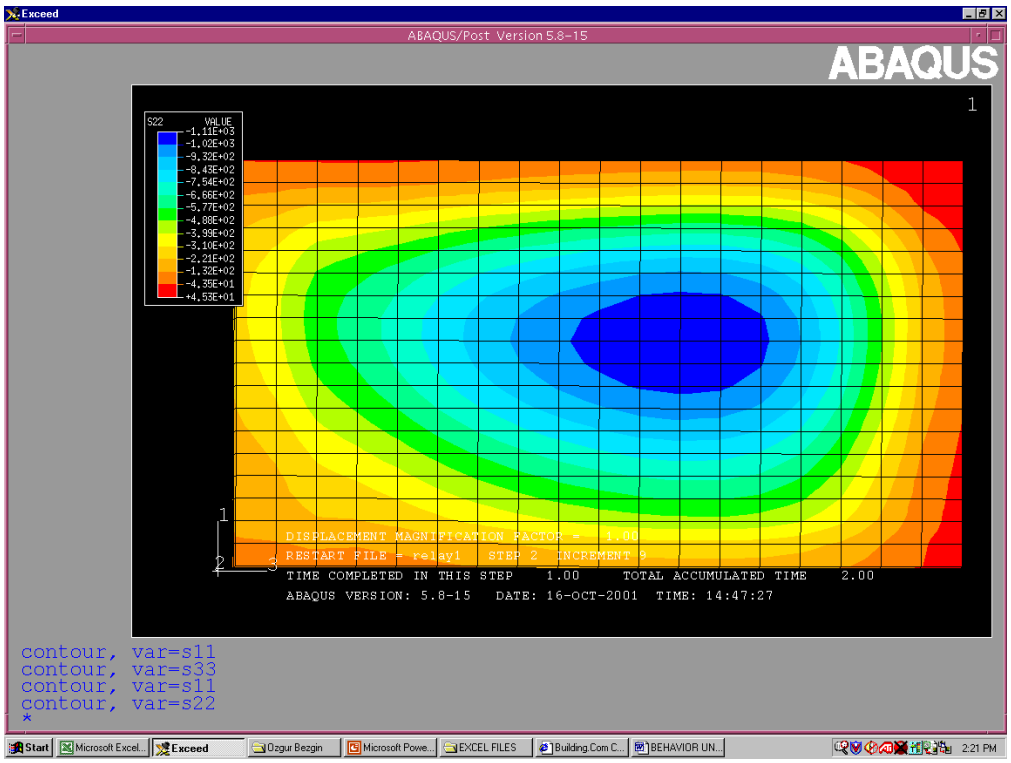

Figure 38. Compressive stress distribution in a rectangular bearing under compression and shear in a typical elastomer layer.

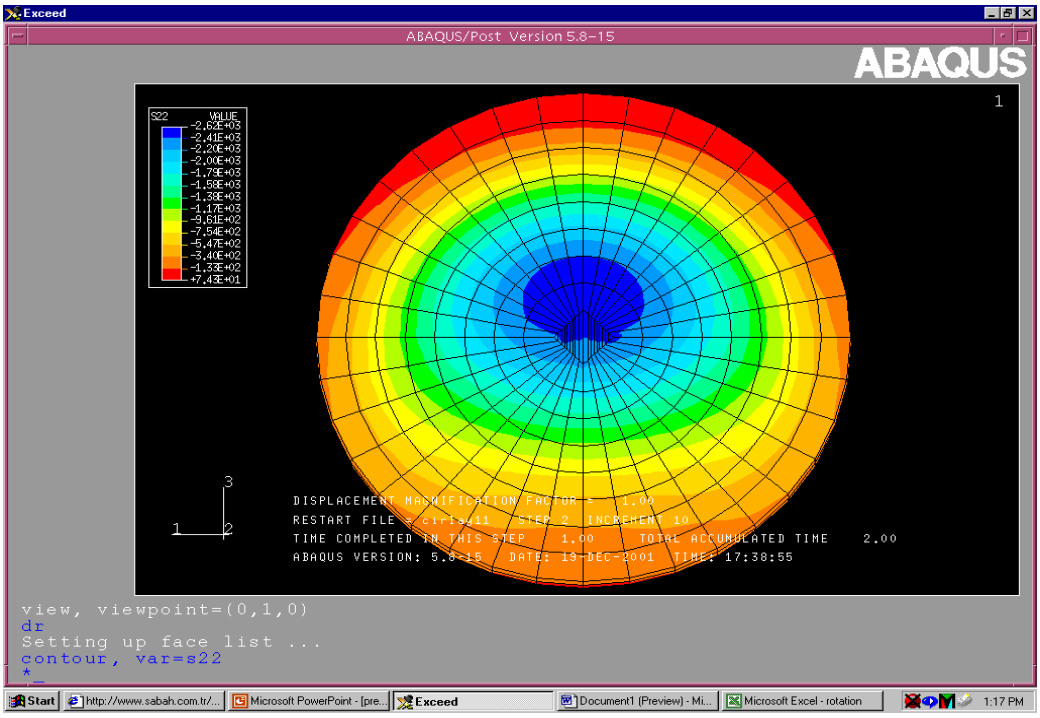

Figure 39. Compressive stress distribution in a circular bearing under compression and shear in a typical elastomer layer.

Figure 39 shows that the stress contours are tangent to the edges, and the geometry of the circular bearing allows the radial dispersion of the stresses along the bearing, thus keeping the local stresses at a certain radial distance the same. There are no discontinuities of the stresses along a certain radial distance away from the center.

STEEL LAMINATED BEARINGS SUBJECTED TO COMPRESSION AND ROTATION (FEA)

Square Bearings

Circular and square bearings were compared under compression and rotation. In order to achieve rotation, variable distributed loads along the surface were applied in order to create an eccentricity of the resultant load with the center of gravity of the bearing. Varying distributed loads, in the shape of a trapezoid, were applied to the square bearing. Five different loading values have been applied. The average height of the profile has been set to be 2000 psi in order to generate measurable rotations. The data used in generating these loads are summarized in Table 6. This table shows location, eccentricity, and moments. Figure 40 shows a schematic representation of the pressure profile on the bearing and the parameters that are used to obtain the applied moment and the total force.

By consecutive application of these loads, the rotation has been calculated from the measured deflections at the ends of the bearing as shown in Table 7.

Table 6. Generation of pressure profile on the square bearing.

c (x=0 in) (psi)	a (x=16 in) (psi)	Slope	Edge Distance (E) (in)	Datum (in)	Eccentricity (e) (in)	Resultant (R) (kips)	Moment (in-kips)
2000	1500	31.25	48	64	0.3814	448	170.88
2250	1250	62.5	20	36	0.7629	448	341.76
2500	1000	93.75	10.67	26.67	1.1443	448	512.64
2750	750	125	6	22	1.5257	448	683.52
3000	500	156.25	3.2	19.2	1.9071	448	854.40

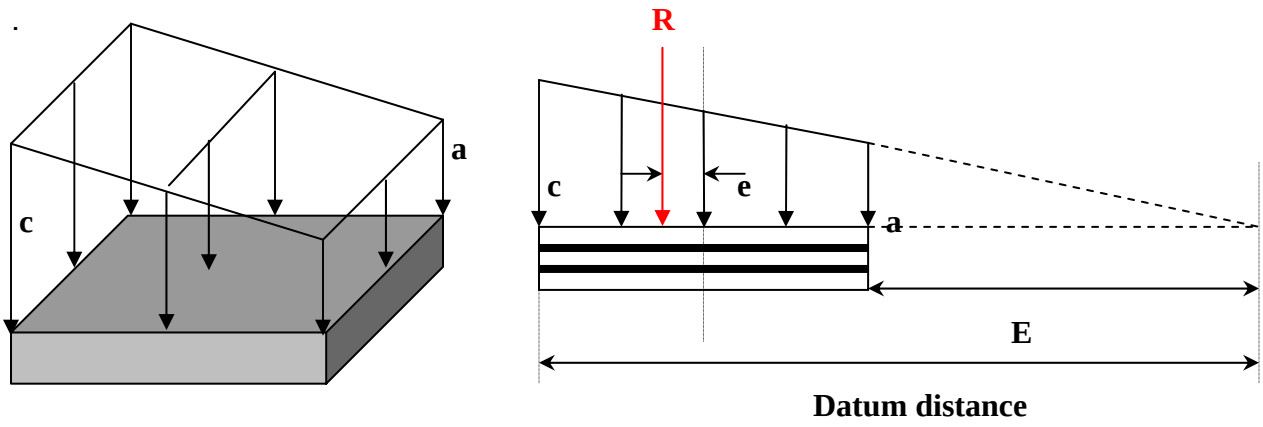

Figure 40. Pressure profile on the square bearing.

Table 7. Deflection data for the square bearing under rotation.

M (in-kip)=	170.88		M (in-kip)=	341.76	
location (in)	deflection (in)	strain	location (in)	deflection (in)	strain
0	-0.0602	-0.020	0	-0.0763	-0.025
15.9999	-0.0232	-0.008	15.95	-0.0117	-0.004
tan (Φ) =	0.0023		tan (Φ) =	0.0040	
(Φ) (rad)=	0.0023		(Φ) (rad)=	0.0040	
(Φ) (deg)=	0.1325		(Φ) (deg)=	0.2313	
M (in-kip)=	512.64		M (in-kip)=	683.52	
location (in)	deflection (in)	strain	location (in)	deflection (in)	strain
0.00	-0.09220	-0.031	0	-0.1080	-0.036
14.77	0.00121	0.0004	16.003	0.0264	0.009
tan (Φ) =	0.0063		tan (Φ) =	0.0084	
(Φ) (rad)=	0.0063		(Φ) (rad)=	0.0084	
(Φ) (deg)=	0.3634		(Φ) (deg)=	0.4813	
M (in-kip)=	854.4				
location (in)	deflection (in)	strain			
0	-0.124	-0.041			
16.003	0.0404	0.013			
tan (Φ) =	0.0103				
(Φ) (rad)=	0.0103				
(Φ)(deg)=	0.5887				

Figure 41 show the compressive stress distribution for a square bearing under compression and rotation in a typical elastomer. Note that the maximum stress region has shifted from the center of the bearing due to the applied moments. Under pure compression the maximum stress region is in the center of the bearing.

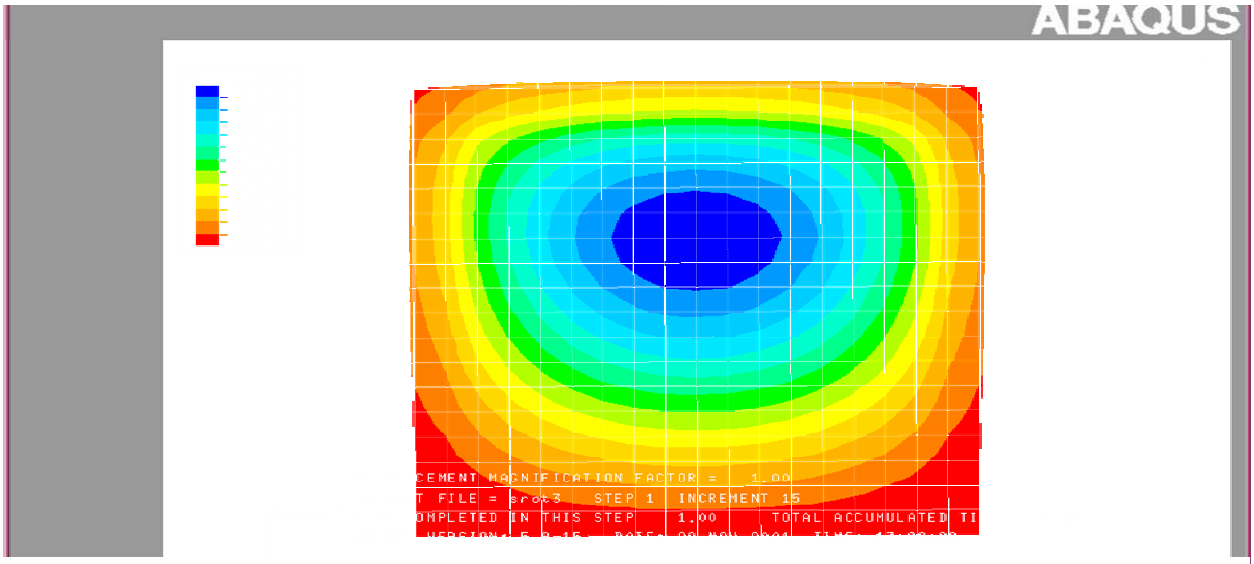

Figure 41. Compressive stress distribution in a square bearing under applied compression and rotation in a typical elastomer layer.

Circular Bearings

In order to compare the behaviors of circular and square bearings under rotation, the same total load and the moment must be applied on the circular bearing. However, this is not as straightforward as it was in the case of square bearing. In the case of the square bearing, the cross section of the loading profile was a trapezoid and did not vary along the surface, however in the case of the circular bearing, the cross section of the loading profile changes along the surface, therefore an equation must be generated in order to keep the loadings and the location of the resultant equal to those in the case of the square bearing. In order to achieve this, an analogy was established between the rotation inducing loading on the bearing, and the pressure profile on a circular plate submerged in a fluid.

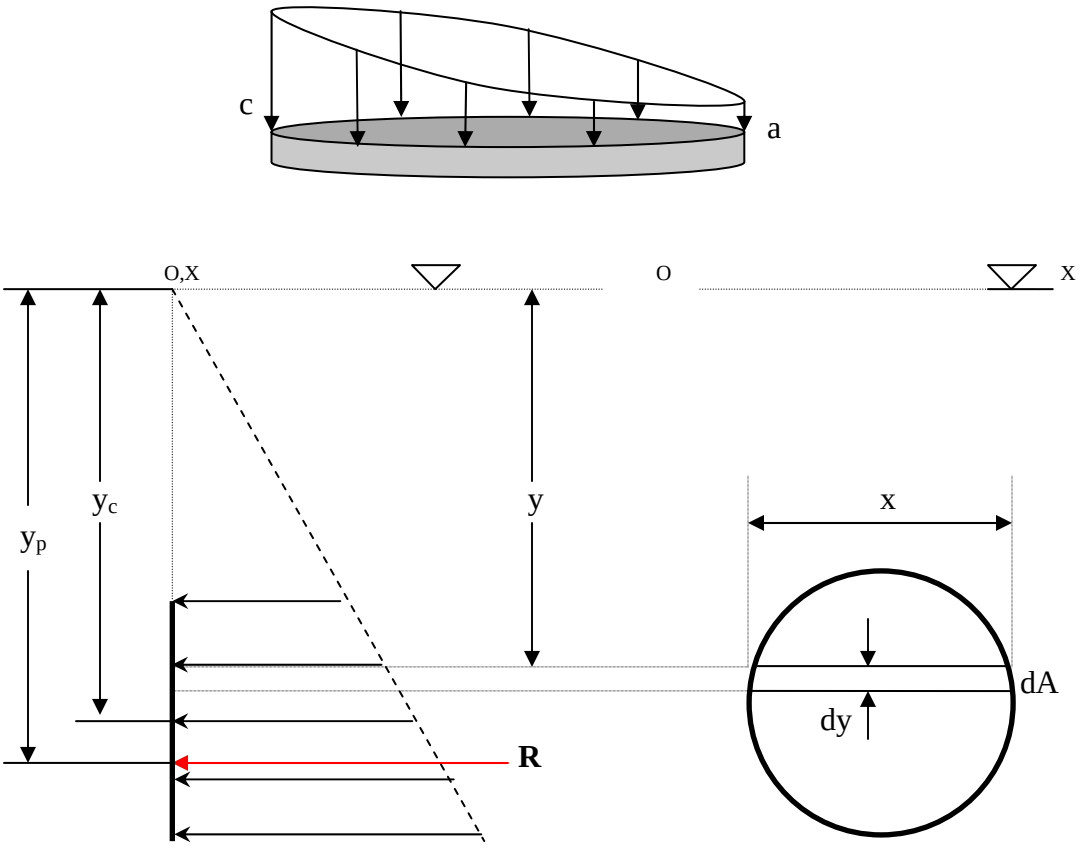

Figure 42. Pressure profile on the circular bearing.

Consider a strip of element dA in Figure 42, where there is a uniform pressure distribution. The infinitesimal element dA=x.dy .

The pressure at depth y is : P = ρ.h where ρ = unit weight of the fluid.

Therefore, the force dF on the horizontal strip is: dF=P.dA = ρ.y.dA and the force on the whole surface is $\int dF=\int \rho.y.dA$

$$\Rightarrow \quad F=\rho.y_c.A \qquad (7)$$

where y_c is the distance from O,X to the centroid C of the circular area, and y_c.A is the static moment of the area about the O,X axis.

The point of application of the resultant pressure force on a submerged area is called the “center of pressure”.

If we take the moment of this elementary force dF around the O,X axis: $y.dF=\rho.y^2.dA$ and integrate it: $\int y.dF = \int\rho.y^2.dA \Rightarrow y_p.F= \rho\int y^2.dA$ where y_p is the location of the center of pressure with respect to O,X axis and F is the total force acting on the circular submerged area. The quantity within the integration is the moment of inertia of the circular surface about the O,X axis, therefore this equation can be summarized as :

$$y_p.F= \rho.I_{O,X} \qquad (8)$$

If equations 7 and 8 are combined, we obtain: $y_p .(\rho.y_c.A) = \rho.I_{O,X} \Rightarrow y_p = \frac{I_{O,X}}{y_c.A}$

Noting that from the parallel axis theorem: $I_{O,X} = A.y_c^2+I_c$, where I_c is the moment of inertia of the area around it's centroidal axis.

Thus $y_p = \frac{A.y_c^2 + I_c}{y_c.A}$

In order to generate the loading profiles along the circular bearing, so that the force and the moment for each loading value is the same as that of the square bearing, equation 2 was reorganized in the form: $(y_c+e).F=\rho\ (I_c+A.y_c^2)$ where e is the eccentricity of the resultant force.

By varying the value of ρ and y_c , the force (F) and the moment (M) values were set equal to the values used for the square bearing. Tables 8 and 9 show pressure profile and deflection data.

Table 8. Generation of pressure profile on the circular bearing.

y_c (in)	e (in)	ρ (pci)	F (kips)	M (in-kips)	a (psi)	c (psi)
47	0.3814	37.416	448.00	170.88	1422	2095
35	0.7629	50.558	448.01	341.77	1315	2225
28	1.1443	63.793	448.00	512.64	1212	2360
21.5	1.5257	84.009	448.00	683.52	1050	2562
17	1.9071	107.63	448.01	854.41	861	2798

Table 9. Deflection data for the circular bearing under rotation.

M (in-kip)=	170.88		M (in-kip)=	341.77	
location (in)	**deflection (in)**	**strain**	**location (in)**	**deflection (in)**	**strain**
2	-0.0602	0.0201	1.6364	-0.0675	-0.0225
18	-0.0232	0.0077	18.0004	-0.0156	-0.0052
tan (Φ) =	0.0021		tan (Φ) =	0.0029	
(Φ) (rad)=	0.0021		(Φ) (rad)=	0.0029	
(Φ) (deg)=	0.1178		(Φ) (deg)=	0.1652	
M (in-kip)=	**512.64**		**M (in-kip)=**	**683.52**	
location (in)	**deflection (in)**	**strain**	**location (in)**	**deflection (in)**	**strain**
1.5	-0.0746	-0.0249	1.3846	-0.0853	-0.028433
18	-0.0057	-0.0019	17.9998	-0.00249	-0.00083
tan (Φ) =	0.0038		tan (Φ) =	0.0046	
(Φ) (rad)=	0.0038		(Φ) (rad)=	0.0046	
(Φ) (deg)=	0.2192		(Φ) (deg)=	0.2636	
M (in-kip)=	**854.41**				
location (in)	**deflection (in)**	**strain**			
1.38462	-0.0986	-0.0329			
18	0.00766	0.0026			
tan (Φ) =	0.0059				
(Φ) (rad)=	0.0059				
(Φ) (deg)=	0.3382				

The compressive stress distribution for circular bearings under compression and rotation in a typical elastomer layer is shown in Figure 43. This figure shows that the maximum stress region has shifted from the center of the bearing due to the applied moments. Figure 43 also shows that there is some distortion in the circular pattern of the compressive stress contours. Under pure compression the maximum stress region is in the center of the bearing and the stress contours are circular.

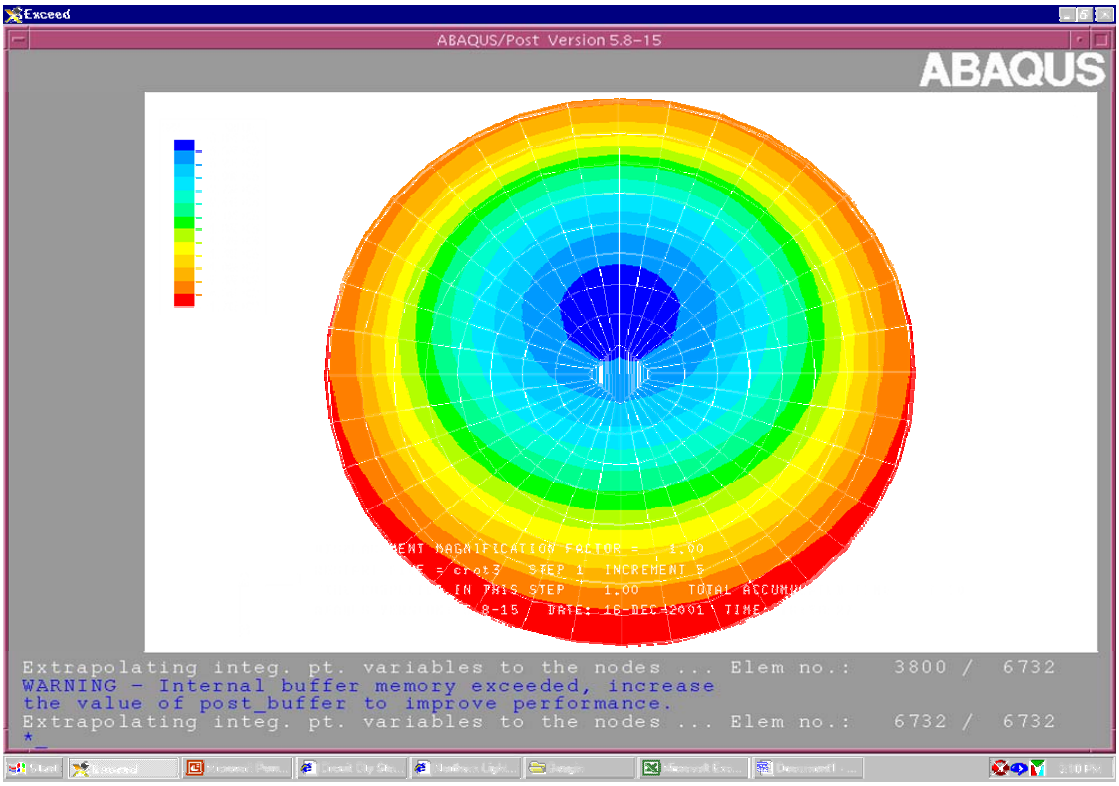

Figure 43. Compressive stress distribution in circular bearing under compression and rotation in a typical elastomer layer.

The moment-rotation relationships for square and circular bearings are shown in Figure 44. As can be determined in this figure, the rotational stiffness of the circular bearing is higher than that of the square bearing. Moreover, the relationship for the circular bearing is not linear, whereas that of the square bearing is linear. These relationships clearly show the effect of bearing geometry on rotational stiffness and magnitude.

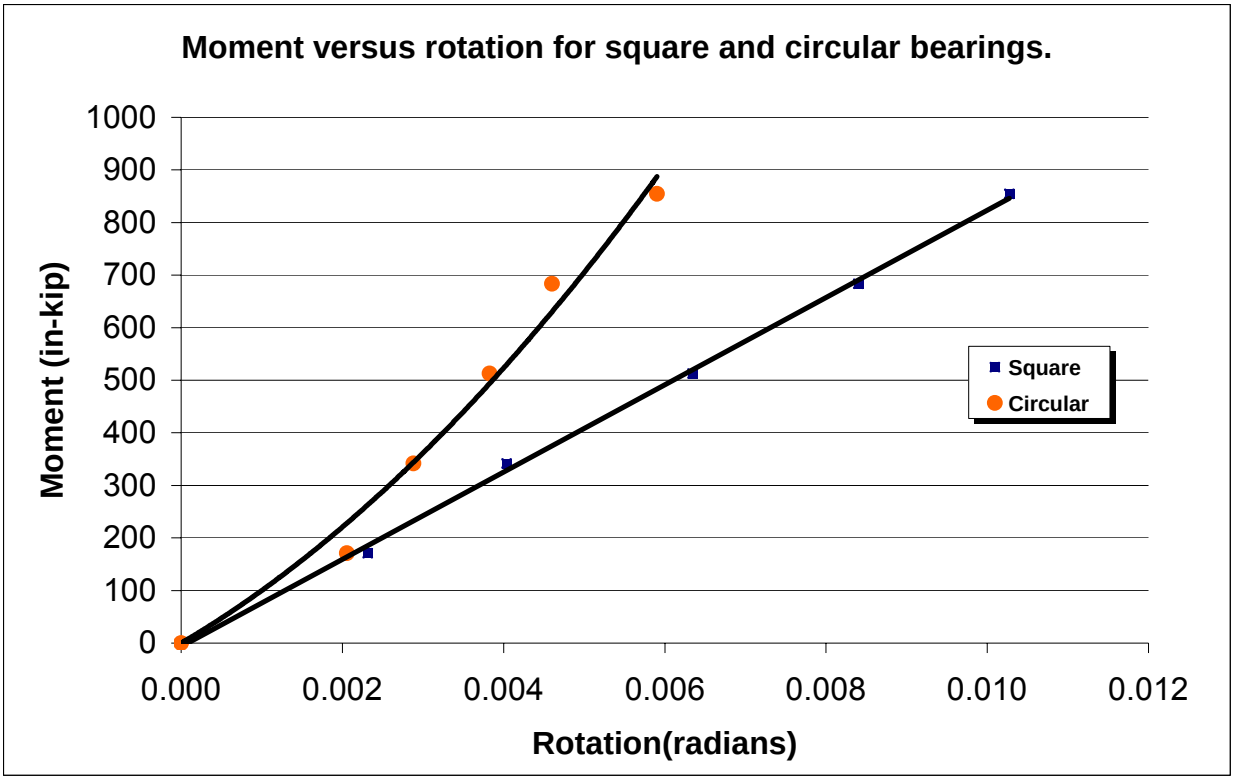

Figure 44. Moment versus rotation for square and circular bearings.

EFFECT OF BEARING THICKNESS ON STIFFNESS OF THE BEARING (FEA)

The effect of bearing thickness on bearing stiffness was evaluated for two bearing types: circular and square bearings. The effect of bearing thickness on stiffness can be seen in Figure 45 and equations (9) and (10). This figure shows a schematic presentation for two bearings: one with a single laminate, and the other with two laminates. Each elastomeric layer has a stiffness K_1 and each laminate layer has a stiffness K_2.

Figure 45. Representation of single laminate and double laminate bearings.

The total stiffness of the single laminate bearing is: $$K_{T1} = \frac{1}{\frac{1}{K_1} + \frac{1}{K_2} + \frac{1}{K_1}} \quad (9)$$

The total stiffness of the two laminate bearing is: $$K_{T2} = \frac{1}{\frac{1}{K_1} + \frac{1}{K_2} + \frac{1}{K_1} + \frac{1}{K_2} + \frac{1}{K_1}} \quad (10)$$

Everything else being the same, as the total thickness and the number of laminates increase, the denominator in the stiffness equations also increases, which in return decreases the total stiffness. To investigate this effect further, three finite element models were generated for square and circular bearings. These models are shown in Figure 46. It was observed from finite element results that as the number of layers increased, the stiffness of the bearing decreased. The three models generated for the square and circular bearings contained steel and composite laminated bearings with three, five, and seven laminates respectively. Each of the bearings in these models was subjected to a distributed compressive load of 1,000 psi and the resulting deflections are tabulated in Table 10.

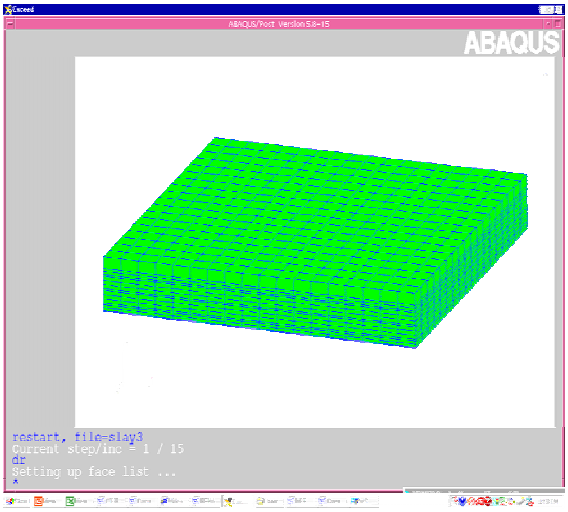

3 layer square bearing

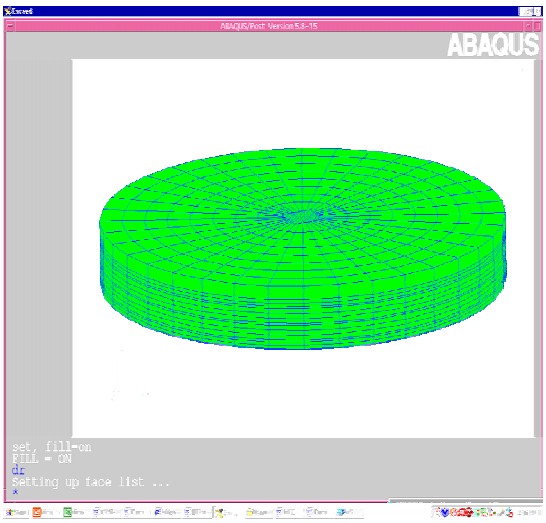

3 layer circular bearing

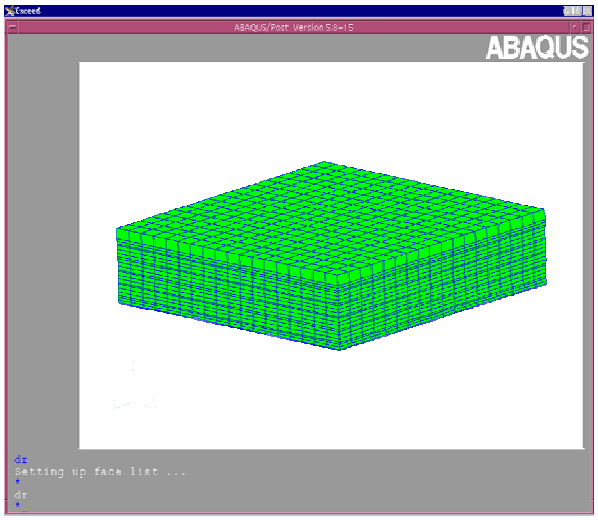

5 layer square bearing

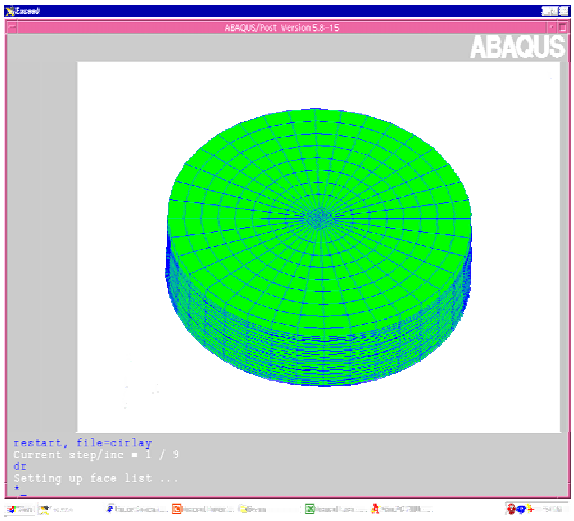

5 layer circular bearing

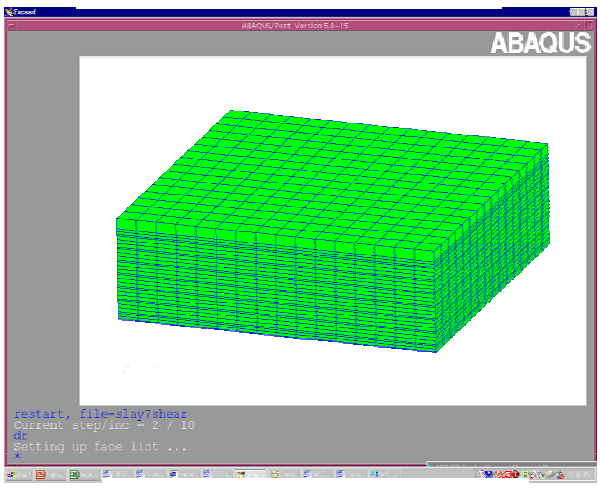

7 layer square bearing

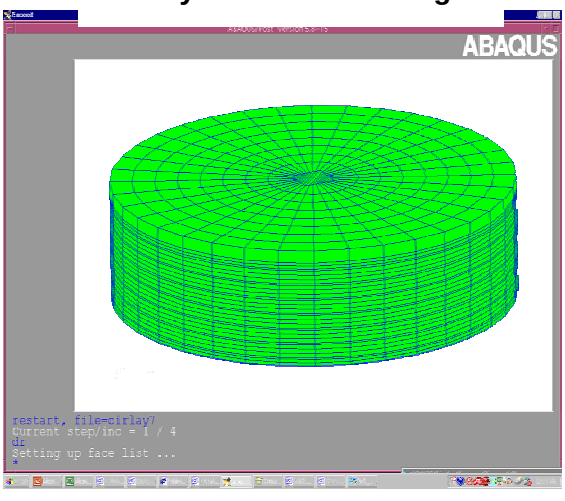

7 layer circular bearing

Figure 46. Finite element models for square and circular bearings with various thicknesses.

Table 10. Deflection data for variable bearing thickness.

Number of steel laminates	Thickness (in)	Deflections (in)			
		Square		Circular	
		Steel	Fiber	Steel	Fiber
3	1.787	0.0134	0.0152	0.0121	0.0139
5	3	0.0257	0.0291	0.0233	0.0267
7	4.211	0.0317	0.0356	0.0314	0.0354

These deflections are plotted versus bearing thickness for steel-laminated bearings in Figure 47 for three, five, and seven steel laminates. This figure shows that for the same bearing area and same applied compressive stress, circular bearings will have less vertical deflections compared to square bearings. The modulus of elasticity used was 7,000, 000 psi and Poisson's ratio was 0.2.

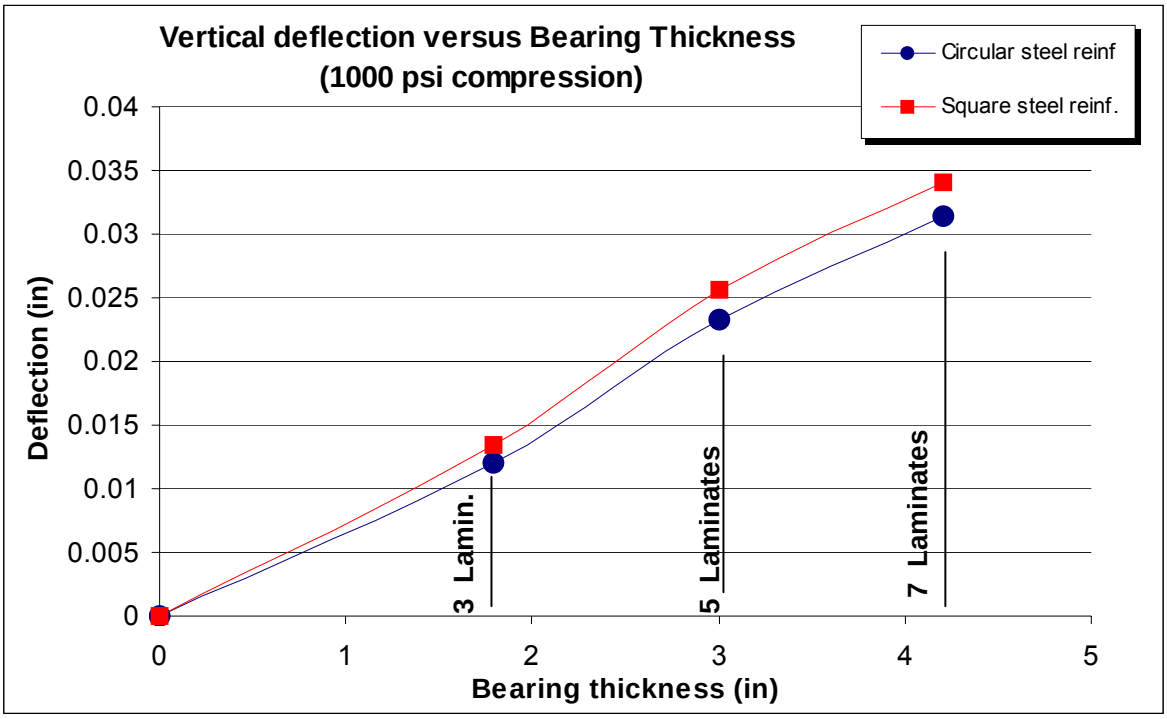

Figure 47. Vertical deflection versus bearing thickness

EFFECT OF LAMINATE TYPE ON STIFFNESS OF ELASTOMERIC BEARINGS (FEA)

In order to evaluate the effect of laminate type on bearing behavior, elastomeric bearings with steel laminates were compared to elastomeric bearings with glass fiber composite laminates (Table 10, Page 56). Each of the bearings was subjected to a distributed compressive load of 1,000 psi. All other bearing parameters were kept the same. The material properties of the glass fiber composite were obtained from manufacturers specifications. These properties are the modulus of elasticity E, and Poisson's ratio μ. The results of the analysis confirmed that the vertical deflection of bearings with steel laminates were lower than those with glass fiber composite laminates. The deflections of bearings with glass fiber composite laminates for the same area and compressive stress were approximately 15 percent higher than bearings with steel laminates. These deflections are plotted in Figures 48 and 49 for square and circular bearings respectively.

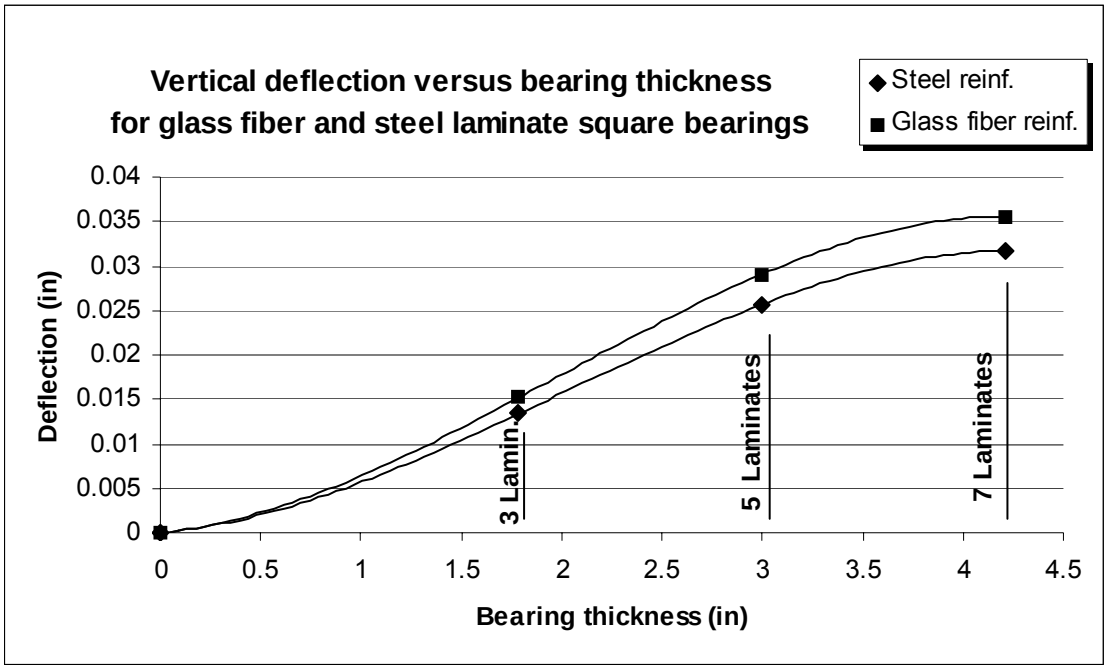

Figure 48. Vertical deflection versus bearing thickness for square bearings with glass fiber composite and steel laminates.

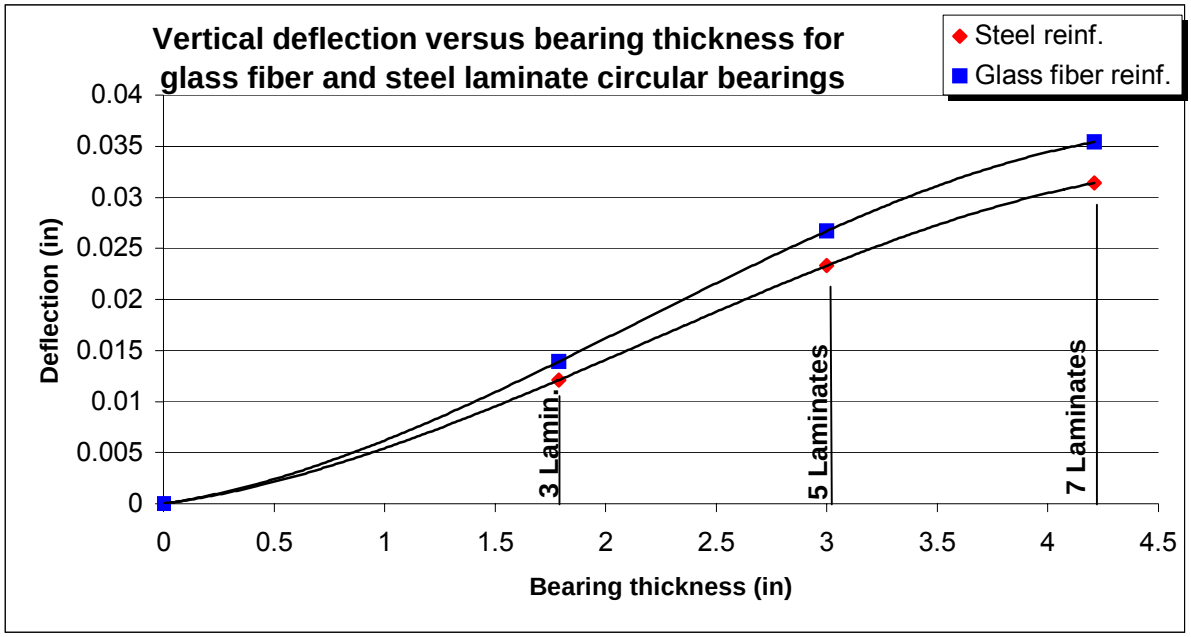

Figure 49. Vertical deflection versus bearing thickness for circular bearings with glass fiber composite and steel laminates.

This is due to the fact that the stiffness of the glass fiber composite laminate is lower than that of steel. No effect on shear resistance has been observed. Based on Figures 47, 48, and 49, it is observed that the trend of deflection versus bearing thickness is such that, as the thickness of the bearing increases, the deflection value approaches a limiting value. The reason for this type of behavior is that as the thickness increases, the slenderness of the bearing also increases, and bending effects start to control the behavior of the bearing due to it's column like behavior.

EFFECT OF TEMPERATURE CHANGES ON SHEAR MODULUS AND COMPRESSIVE STIFFNESS (FEA)

In order to analyze the effect of temperature changes on the compressive stiffness of layered elastomeric bearings, a 16" by 16" square elastomeric bearing with 5-steel layers and a 5 steel layered 18" diameter circular bearing were analyzed under a 1000 psi distributed compressive load for 5 different values of shear modulus (G) for the elastomer which corresponded to 5 different temperatures values. The bearing dimensions were chosen such that they had the same surface area.

The variation of shear modulus with temperature for neoprene was obtained from a chart produced by CALTRANS. This graph was shown in Figure 3 on page 20 of this report. The compressive stiffness of elastomeric bearings is directly related to the shear modulus (G) and the shape factor (S). This relationship is stated in an equation given by AASHTO, which relates the compressive modulus, Ec of the bearing to the mentioned parameters.

$$E_c = 3G(1+2kS^2) \quad \textbf{(11)}$$

Where G is the shear modulus, S is the shape factor and k is a constant based on hardness of the elastomer. Table 11 shows the variation of deflections with temperature.

Table 11. Variation of vertical deflections with temperature for square and circular bearings.

Temperature (F^o)	Temperature (C^o)	Shear modulus	Circular	Square
			Deflection (inch)	
68	20	150	0.0305	0.0336
50	10	170	0.0271	0.0299
19.4	-7	200	0.0233	0.0257
14.0	-10	220	0.0213	0.0235
-0.4	-18	250	0.0189	0.0209

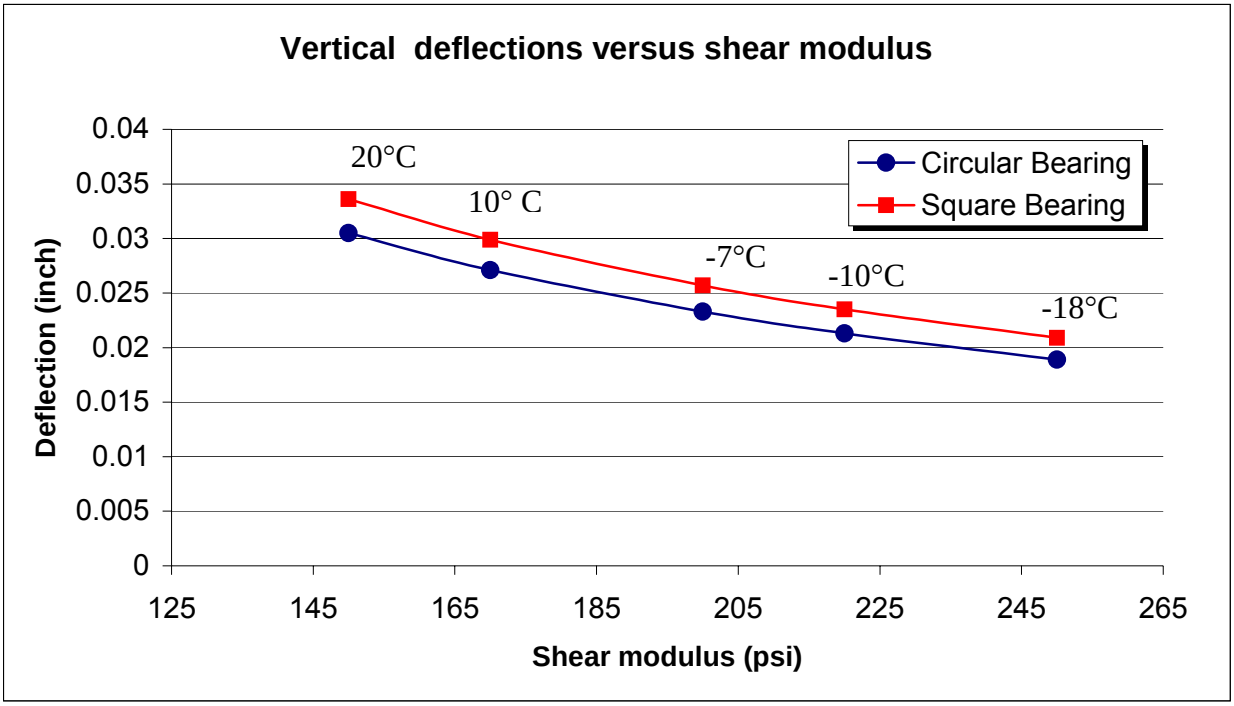

Figure 50. Vertical deflections versus shear modulus.

Figure 50 shows the variation of the compressive deflection with the change in shear modulus. This variation in compressive strength reflects the relationship between the compressive elastic modulus Ec and the shear modulus G given in equation (11). The deflection increases as the compressive modulus increases and since the compressive modulus depends on G (Eq. 11), hence the deflection depends on G. The non-linear relationship observed in Figure 50 arises from the fact that in equation (11), the compressive stiffness is not only related to shear modulus, but also related to the hardness of the elastomer, k, which is in turn, is related to the shear modulus. So, although it seems from equation (11) that compressive modulus and the shear modulus are linearly related to each other, because the k factor is not constant, a non-linear relationship exists. Figure 50 also shows that, due to the higher shape factor of the circular bearing, the compressive deflections are approximately 10 percent smaller than the deflections of the square bearing loaded under the same temperature conditions.

EFFECT OF BEARING SLIP ON STEEL-LAMINATED BEARING BEHAVIOR (FEA)

There are instances of elastomeric bridge bearings slipping or “walking out” from their position under bridge girders rather than remaining in their original location and responding to the bridge movement by elastomer deformation. The walking out phenomena causes the area of contact between the bearing and the girder to decrease leading to higher stress on the remaining area. There are cases in which the girder shifts above the bearing, thereby causing a reduction in the bearing area between the elastomeric bearing and the supported beam or the girder.

The phenomenon of bearing slippage was analyzed considering a loss in contact area. This loss was chosen to be 10% of the original contact area for the square and circular bearings. An equivalent portion of the top rigid plate, which represents the bottom flange of the member, was removed in order the model the partial loss of contact surface. The bearing slip models were subjected to two types of loading: 1) a uniform compression of 1,000 psi, and 2) a combined load of 1,000 psi uniform pressure and a lateral load equal to 15 percent of the applied vertical load. Bearing models for square and circular bearings are shown in Figures 51 and 52 respectively. The compressive stress distributions for bearings with known slip are shown in Figure 53 for square bearings and in Figure 54 for circular bearings. The results of the analysis showed that due to slip, the compressive stress distribution is not uniform across the bearings as was the case without slip (see Figures 16 and 28 on pages 30 and 38 of this report). The maximum compressive stresses for circular bearings without slip were about 4.8 percent higher than those with slip. For square bearings, the maximum compressive stresses without slip were about 8.0 percent higher than those with slip. It is worth noting that the compressive stress distribution in bearings with slip is similar to that of bearings without slip subjected to compression and shear.

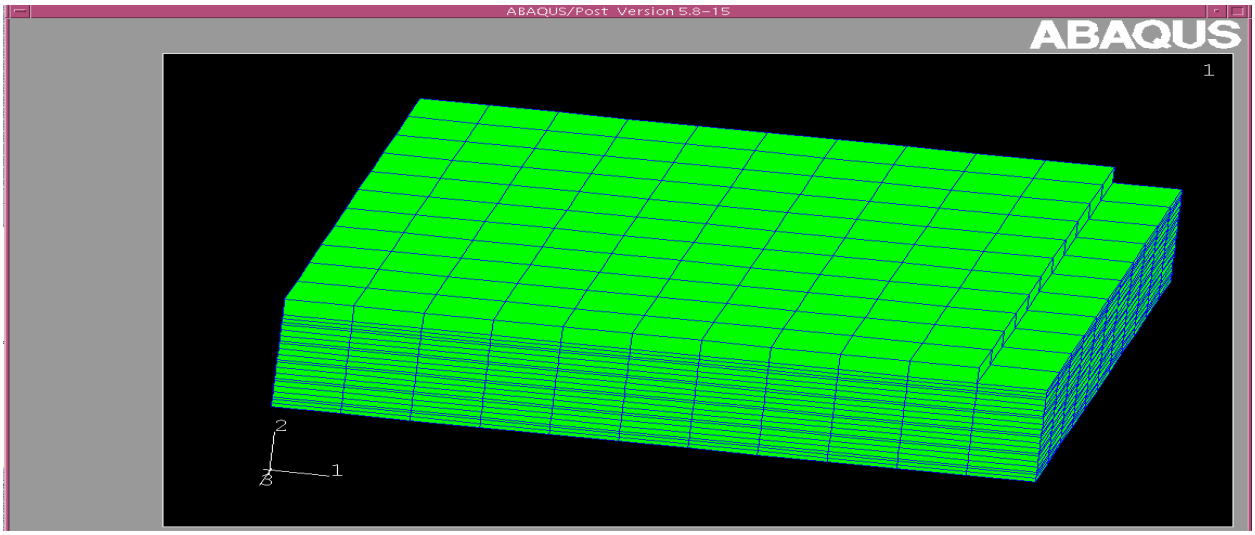

Figure 51. Laminated square bearing model with partial contact area loss.

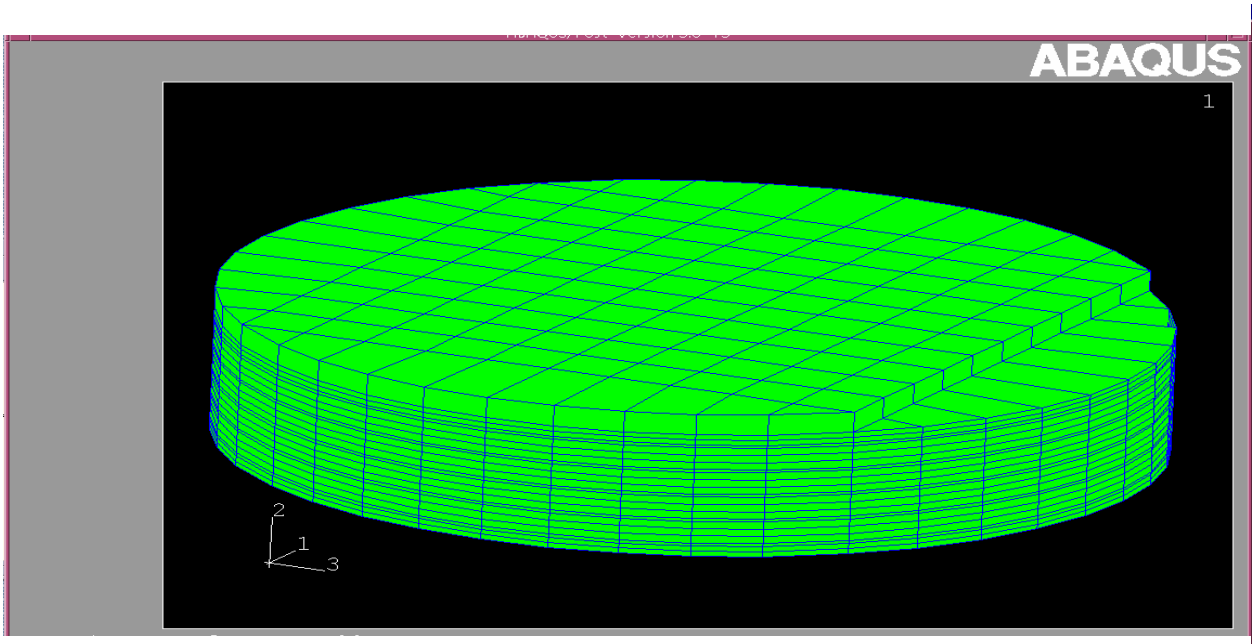

Figure 52. Laminated circular bearing model with partial contact area loss.

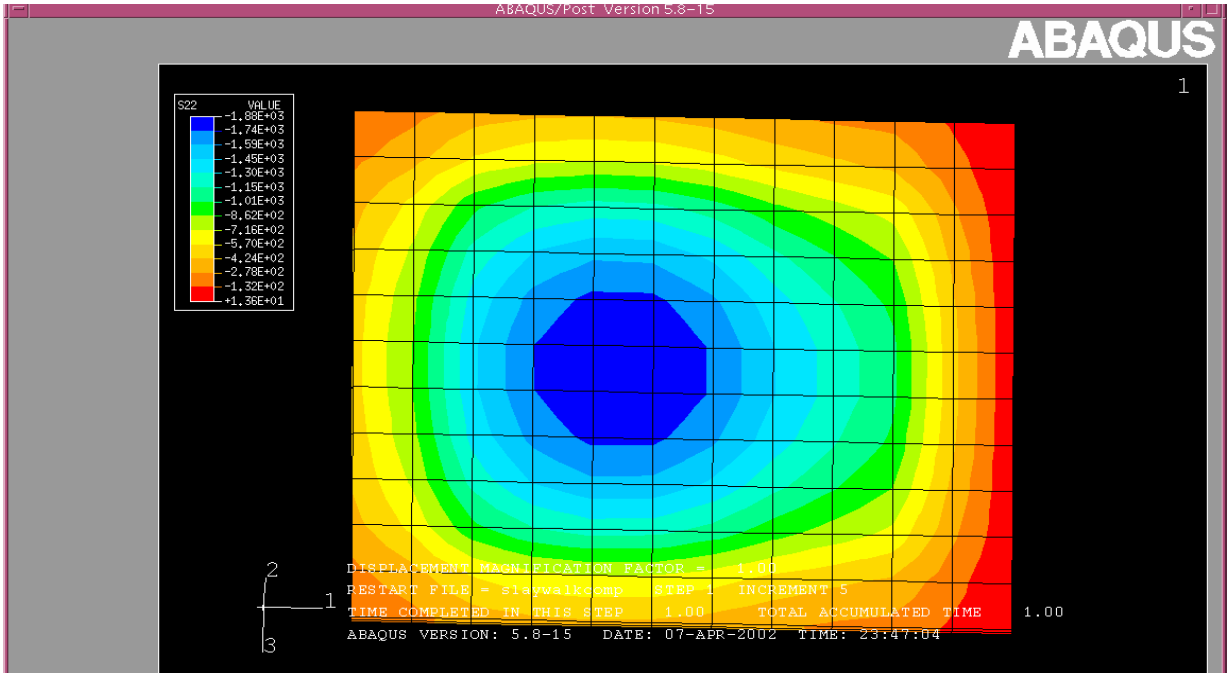

Figure 53. Compressive stress distribution in an elastomer layer under compression for a square bearing of known slip.

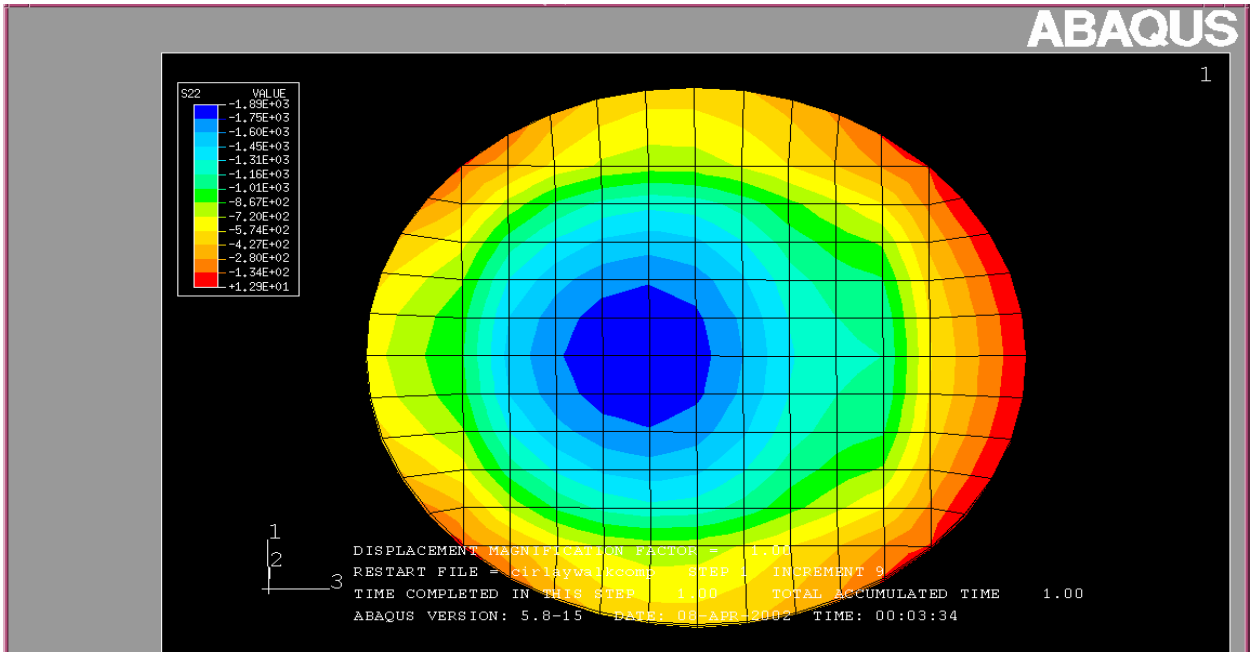

Figure 54. Compressive stress distribution in an elastomer layer under compression for a circular bearing of known slip.

It was also observed that the vertical deflections in the circular bearing are approximately 15 percent less than the deflections within the square bearing. This difference is due to a higher shape factor of the circular bearing, and does not seem to be affected by bearing slip. Vertical deformations for square and circular bearings are shown in Figures 55 and 56, respectively.

Also, note that since a part of the plate is not loaded, the resultant force has shifted from the center of gravity of the bearing. This shift in the location of the resultant force has created a difference between the deflections of the ends of the bearing. However, the average deflection of the circular bearing is less than the square bearing which is similar to what was observed when there was no bearing slip.

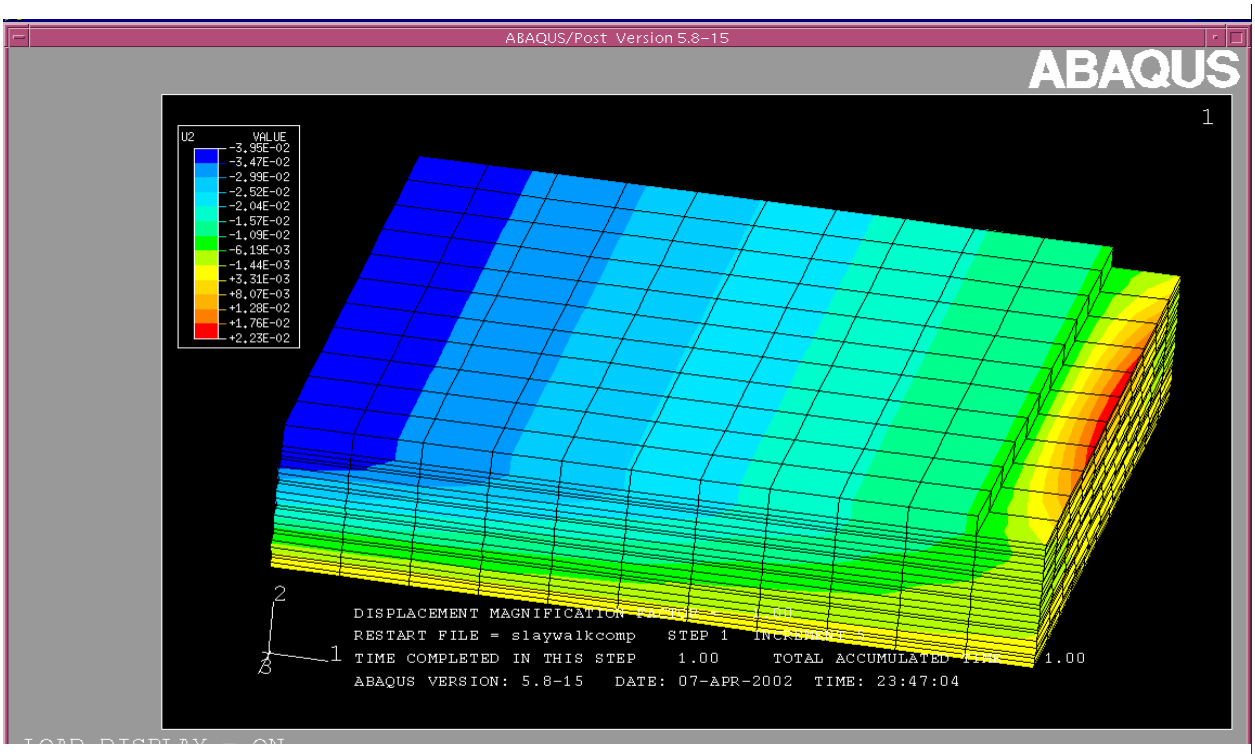

Figure 55. Deflection of the square bearing under compression.

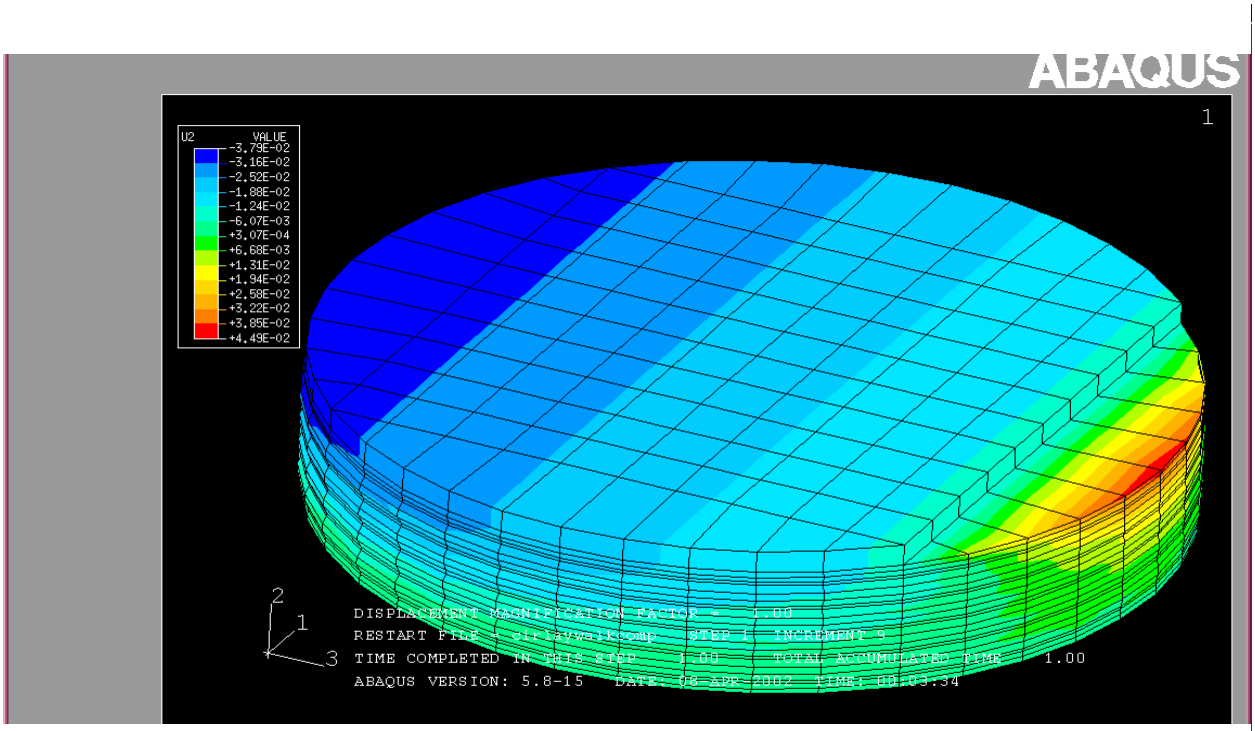

Figure 56. Deflection of the circular bearing under compression.

CONCLUSIONS

Based on the data collected from the bearing survey, the following conclusions may be drawn:

1- There is no evidence to prevent consideration of circular elastomeric bearings as an alternative to square or rectangular elastomeric bearings.

2- Eight states already use circular bearings in their bridges. Texas and New Hampshire provide standard drawings for circular elastomeric bearings and recommendations on their use.

3- Twelve states are willing to consider circular bearings and provide no reason why they cannot be used. Some states believed circular bearings might be more expensive than square bearings.

4- Circular bearings are used on skewed and curved bridges with span lengths less than 100 ft. In some cases, circular bearings have been specified for spans up to 150 ft.

5- The majority of circular bearings used have diameters varying from 12 in to 24 in. Few states used diameters between 24 in and 36 in.

6- The majority of circular bearings used are between 2 in and 3 in thickness. A few states used 3 in to 4 in thick bearings.

7- Most of the states using circular bearings did not have enough data to compare maintenance of circular bearings to square or rectangular bearings. A few states reported insignificant differences in maintenance.

8- Most of the states using circular bearings did not have enough data to compare the cost of circular bearings to square bearings. Texas reported a slight increase

(about 10 percent) in the cost of circular bearings. Results from the bearing suppliers and manufacturers showed only minor differences in the cost between circular and square bearings.

9- Only one state reported instrumentation of elastomeric bearings (Texas) where longitudinal movements of rectangular bearings were monitored. Results showed reasonable movements comparable to design values. Later Texas decided to discontinue monitoring bearing movements.

10- Ohio DOT reported that field research on monitored laminated rectangular bridge bearing movements showed that short-term monitoring of bearings is more practical than long-term monitoring, and that lab tests showed that laminated rectangular bearings under fatigue loads did not have any substantial loss of vertical or shear stiffness.

Based on the data collected from the finite element analysis, the following conclusions may be drawn:

1- For compression, smaller vertical deflections were observed in circular laminated bearings compared to square bearings with the same thickness and surface area. Vertical deflections of circular bearings were about 10 percent lower than of square bearings. This can be attributed mainly to the larger shape factor (higher stiffness) of circular bearings.

2- Under combined normal stress and shear, tensile stresses were observed at the interface between upper elastomer layer and steel plate for both circular and square bearings. The level of tension was approximately 75 psi for circular bearings compared to 100 psi for square bearings.

3- When a portion of the bearing is not in direct contact with the girder, due to bearing walking out or uplift, the tensile stresses observed in Conclusion 2

became higher. For 15 percent of the area of the bearing with no contact, the tensile stresses at the interface increased form 100 psi to 150 psi for square bearings and from 75 psi to 100 psi for circular bearings.

4- Finite element analysis proved that there are concentric stress contours for laminated circular bearings and square contours for the laminated square bearings, especially away from the center. Discontinuities in the stress contours were observed in the laminated square and rectangular bearings while no discontinuities were observed in laminated circular bearings. These discontinuities were amplified when applied shear stresses are added to the applied compressive stresses.

5- The behavior of laminated circular bearings and square bearings under applied load and rotation showed that square bearings have an approximate linear load-rotation relationship. For circular bearings, the load-relationship was non-linear. For the same applied load, less rotation was observed in circular bearings when compared to square bearings, indicating a higher rotational stiffness of circular bearings (this observation was contradictory to the experimental results, see Recommendation 3).

6- The vertical deflections of elastomeric bearings with glass-fiber composite laminates were higher than those with steel shims, by approximately 10 to 15 percent. This is due to the lower stiffness of the composite laminates compared to steel laminates. To maintain compressive strain limits comparable to bearings with steel laminates, the maximum stress limits on bearings with glass-fiber composite laminates need to be reduced by 10 percent to 15 percent.

7- The magnitude of the normal stresses in the bearing between the center and the edge of the bearing is not constant. The normal stress is at its maximum at the center and drops to a much smaller value at the edge while the average stress

remains equal to the applied stress. This was observed for all three bearing geometries.

8- The variation of the normal stress between the center and the edge of the bearing is non-linear with a sharp drop close to the edge. For the laminated square and the rectangular bearings, the drop along the diagonal was less than those along the longitudinal and the transverse directions. Comparing the three bearing geometries, the laminated circular bearing showed a milder drop in normal stresses between the center and the edge.

Based on the data collected from the limited experimental study (see Appendix, Page 75), the following conclusions may be drawn:

1- The stress strain curves of square, circular, and rectangular laminated bearings from compression tests, showed similar trends to those from the finite element investigation. For the same area and same compressive load, test results and the finite element analysis showed that circular bearings had the lowest compressive strains compared to square and rectangular bearings. The higher shape factor of circular bearings resulted in their lower compressive strains.

2- The stress-strain relations in pure compression of laminated circular, square, and rectangular bearings tested in this study follow a trend similar to that of the AASHTO LRFD design guide curves in Section 14.7.5.3.4.

3- The effective compression moduli Ec of circular and square bearings from tests were about 10 percent higher than AASHTO LRFD approximate values. For rectangular bearings, Ec was about 20 percent higher than AASHTO LRFD values.

4- The measured moment capacity versus rotation of circular bearings and rectangular bearings rotated about their major axis (strong axis, see Figure 1A, Page 76) are similar to the predicted AASHTO LRFD moment capacity at low

rotations. The square bearings had a higher moment capacity than the moment capacity predicted by AASHTO LRFD at low rotations. For square bearings, the measured moment capacity versus rotation is not as linear as expected. For rectangular bearings rotated about their minor axis (weak axis), the measured moment capacities were lower than those from the AASHTO LRFD equation for rotations greater than 0.005 rad. This reduced moment capacity needs further investigation.

5- The shear load versus displacement curves for laminated circular and square bearings from experimental results (below the AASHTO LRFD maximum service shear deformations, 28.5 mm for the tested specimens) were approximately linear. Below the maximum service shear deformations, the experimental and the theoretical shear stiffness are similar except at the beginning of the test, when the experimental shear stiffness is higher possibly due to bearing constraints from the test assembly.

6- For the same bearing area and the same applied moment, the experimental results showed that laminated circular bearings had more rotation compared to laminated square bearings and rectangular bearings about their major axis. This observation was not in agreement with the finite element results (see Recommendation 3).

RECOMMENDATIONS

Based on the results of this study, the following recommendations may be made:

1- Laminated circular bearings should be considered as an acceptable bearing geometry along with laminated square and rectangular bearings for bridges. The surveys, the finite element analysis, and the experimental results confirmed that there was no significant difference in cost and performance between laminated

circular, square, and rectangular bearings with the exception of the conflicting results for rotation, which needs further investigation (see Recommendation 3).

2- In situations where the direction of rotation is not well defined (highly skewed and curved bridges), laminated circular bearings have an advantage over laminated rectangular and square bearings because their rotational capacity is the same in all directions while those of rectangular and square bearings are dependent on the axis of rotation.

3- Laminated circular bearings subjected to large rotations should be carefully evaluated. For the same bearing area, the experimental results showed that laminated circular bearings had more rotation compared to laminated square bearings and rectangular bearings about their major axis. The finite element analysis showed that laminated square bearings had more rotation compared to laminated circular bearings. There is a need for more analysis and testing to reconcile the difference between the analytical and experimental results. Accurate prediction of bearing rotational capacity will be required when designing bearings for situations with large rotations. Alternatively, details that eliminate or minimize rotations at the bearings can be used, and in this case bearing geometry will not be a factor.

4- Although, the experimental tests covered all three bearing geometries, they were limited to one bearing thickness, one rubber material, and one bearing size. There is a need for a comprehensive experimental investigation of laminated elastomeric bearings under compression, compression and rotation, compression and shear, and cyclic loads.

5- There is a need for field instrumentation of laminated bearings to assess and compare their behavior. Also the field data will help validate AASHTO LRFD design criteria for laminated elastomeric bearings.

REFERENCES

1. ABAQUS Structural Analysis Program, User's Manual version 5.8–15, 2001.

2. Bezgin, N., O.," Analytical Investigation of Circular, Square, and Rectangular Elastomeric Bearings", Master's Thesis in Progress.

3. Billings, L., J., Dissertation," Finite Element Modeling of Elastomeric Seismic Isolation Bearings,", University of California at Irvine, 1992.

4. Culmo, Michael, CME Associates, Inc., Chairman, NESBC Bearing Sub-Committee. Private communication.

5. Hamzeh, O. N., Tassoulas, J. L., and Becker, E. B. ,"Behavior of Bridge Elastomeric Bearings: Computational Results,", Journal of Bridge Engineering, Vol. 3, No. 3, August 1998, pp. 140-148.

6. Herrman, L. R., Hamidi, R., and Shafigh-Nobari, F. and Ramaswamy, A.,"Nonlinear Behavior of Elastomeric Bearings: II. FE Analysis and Verification,", Journal of Engineering Mechanics, ASCE, Vol 114, 1988, pp. 1831-1853.

7. LRFD Bridge Design Specifications. AASHTO, 2nd Edition, Washington, D.C., 1998.

8. Lindley, P. B.," Plane-Stress of Rubber at High Strains Using Finite Elements", Journal of Strain Analysis, Vol. 6, No. 1, 1971, p. 45-52.

9. Lindley, P. B.," A Finite Element Program for the Plane Strain Analysis of Rubber at High Strains Using Finite Elements", Journal of Strain Analysis, Vol. 10, No. 1, 1975, p. 25-31.

10. McDonald, J., Heymsfield, E., Avent, R.," Slippage of Neoprene Bridge Bearings ", Journal of Bridge Engineering, Vol. 5, No. 3, August 2000, pp. 216-223.

11. Massachusetts Highway Department, Bridge Manual-Part I and II, 1995, Boston, MA.

12. Michigan Department of Transportation, Bridge Design Manual, 1996, Lansing, MI.

13. Minor, J. C., and Egen, R. A., " Elastomeric Bearing Research,", NCHRP Report 109, TRB, National Research Council, Washington, D.C. 1970, 62 pp.

14. Muscarella, J.V., and Yura, J. A. "An Experimental Study of Elastomeric Bridge Bearings With Design Recommendations,", Research Report No. FHWA/TX-98/1304-3, Texas Department of Transportation, Oct 1995, 192 pp.

15. New Jersey Department of Transportation, Bridge Design Manual, 1997, Trenton, NJ.

16. Nims, D.," Instrumented Elastomeric Bridge Bearings,", ODOT Report NO. FHWA/OH-2000-010, Ohio Department of Transportation, June 2000.

17. Roeder, C.W., Stanton, J. F., and Feller, T.,"Low Temperature Behavior and Acceptance Criteria For Elastomeric bridge Bearings,", NCHRP Report 325, TRB, National Research Council, Washington, D.C. Dec 1989, 80 pp.

18. Roeder, C.W., Stanton, J. F., and Taylor, A. W.,"Performance of Elastomeric Bearings,", NCHRP Report 298, TRB, National Research Council, Washington, D.C. Oct 1987, 100 pp.

19. Seki, W. et al., “A Large-Deformation Finite Element Analysis for Multilayer Elastic Bearings,“, Rubber Chemistry and Technology, Vol. 60, No. 5, 1987, pp. 856-869.

20. Standard Specifications for Highway Bridges. AASHTO, 16th Edition, Washington, D.C., 1996.

21. Stanton, J. F., and Roeder, C.W., “Elastomeric Bearings Design, Construction, and Materials,”, NCHRP Report 248, TRB, National Research Council, Washington, D.C. Aug 1982, 82 pp.

22. Takayama, M., Tada, H., and Tanaka, R.,” Finite Element analysis of laminated Rubber Bearing Used in Base Isolation System,”, Presented at a meeting of Rubber Division, American Chemistry Society, Washington, D.C., October 1990.

23. Texas Department of Transportation, Bridge Design Manual, 1998, Austin, TX.

24. Yazdani, N. Eddy, S., and Cai, C. S. ,“Effect of Bearing Pads on Precast Prestressed Concrete Bridges,“, Journal of Bridge Engineering, Vol. 5, No. 3, August 2000, pp. 224-232.

APPENDIX

EXPERIMENTAL INVESTIGATION (Laminated Bearings)

Materials

The experimental program was comprised of testing reinforced elastomeric bearings in compression, compression and rotation, and compression and shear. Three different bearing geometries were tested: circular, square, and rectangular. The circular bearings were 228.6 mm (9 in) in diameter, the square bearings were 203.2 x 203.2 mm (8 inx 8 in), and the rectangular bearings were 254 x 152.4 mm (10 in x 6 in). Three specimens were tested for each bearing geometry. The total thickness of reinforced bearings was 76.2 mm (3 in). The bearing dimensions were chosen such that surface areas of all three bearing geometries were the same. Each reinforced bearing had six 3.2 mm thick mild steel shims and seven elastomer layers. Each of the five interior elastomer layers was 9.5 mm thick and the total thickness of the elastomer was 56.9 mm. The top and bottom elastomer layers had a thickness of 4.7 mm. All laminated pads had an edge cover of 6.4 mm. Bearing and elastomer dimensions are shown in Figure 1A, as well as the orientation of rectangular bearings. The elastomer material was natural rubber having a hardness equal to 55$\pm$5 durometer. All specimens were tested at an ambient temperature equal to 23 ^{o}C $\pm$ 2 ^{o}C (74 ^{o}F $\pm$ 5 ^{o} F). A summary of the experimental program is shown in Table 1A.

Table 1A- Experimental Program

Tests	Reinforced Bearings		
	Circular	Rectangular	Square
Pure compression	3	3	3
Compression with rotation	3	2 (major) 2(minor)	3
Compression with shear	2	2	2

Laminated Elastomeric Bearing Dimensions

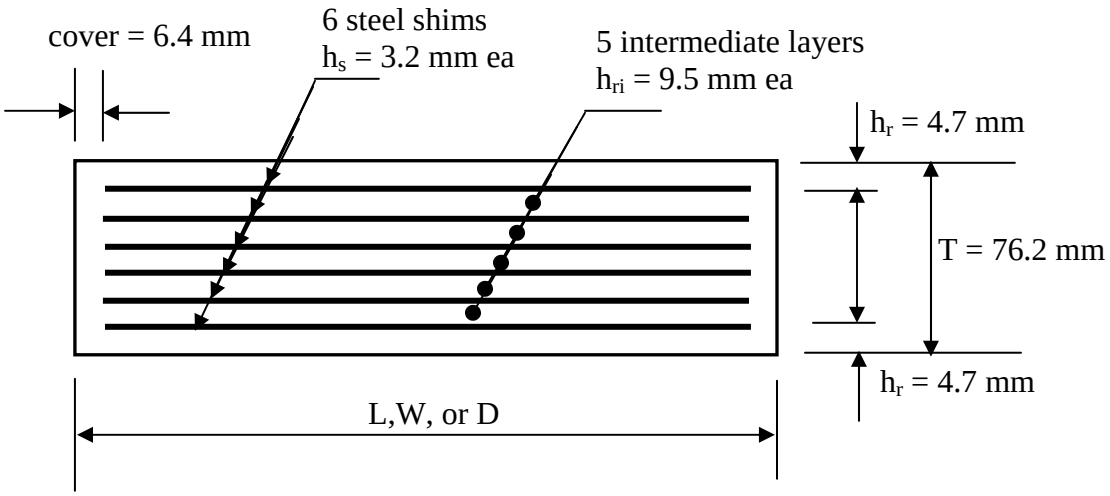

Circular, D = 228.6 mm
Square, L = W = 203.2 mm
Rectangular, L = 254 mm, W = 152.4 mm
Total thickness of the elastomer, hrt = $\Sigma h_{ri}+2h_r$ = 56.9 mm
Elastomer: Natural Rubber 55±5 durometer hardness

Rectangular Bearing Orientation

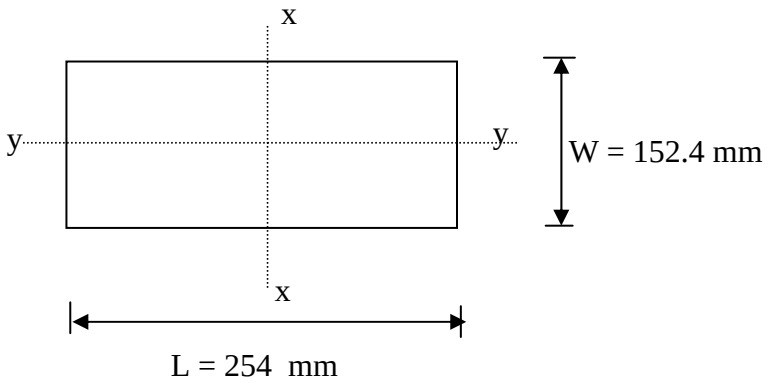

x - x = strong (major) axis
y - y = weak (minor) axis

Figure 1A. Dimensions of laminated elastomeric bearings used in this study and orientation of rectangular bearings.

Testing Procedure

Three types of tests were conducted for each set of the three bearing geometries: 1) compression, 2) compression and rotation, and 3) compression and shear. All tests were carried out using a 1780 KN (400,000 lbs) Tinius-Olsen hydraulic testing machine equipped with a swivel-head platen. To ensure uniform compressive stress distribution on the bearings, 50 mm thick steel plates were provided on top and bottom of the bearing. Test setup of the compression test is shown in Figure 2A. The test assembly for compression and rotation was similar to that of compression except that the load was applied eccentric to the bearings to produce bending (see Figures 3A and 4A). The compression and shear test assembly shown in Figures 5A and 6A consisted of two 50 mm thick exterior steel plates and an interior 50 mm thick steel plate compressed against a pair of bearings using four anchor bolts.

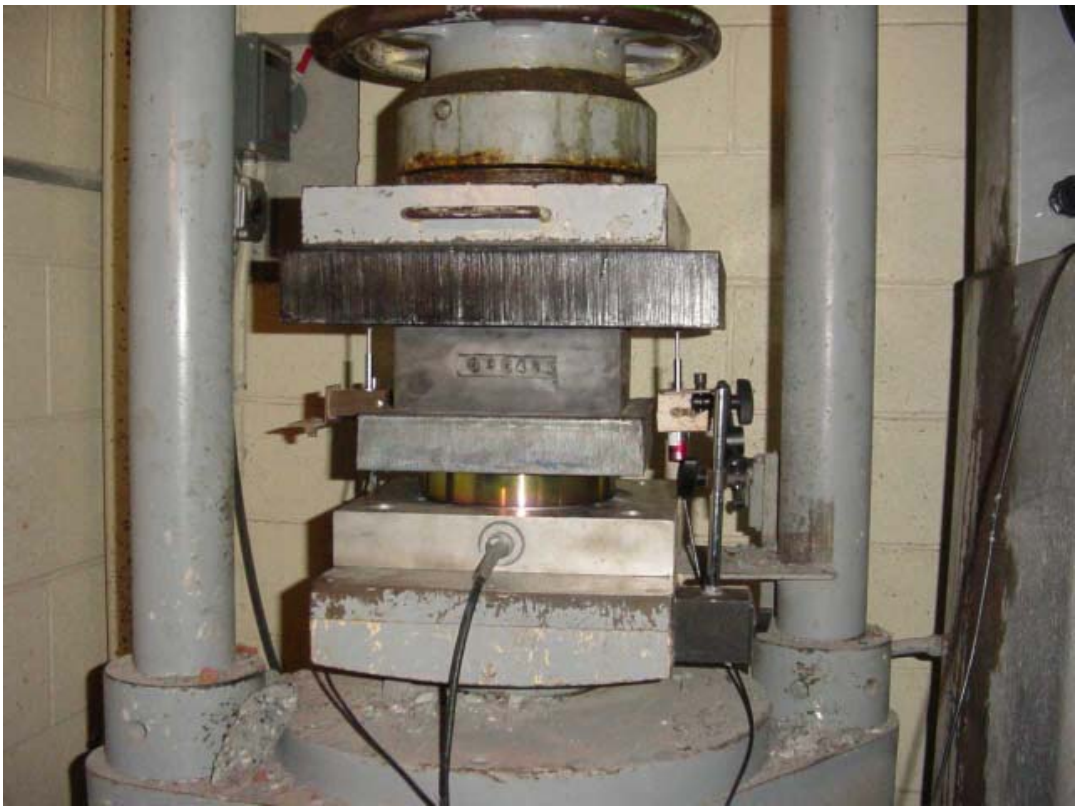

Figure 2A. Square bearing being tested in pure compression.

The bearings were glued to the exterior steel plate and the interior plate to prevent slip and the bolts were then tightened to provide a compressive stress of 8.5 MPa (1.25 ksi). A load was applied to the interior plate, which provided shear forces on both bearings.

For each test, load and deformations were recorded using a SOMAT data acquisition system. The load was measured using a 900-KN (200 kips) load cell placed at bottom of test setup and deformations were measured using LVDT's on both sides of the bearing. LVDT's with ±6.25 mm maximum stroke were used for compression and compression and rotation tests and ± 50.8 mm maximum stroke LVDT's were used for the compression and shear tests. For the compression tests, the load was applied at the center of the compression test set up and data were collected until the bearing bulged outwards. For compression and rotation tests, the eccentric load was applied to the test setup and the data were collected until the average compressive stress exceeded the maximum permissible stress for each bearing. For compression and shear tests, the test data were collected until the bearing became distorted or the maximum deflection of the LVDT was reached. Since the presence of compressive stress on elastomeric bearings lowers their shear capacity, the compressive stress chosen for compression and shear tests was 8.5 MPa (1.25 ksi). This value was slightly higher than the maximum permissible stress by AASHTO-Method B (1.66GS = 1.220 ksi) and would represent the worst case for bearings in compression and shear. Figures 3A and 4A show square and circular bearings being tested in compression and rotation, while Figures 5A and 6A show square and circular bearings being tested in compression and shear.

Figure 3A. Square elastomeric bearing during compression and rotation tests.

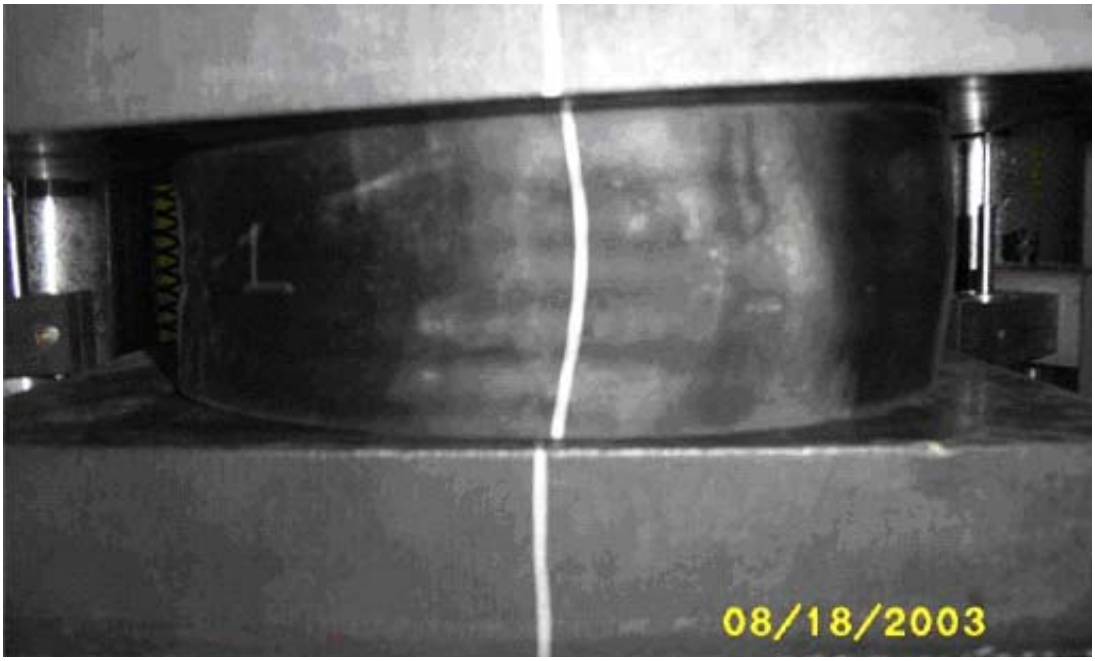

Figure 4A. Circular Elastomeric bearing during compression and rotation test.

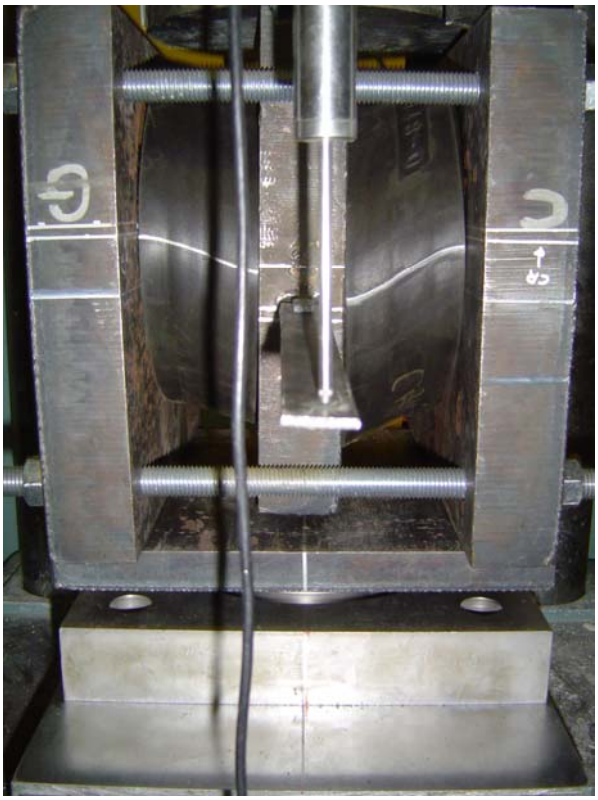

Figure 5A. Circular elastomeric bearing in shear and compression test.

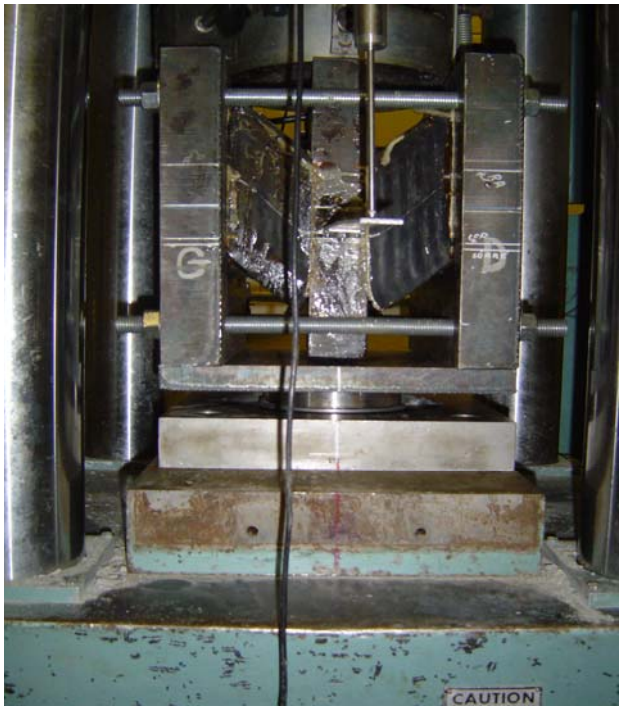

Figure 6A. Square elastomeric bearing in shear and compression test.

TEST RESULTS AND DISCUSSION

Compression

The results of the compression tests for the total stress strain curves and the initial portion of the curves are shown in Figures 7A and 8A respectively. Each of the plots shown in these figures represents the average of three tests. As expected, the stress strain curves for square and rectangular bearings had only minor differences because their shape factors (S) were close. The circular bearings had a higher axial stiffness than square and rectangular bearings because of their higher shape factor. Figure 8A also shows AASHTO's approximation of the effective modulus Ec (slope of the initial portion of the stress-strain curve) . The graphs in Figure 7A show that the stress strain curve remains linear up to compressive stress approximately equal to 8 MPa and compressive strains equal to 6%. The values of Ec obtained from test data for circular and square bearings are about 10 percent higher than that from the AASHTO approximate equation (see Figure 8A). For rectangular bearings, the value of Ec from test data is about 20 percent higher than that of AASHTO. The plots in Figure 7A also show that for the range of compressive stresses allowed in AASHTO Method B (up to σ_{max}), the stress-strain curves for all three bearings were linear. The graphs in Figure 8A show similar trends to those in Figures C14.7.5.3.3-1 in AASHTO LRFD Specifications. The AASHTO LRFD graphs are for 50 and 60 durometer hardness while the elastomer used in this study had 55 $\pm$ 5 durometer hardness.

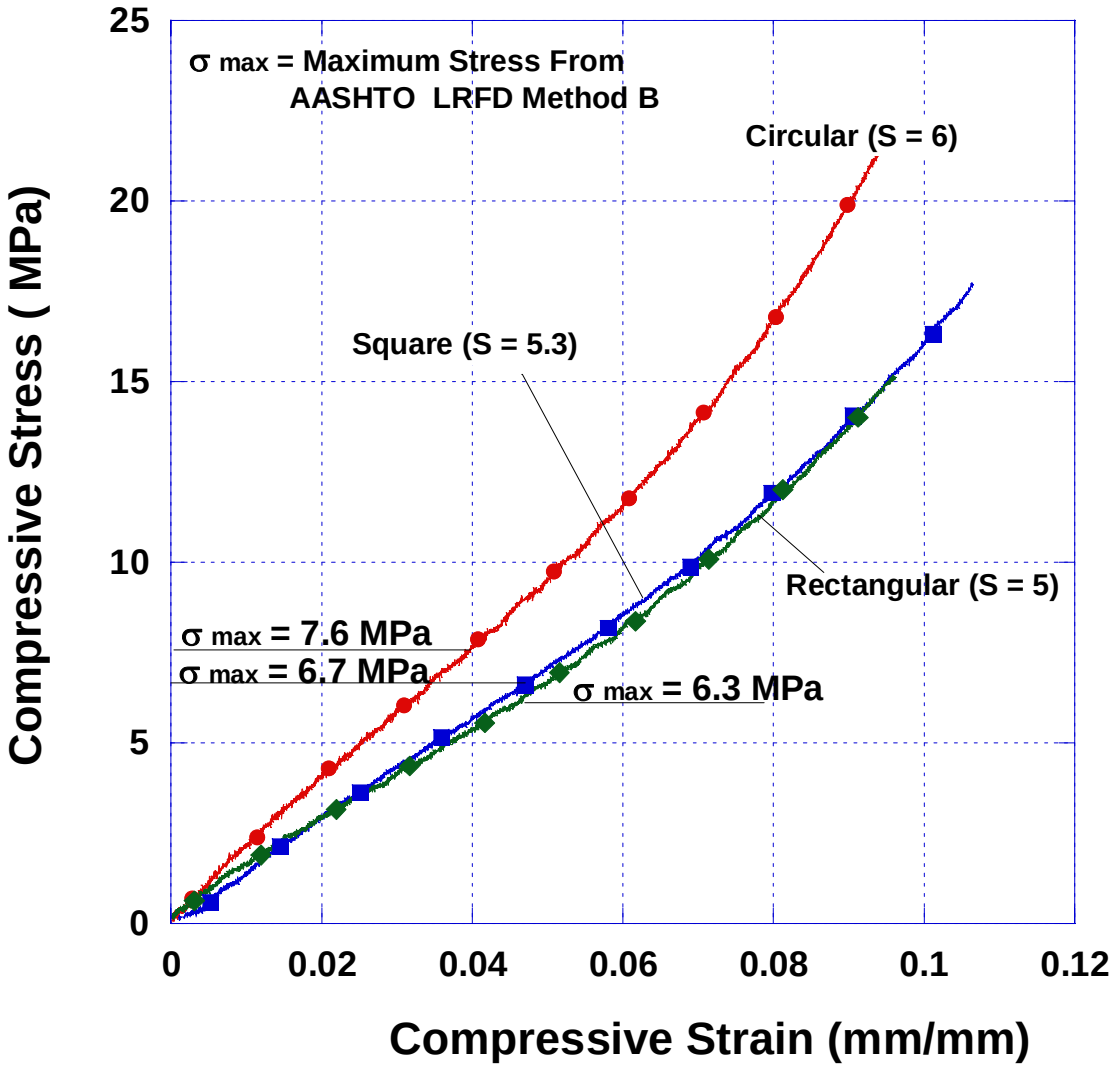

Figure 7A - Compressive stress versus strain for various bearing geometries from test results.

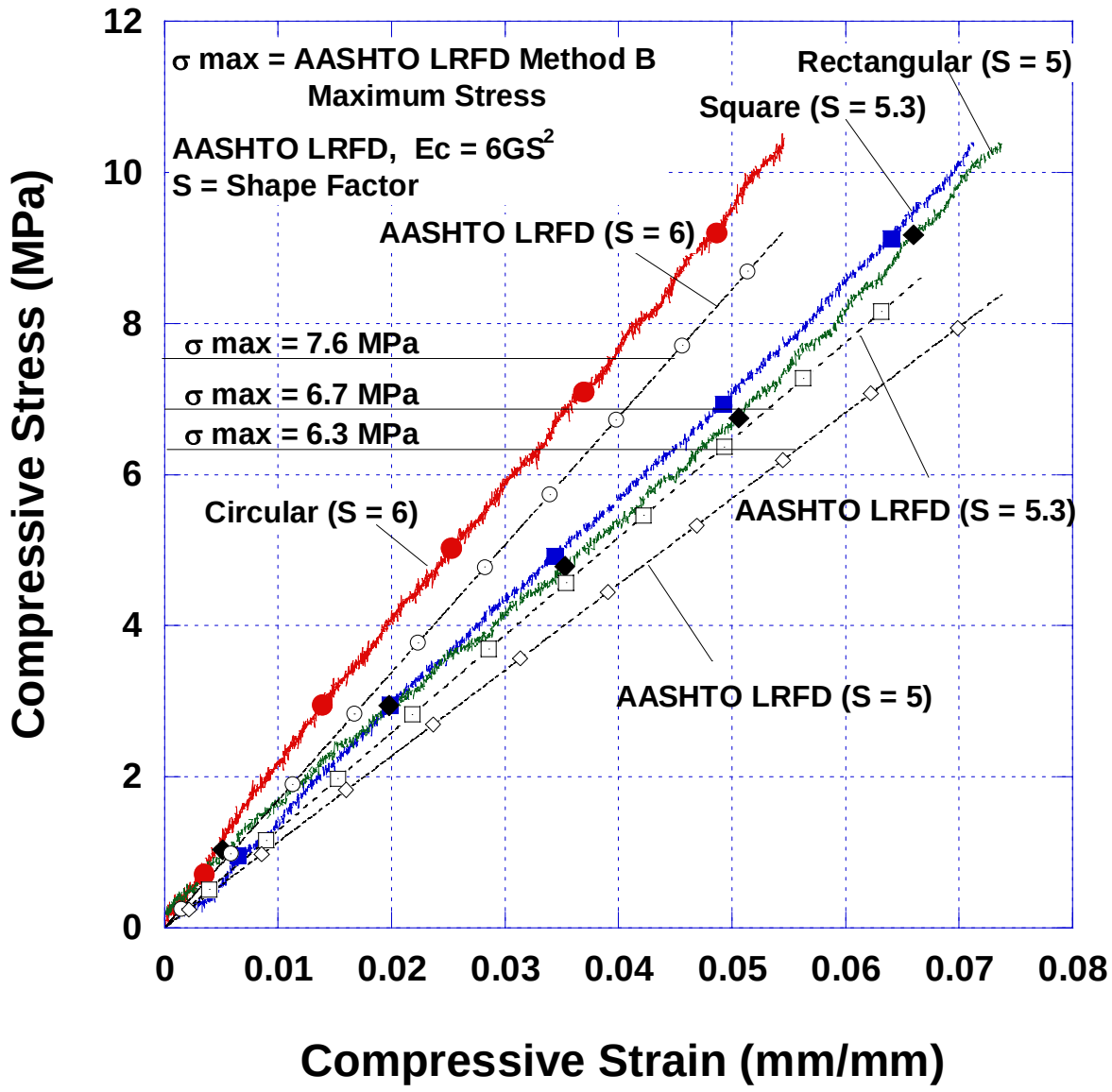

Figure 8A - Initial portion of the compressive stress versus strain curve from test results and from AASHTO LRFD prediction equation.

Compression and Rotation

Test results for compression and rotation are shown in Figures 9A and 10A for the total curve and the initial portion of the curve respectively. Figure 9A shows that the square bearings and the rectangular bearings rotated about their major axis (see Figure 1A, Page 76) had a higher flexural stiffness than the circular bearings although the circular bearings had a higher shape factor. The test results in Figure 9A also show that the

orientation of rectangular bearings had a significant effect on their rotational capacity. A rectangular bearing rotated about its minor axis had about 2.5 to 3 times the rotational capacity of the same bearing rotated about its major axis. The significant difference in the rotational capacity of rectangular bearings about its major and minor axes of symmetry makes it important to accurately predict the actual direction of rotation of the bridge girder. Rectangular bearings should be oriented such that their direction of rotation is about the minor axis. In those situations where the direction of rotation is not well defined (highly skewed and curved bridges), circular bearings would be more appropriate because its rotational capacity is the same in all directions. This study did not include rotation tests of square and rectangular bearings about axes other than their axes of symmetry. The moment versus rotation relationships in Figure 9A for square bearings, circular bearings, and rectangular bearings (rotated about their major axis) are linear at relatively low rotations (less than 0.02 rad) compared to rectangular bearings rotated about their minor axis (which are linear up to 0.03 rad). Figure 10A shows the initial linear portion of the moment versus rotation relations for all bearings. The relationship is compared to AASHTO LRFD prediction equations for the moment capacity. It is observed that the measured moment capacity versus rotation of circular bearings and rectangular bearings rotated about their major axis are similar to the predicted moment capacity at low rotations. The square bearings had a higher moment capacity than the moment capacity predicted by AASHTO LRFD at low rotations. In the case of the square bearing, the measured moment capacity versus rotation is not as linear as expected. For rectangular bearings rotated about their minor axis, the measured moment capacities were lower than those from the AASHTO LRFD equation for rotations greater than 0.005 rad. This reduced moment capacity needs further investigation.

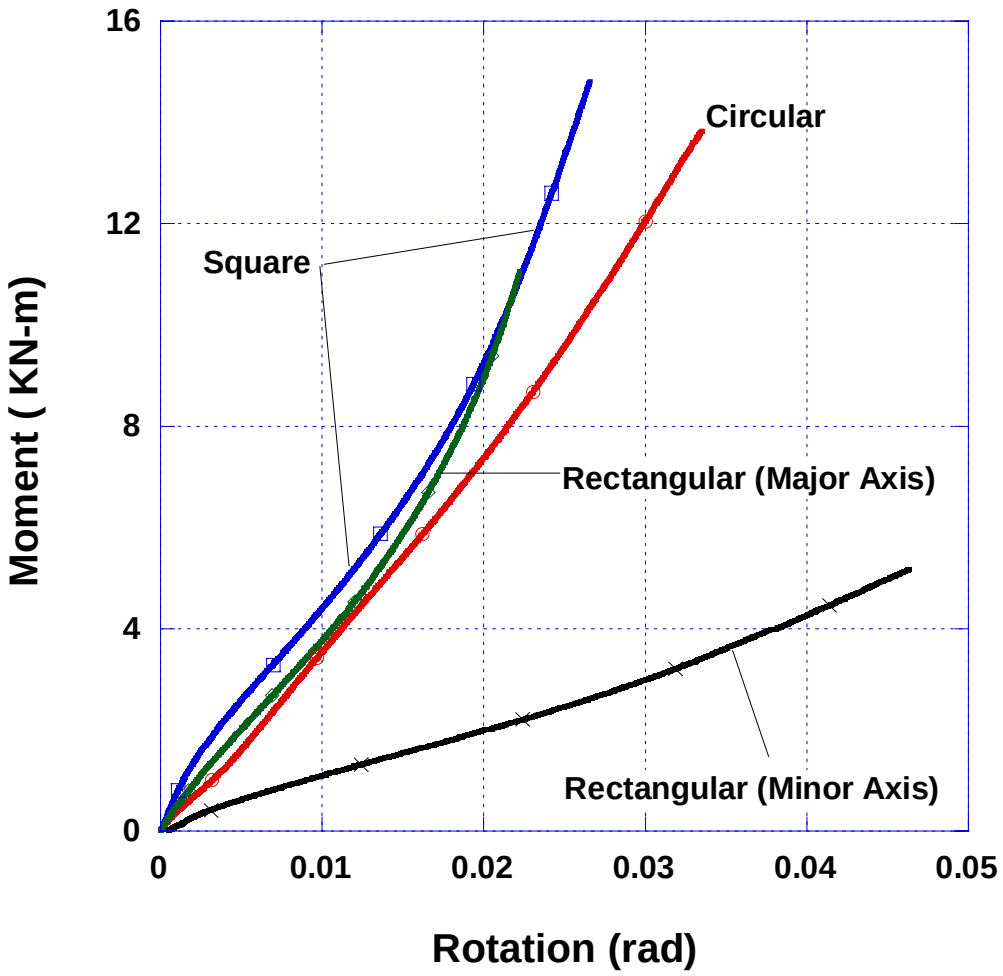

Figure 9A - Moment versus rotation for various bearing geometries from test results.

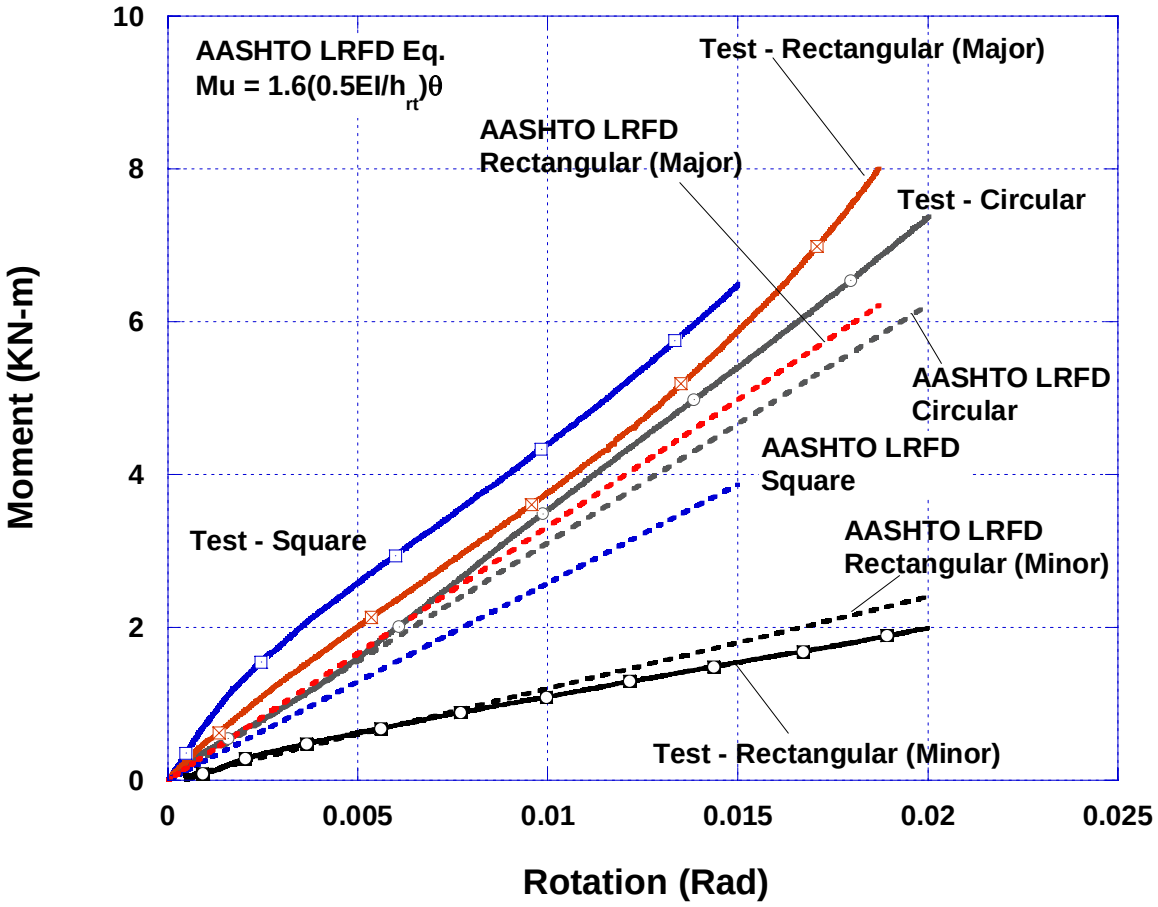

Figure 10A - Initial portion of the moment versus rotation relationship for various bearing geometries from test results and from AASHTO LRFD prediction equation.

The AASHTO LRFD Method B for the interaction between compressive stress and rotation are plotted in Figure 11A along with experimental data for square and circular bearings. The graph shows that the experimental values are much closer to the uplift stress equation than to the edge equation. This seems to indicate that the uplift stress line will likely control the stress-rotation interaction at the compressive stress level used in these tests. Circular bearings fall slightly below the AASHTO LRFD Method B uplift stress line while the square bearing is slightly above that line. The effect of compressive

stress level on the rotational capacity of circular bearings needs further evaluation.

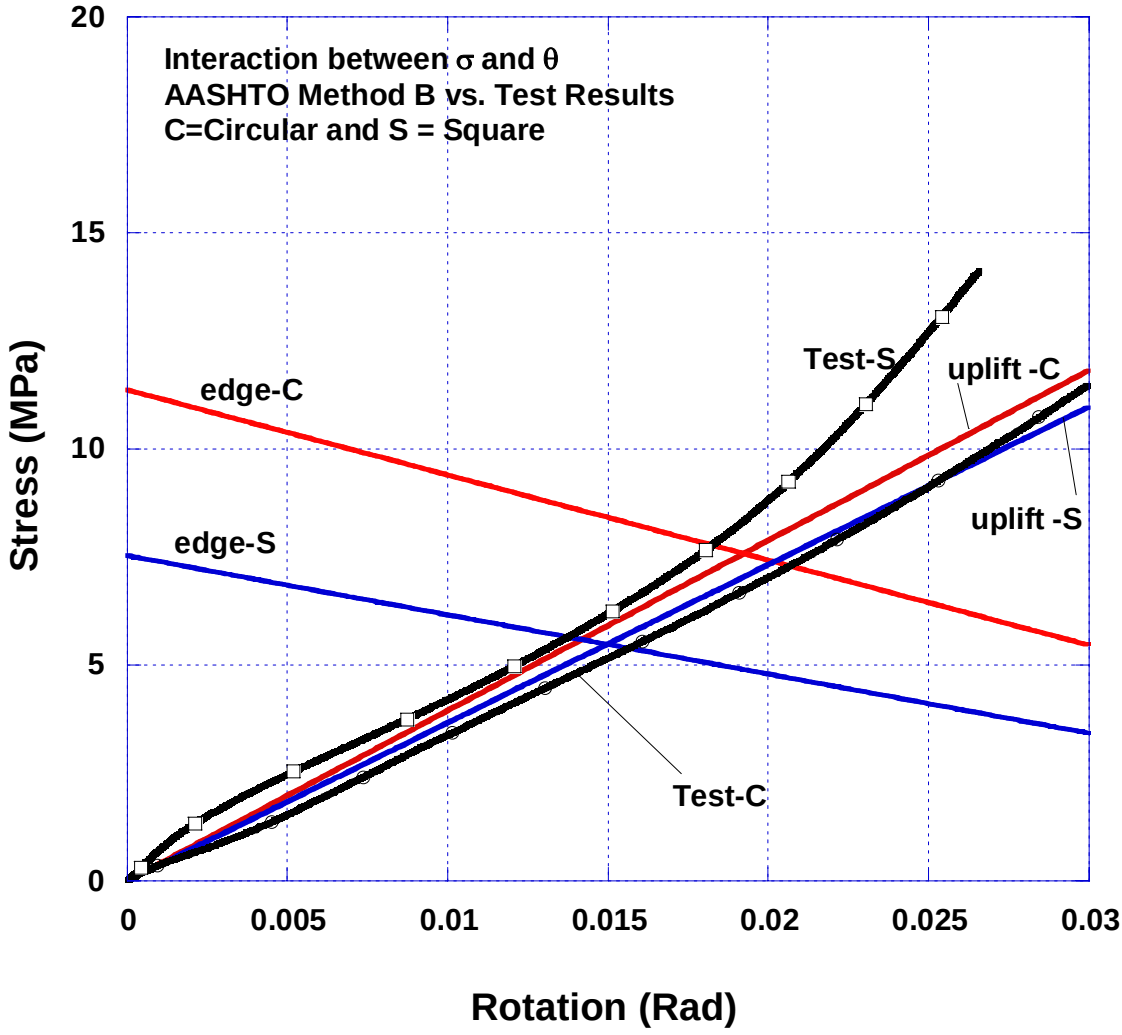

Figure 11A - Interaction between stress and rotation of elastomeric bearings from test results and from AASHTO Method B.

When comparing the same experimental stress versus rotation interaction to AASHTO LRFD Method A as shown in Figure 12A, all experimental curves fall well above the uplift stress equation from Method A except for the rectangular bearings rotated about their minor axis where the experimental and AASHTO Method A plots coincide with each other. By comparison, for AASHTO Method B, the measured stress versus

rotation of rectangular bearings rotated about their minor axis fell well below the uplift stress (not shown in Figure 11A). Rectangular bearings rotated about their minor axis should be carefully designed for uplift when using AAHSTO LRFD Method B.

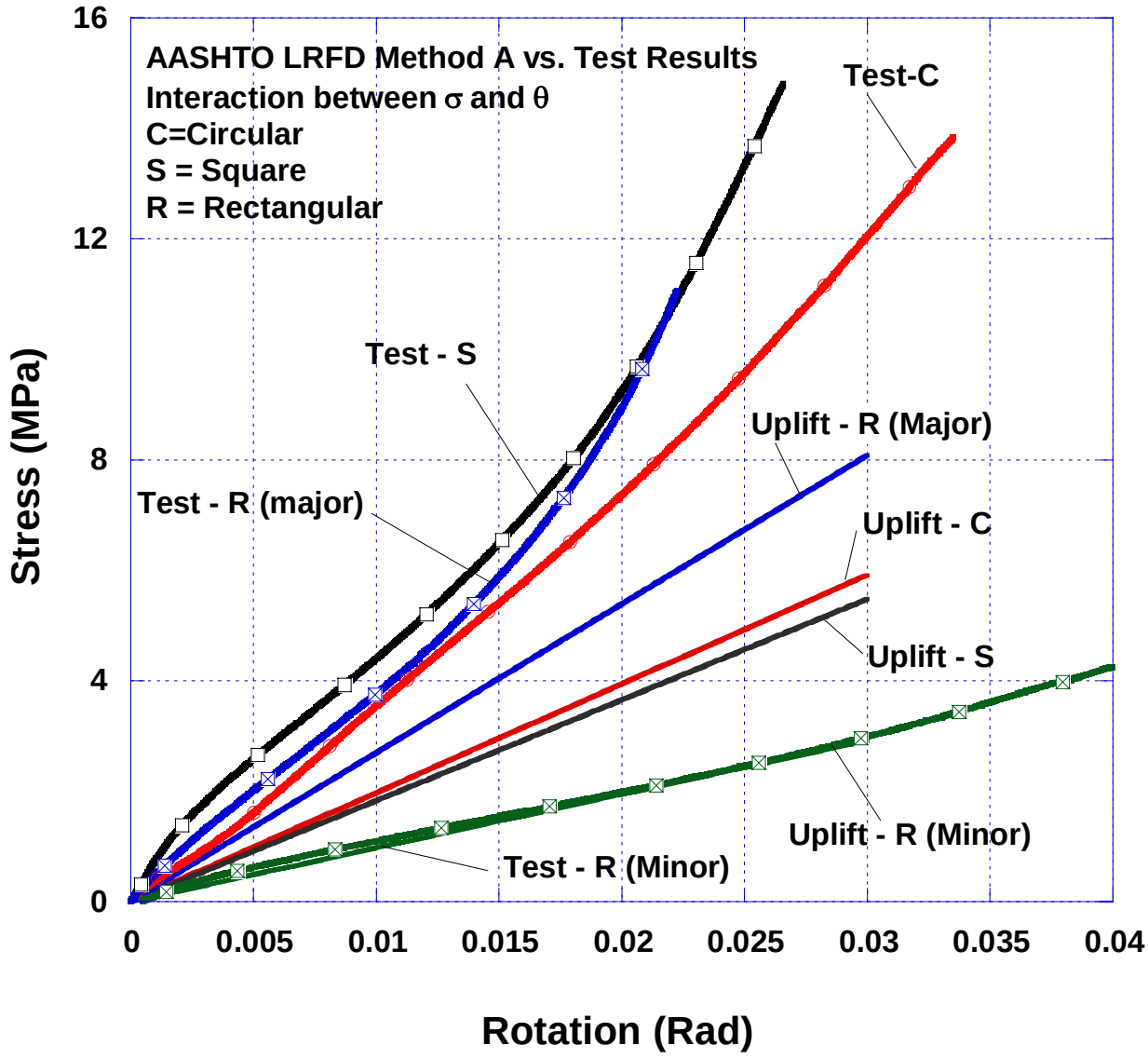

Figure 12A- Interaction between stress and rotation of elastomeric bearings from test results and from AASHTO Method A uplift equations.

Compression and Shear

Results of compression and shear tests conducted on circular and square bearings are shown in Figure 13A. The graphs shown in Figure 13A are for bearings with a compressive stress equal to 8.5 MPa (1.25 ksi). The measured shear force versus horizontal displacement relationship is approximately linear for square and circular bearings up to the AASHTO maximum service shear deformation ($\Delta_s = h_{rt}/2 = 28.5$ mm). Beyond that displacement, the relationship becomes non linear with a lower shear stiffness. The non-linear behavior in circular bearings was more than that of the square bearings. It is believed some slip has occurred in both bearings during the test as the load increased and that contributed to lower stiffness at higher loads. Also it was observed that there were some distortions near bearing edges at high loads and part of the bearing area lost contact with the steel plates. This was observed in both bearings and is believed to have contributed to lower shear stiffness at higher loads. The effect of the compressive stress level on the shear load versus deformation was not included in this study. The effect of compressive stress level on shear capacity of circular elastomeric bearings needs further evaluation. The theoretical shear stiffness (slope of AASHTO equation) of the bearings is also shown in Figure 13A. The theoretical shear stiffness agrees with the measured shear stiffness up to the AASHTO maximum service shear deformations, although the measured values have a steeper slope than the theoretical values at the beginning of the test. This steepness at the beginning of the curve may be attributed to setup restraints. Loading and unloading the specimens with small loads would have eliminated this higher slope in the beginning.

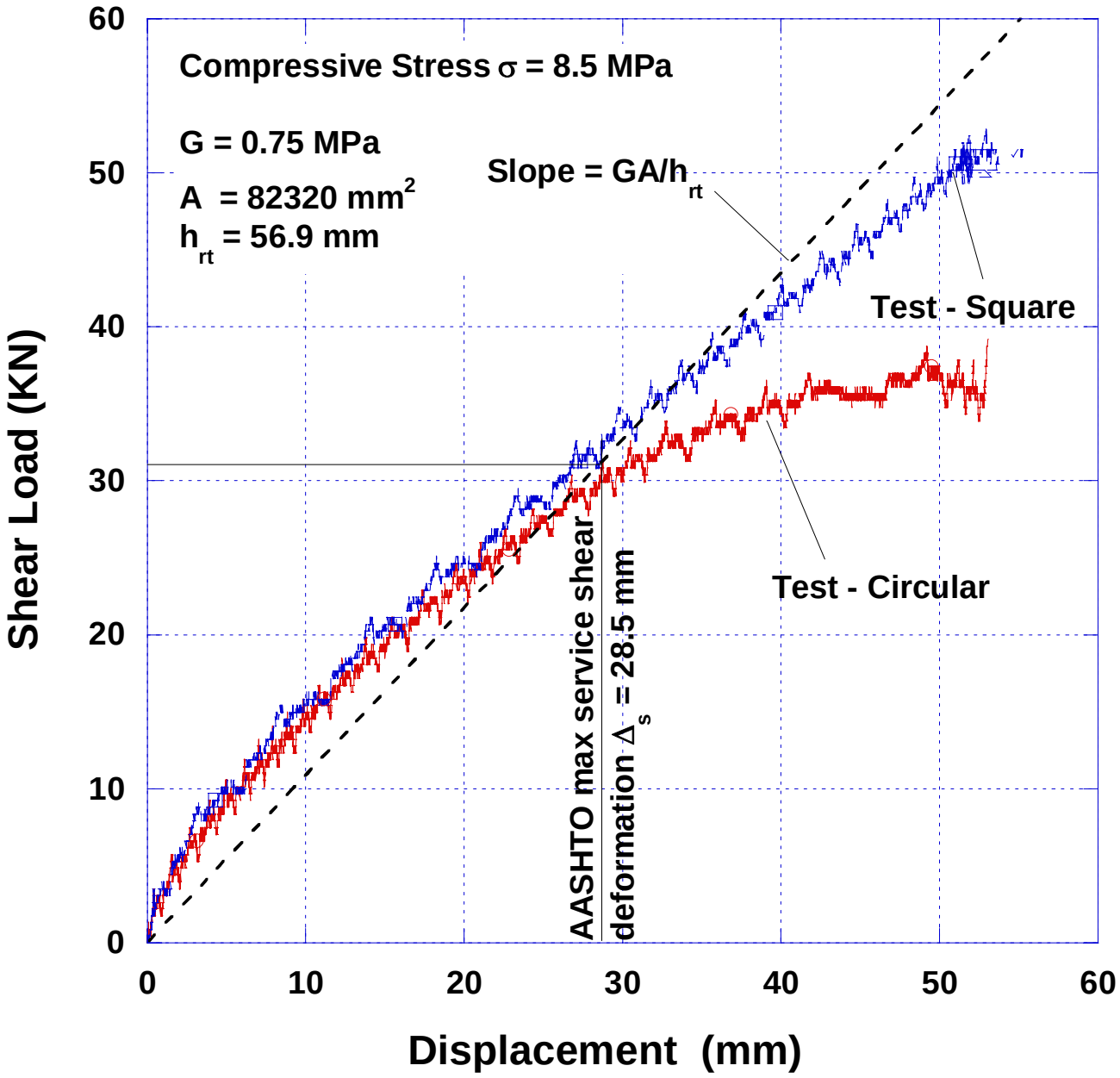

Figure 13A- Shear load versus bearing displacement for circular and square bearings from test results and from theoretical prediction.